

2.2. SIGNIFICANCE AND BACKGROUND INFORMATION AND TECHNICAL APPROACH

I. IDENTIFICATION AND SIGNIFICANCE OF THE OPPORTUNITY

For several decades photomultiplier tubes (PMT) have been the key technology for sensing light for most particle physics research operations [Kleinknecht]. High energy particle physics experiments regularly employ thousands of photomultipliers of many different sizes. The most dramatic example is the Super Kamiokande detector in Japan [<http://superk.physics.sunysb.edu>, Kleinknecht]. This detector is a 50,000 ton tank of pure water viewed by over 11,000 photomultiplier tubes, each 50 cm in diameter. This experiment has detected flashes of Cherenkov light from reactions of neutrinos from the sun as well as the atmosphere. Dr. Masatoshi Koshiba shared the 2002 Nobel Prize in physics for this research. PMTs are also used widely in calorimetry and scintillation tracking devices. The key advantage of PMTs in all these applications is their large amplification ($\sim 10^6$) with low noise which enables them to achieve high sensitivity for single photoelectron detection. Although extraordinarily successful, the PMT technology also has a number of limitations: large PMTs are expensive and cannot be mass produced, they cannot operate under pressures exceeding a few atmospheres, their sensitivity is limited over a small wavelength band, their optical quantum efficiency is low, they cannot operate under high magnetic fields, and they are bulky. As a result, there is a need for alternative designs of large photosensors that can address some of the limitations of PMTs in many high energy and nuclear physics experiments and in other astrophysical applications.

One promising solid state replacement for a PMT is the silicon avalanche photodiode (APD) [Farrell 94, Shah 01, Huth, Knoll]. An APD (like PMT) exhibits gain created by impact ionization process in the device. Also, silicon APDs exhibit high optical quantum efficiency (up to four times higher than PMTs) and much wider spectral response. APDs are insensitive to magnetic fields [Marler]. RMD has been investigating a deep-diffused APD design that provides high gain (10^3 - 10^4) [Farrell 94]. Early designs of these APDs utilized beveled edges to prevent premature breakdown in order to achieve such high gain. Such beveled edge APDs require manual fabrication and as a result, their cost is generally high ($\sim \$1000$ for 1-2 cm^2 device). Furthermore, it is very difficult to produce very large devices with this approach, again due to the need for manual fabrication. The largest APDs that are commercially available with this design are about 2 cm^2 . Due to their high cost and relatively small size, such beveled edge APDs are not suitable for many high energy physics applications.

Recently, RMD has developed a planar process to fabricate deep diffused APDs that do not require the beveled edges [Shah 01]. The performance of such planar APDs is comparable to the beveled edge APDs. Prior to the Phase I research, large area APDs (10 cm^2 area) and monolithic multi-element arrays (28 x 28 elements, 1 mm pixels) had been fabricated using this process. The planar process is well suited for fabrication of APDs in a variety of shapes. Furthermore, this APD fabrication process can be automated, which would enable significant reduction in the cost of the APDs upon mass production. In view of these advances and the need for very large, solid-state optical detectors in the high energy physics community, the goal of the proposed effort is to build very large APDs ($\geq 40 \text{ cm}^2$ area) using the planar process with performance suitable for high energy physics applications. While this goal is very ambitious, our recent progress has been very promising. If such large APDs are successfully developed in the proposed effort, they should be

able to challenge PMTs in many existing as well as future particle physics experiments. Such large APDs ($>40 \text{ cm}^2$ in size) with high sensitivity over a wide wavelength region, low magnetic field susceptibility, high pressure tolerance, and low cost through mass production could eventually make detectors that are much larger than Super Kamiokande possible for high energy physics studies. Calorimetry experiments would also benefit from the advancement in the large APD technology.

The Phase I research was aimed at detailed investigation of the design, fabrication aspects as well as signal, noise and optical sensitivity of very large APDs. During the Phase I program, we successfully fabricated very large APDs ($\sim 45 \text{ cm}^2$ area) using the planar process, which are the largest functioning APD in the world. Packaging design for such large APDs was optimized to allow cooling of these devices to liquid nitrogen temperature without any damage to the large APDs due to thermal stress. Gain and noise of these large devices were initially measured at $-40 \text{ }^\circ\text{C}$, and the optimal gain was measured to be ~ 5000 with the corresponding noise of ~ 70 electrons (rms). Scintillation spectroscopy was performed by coupling a 45 cm^2 APD to a CsI(Tl) scintillator and irradiating it with 662 keV gamma rays (^{137}Cs source). Energy resolution of $\sim 10\%$ (FWHM) was recorded for the 662 keV photopeak in this study at $-40 \text{ }^\circ\text{C}$. Optical quantum efficiency was evaluated for the large APDs and the quantum efficiency $\sim 60\%$ or higher was recorded in 400-800 nm wavelength region. Even in the deep ultraviolet (DUV) region reasonably high quantum efficiency ($\sim 40\%$ at 200 nm) was recorded for the planar APDs. Risetime of $\sim 2 \text{ ns}$ was recorded for the 45 cm^2 APDs upon direct interaction of 5.5 MeV alpha particles, confirming that fast response is achieved with these very large devices. Finally, when these 45 cm^2 APDs cooled to liquid nitrogen temperature, gain of up to 10^4 and dark current of $\sim 30 \text{ pA}$ were achieved. By performing careful studies at LN_2 temperature with the 45 cm^2 APD, electronic noise of 0.8 electrons (rms) was measured. This indicates that detection of low intensity optical signal can be achieved with these large APDs at LN_2 temperature, which was demonstrated in our study. Overall, based on the results of the Phase I program, the feasibility of the proposed approach was adequately demonstrated. The Phase I research was a collaboration between RMD and the Brookhaven National Laboratory team of Dr. Laurence Littenberg, Dr. Michael Sivertz, Dr. Milind Diwan and Dr. Peter Yamin

During the Phase II project, we will continue the advancement of this promising large APD technology. Larger APDs (up to 60 cm^2) will be designed and built in the Phase II project. Extensive evaluation of these large APDs will be conducted. Gain, noise, and quantum efficiency will be evaluated as a function of temperature. Spatial variation of gain for the very large APDs will also be studied. Surface treatment and design aspects of the APDs will be examined to optimize their noise, sensitivity in blue-UV region as well as their timing characteristics. Electronic readout issues will be examined to achieve low noise and fast response with the large APDs. The BNL team will evaluate the potential of the large APDs in water Cherenkov studies and in high energy physics experiments such as KOPIO (where the goal is to use an intense beam of kaons to study special very rare decays such as a kaon decaying into a neutral pion, a neutrino, and an antineutrino [www.bnl.gov/rsvp/KOPIO.htm]) and MECO (Muon to Electron Conversion [www.bnl.gov/rsvp/MECO.htm])). APDs with sizes up to 4 cm^2 and 4.5 cm^2 will be investigated for KOPIO and MECO, respectively. Finally, the large APDs will be evaluated as UV sensors in a liquid Xe detector by Dr. Priscilla Cushman at University of Minnesota in the Phase II study.

The Phase II research will be a collaboration between RMD and the Brookhaven National Laboratory (BNL) team of Dr. Laurence Littenberg, Dr. Michael Sivertz, Dr. Milind Diwan and Dr. Peter Yamin. The BNL group has significant experience in the area of detectors for high energy

physics applications and will provide input regarding the detector requirements and will perform testing of the large APDs. Dr. Stephen Reucroft at the Northeastern University will participate in the basic APD evaluation in the Phase II project. Dr. Cushman at the University of Minnesota will also collaborate on the Phase II project, particularly in evaluation of large APDs as UV sensors in a liquid Xe detector. Both, Dr. Reucroft and Dr. Cushman, have considerable experience in particle physics detectors including APDs. It is our expectation that upon sufficient investigation, initially by the RMD team and our BNL, University of Minnesota, and Northeastern University collaborators, and later by a wider spectrum of the high energy physics community, such large APDs will eventually be considered for large high energy physics detector applications such as water Cherenkov detectors and calorimetry. Experiments such as KOPIO and MECO are expected to be near-term applications of the proposed technology while water Cherenkov detection and liquid Xe calorimetry are anticipated to be longer-term applications of the very large APDs. Canberra Industries (Meriden, CT) will participate in the Phase II evaluation of the large APDs using their own resources. Canberra will also be our partner in the Phase III commercialization project.

II. BACKGROUND AND TECHNICAL APPROACH

A. DETECTOR REQUIREMENTS IN HIGH ENERGY PHYSICS EXPERIMENTS

1. Water Cherenkov Detectors

One of the most demanding potential application for large area APDs will be a new very large underground water Cherenkov detector [Diwan]. At present, Super Kamiokande (SK) detector in Japan (see **Figure 1**) is the largest water Cherenkov detector in the world and it has been used to detect neutrinos from the sun as well as the atmosphere [Fukuda]. The SK detector has a total mass of 50 kT of pure water that is viewed by approximately 11000 PMTs, each with a diameter of 50 cm. In such water Cherenkov detectors, high energy charged particles (such as electrons, muons etc.), produced upon neutrino interactions, create optical photons (from UV to visible range) in a cone. About 300 photons are produced per cm of charged particle track in water. These photons are viewed by the photodetectors (such as PMTs) placed on the walls of the tank, and the measurement of time (with few nanosecond resolution) and charge signal at each PMT can be used to reconstruct the trajectory of the particle. While excellent performance has been recorded with the SK detector, PMT is a limitation in the detector design. For example, nearly 7000 out of 11000 PMTs were destroyed in a pressure related chain reaction in the SuperK detector in November of 2000. Investigation revealed that a single faulty phototube at the bottom of the tank imploded and created shock waves that destroyed the rest. The detector has been rebuilt with about half the original number of phototubes.

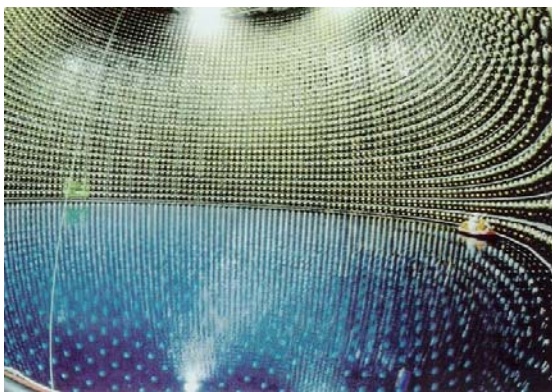


Figure 1. Super Kamiokande detector filled about half-way with water.

The next generation detector of this kind is being considered for several different locations [Diwan] and will be at least 500kT in mass. The physics agenda for such a large detector includes proton decay [Shiozawa], detection of neutrinos from astrophysical sources (such as the sun, cosmic rays, and super-novae) as well as man made sources such as accelerators. The

photosensor for such a large detector will be very challenging. It is unclear if the large 50 cm diameter PMTs can be used for such a large detector because of the increased pressure on the tubes and the difficulty of handling large photomultipliers inside a large underground cavity. A large diameter APD should be examined for this application. As already mentioned, the APD has a number of advantages such as pressure tolerance and high quantum efficiency. However, to make the APD a viable option for water Cherenkov detectors it needs to have a larger size (60 cm² in area or more). Furthermore, the large APDs need to show fast timing performance with an ability to detect single photons. Our recent studies indicate that large APDs do indeed show fast timing performance. To achieve single photon detection, these APDs will need cooling with LN₂.

It has been suggested that the performance of a water Cherenkov detector could be enhanced by a ring imaging readout. In such a detection scheme, mirrors or lenses could be used to focus the Cherenkov light onto an array of photosensors or a single position sensitive photosensor [Antonioli]. Our colleagues at BNL are considering this possibility. A large imaging APD with pixilated readout (~1 cm² pixels) could be well suited for such an application. An optimum size for APD pixel size could be obtained by considering the requirements of high spatial resolution and low noise. As part of Phase II we will evaluate these approaches and the requirements on APDs.

In the Phase I project, our aim was to demonstrate that large APDs (≥ 40 cm²) can indeed be produced and then explore the design and the operating conditions under which various performance parameters of such APDs are enhanced. Such APDs will then be further optimized and evaluated in detail in the Phase II project and their size will be scaled-up. While this overall goal is very challenging, a continued advancement in the large APD technology during and beyond the Phase II project is expected to result in the photodetectors that can challenge the PMTs for optical detection in the large Cherenkov detectors of the future.

2. Calorimetry

Low cost APDs in some cases with large sizes are also required in other high energy physics applications such as calorimetry based on solid-state inorganic scintillators such as PbWO₄ [Zalesky]. High quantum efficiency, wide spectral response, high gain, low noise, high radiation hardness, compact size and magnetic field insensitivity are important advantages of APDs in this application. There are two potential calorimetry applications of immediate interest for large APDs. In the following sections we will briefly describe the experiments, KOPIO and MECO, at Brookhaven National Laboratory. Both KOPIO and MECO are part of the RSVP (Rare Symmetry Violating Processes) project at BNL [<http://www.bnl.gov/rsvp>]. This project is funded by the National Science Foundation as Major Research Equipment and Facilities Construction program and will start construction towards the end of the proposed Phase II project. It has been reviewed and approved by all levels of the Foundation and has been recommended for funding by the National Science Board. It is essential for both of these projects to have clear evaluation of APDs for their calorimeter systems before construction starts. The applications for KOPIO and MECO are for the near future, and we also discuss calorimetry with noble liquid gases as longer-term application for the large APDs.

a. KOPIO

KOPIO will search for the decay of a kaon via the rare CP violating decay mode $K_L \rightarrow \pi^0 \nu \nu$. This decay mode of the neutral kaon is considered crucial to our understanding of CP or charge and parity symmetry. Violation of the CP symmetry (in which reversing the charge of the particle and

taking the mirror image leaves all other properties unchanged) is fundamental to understanding how the universe is composed of matter rather than anti-matter. Experimentally, however the decay occurs very infrequently (~ 3 parts in 10^{11}) and therefore the crucial experimental requirement is the suppression of all other background processes. The success of KOPIO will depend on the detection and rejection of the much more common decay modes that include extra gamma rays and charged particles. To be fully efficient, the gamma detectors must be sensitive to gammas from energies down to 1 MeV and up to 1.5 GeV. These gammas will be detected with lead/scintillator modules which convert the deposited energy to visible light. Low energy gammas yield very little light, making the observation of low intensity light signals of great importance.

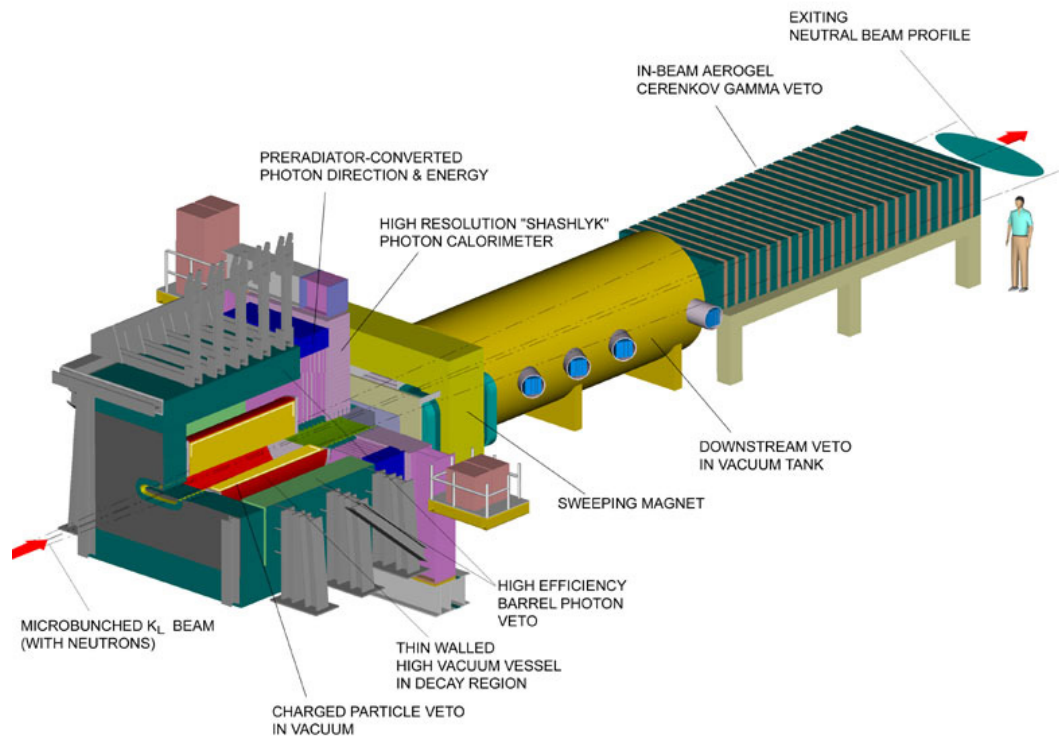


Figure 2. Schematic of the KOPIO detector. Low energy kaons enter the apparatus at lower left of the picture. The decays that occur in the thin walled vacuum vessel are analyzed by large number of scintillation counters that almost completely surround the decay.

KOPIO makes use of plastic scintillator to identify charged particles and photons. **Figure 2** shows a schematic diagram of the KOPIO detector. Current designs anticipate the use of 3000 phototubes with 2" diameter as part of a photon calorimeter and 1000 additional phototubes to be used as part of a photon veto counter. If large APDs with desired performance were available for this experiment, many advantages would accrue. Several of the KOPIO subsystems are considering using APDs as the light detection device, provided the performance in critical areas can be achieved. These critical areas are: sensitivity to low intensity light signal, timing response, and variation of these performance parameters as the devices size is increased. It is crucial that we complete the study of APDs for this experiment during the Phase II program so that the construction of the KOPIO detector can begin towards the end of the Phase II project. Subsystems that are

considering APD use include the Calorimeter, Outer Veto, Barrel Veto, and Downstream Veto. Although the technical challenges vary, much of the APD research for the Phase II proposal is common to all of the subsystems. APDs with area up to 4 cm² area required for KOPIO. Our BNL collaborators will explore the possibility of using large APDs in KOPIO during the Phase II project.

b. MECO

After the discovery of the muon it was realized that it could decay into an electron and a gamma ray (e-gamma) unless the number of muons and electrons is conserved or always constant in the universe. A related process is the conversion of muons into electrons in the field of a nucleus. Experimentally the conversion process is favored because it is easier to detect. After decades of effort there is still no evidence of either muon to e-gamma decay or muon to electron conversion. There is new interest in these processes because of new theoretical understanding in recent years which has predicted this process to occur at very small rates.

The MECO experiment is a search for the Standard Model-forbidden decay $\mu \rightarrow e$ at sensitivity of about one part in 10¹⁷. The experiment will be performed in a new pulsed muon beam to be constructed in the experimental hall of the Alternating Gradient Synchrotron at Brookhaven National Laboratory. **Figure 3** shows a schematic diagram of the MECO experiment.

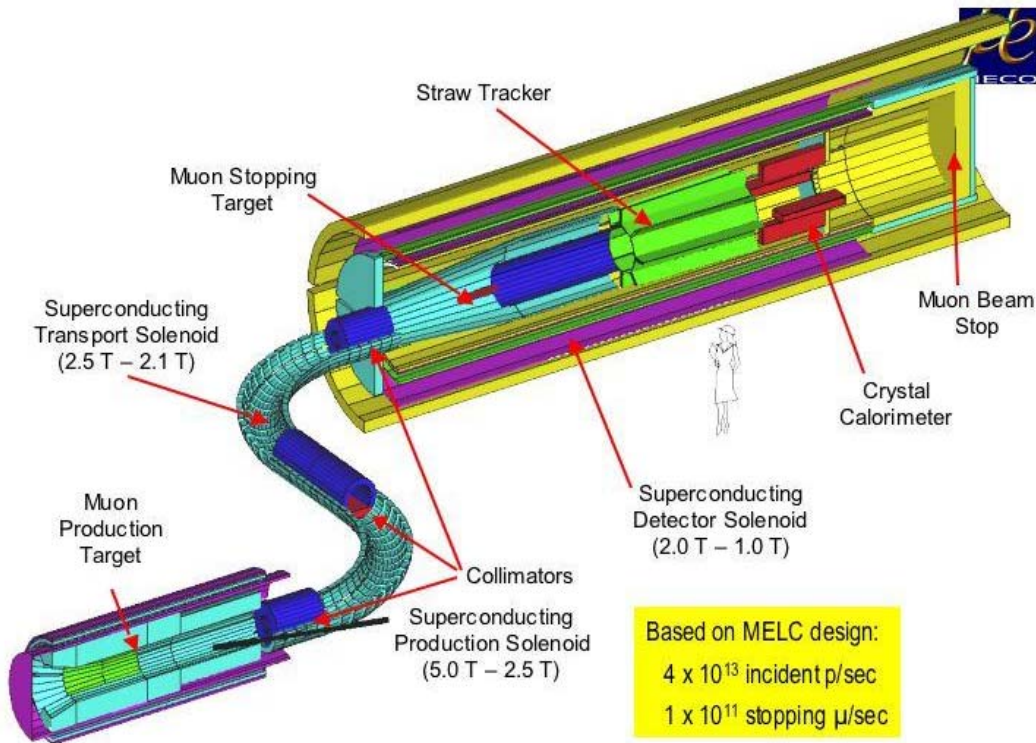


Figure 3. Schematic of the MECO experiment. Low energy muons are produced in the smaller superconducting solenoid by 28 GeV protons impinging on a target. These muons are transported to a stopping target in the larger solenoid. The spectrometer inside the larger solenoid will analyze the product of muon decays or conversions. The crystal calorimeter is used to measured the energy of the electrons produced in the decays or conversions.

The critical parts of the experiment are the muon production target, the superconducting solenoids which both capture the muon and help in analyzing the momentum of the conversion electron, the straw tube spectrometer which detects the helical orbit of the conversion electron in the

magnetic field, and the crystal calorimeter which stops the conversion electron and measures its energy. The expected signal in MECO experiment is a monoenergetic 105 MeV electron in a much larger, though rapidly falling, background. The precise determination of the electron energy in MECO will be made by tracking through a magnetic field, but the decision on whether or not to record the event (trigger) will be made on the basis of the energy deposited by stopping the electron in a calorimeter composed of ~ 2000 PbWO_4 scintillator blocks, each with $3 \times 3 \times 14 \text{ cm}^3$ size. Since the trigger rate falls as the eighth power of the calorimeter energy resolution near 105 MeV, energy resolution better than 5% is required. The calorimeter will reside in the region of 1 Tesla tracking field, so read out by photomultiplier tubes is not feasible and APDs will be required. Thus large APDs are needed to read out the light from the crystal calorimeter in the MECO experiment. In addition to good energy resolution, the other requirements are good timing resolution and capability to handle high count-rates.

c. Noble liquid gas calorimetry.

Calorimetry based on scintillation from liquid noble gases (such as liquid Xe that emits $\geq 40,000$ photons/MeV at 174 nm [Doke, Séguinot, Williams]) can also be a possible application for large APDs. It should be noted that RMD's high gain APDs have good quantum efficiency ($\sim 40\%$) at 174 nm and further improvement can be obtained by optimizing the front surface and the device structure. In this application, large APDs could be immersed in liquid Xe because the signal to noise ratio of the large APDs is expected to be excellent under cryogenic cooling. Another medium of interest is liquid Ar with a 3% addition of Xe to shift the emission wavelength of 128 nm for liquid Ar to 174 nm. This technique also appears to considerably increase the attenuation length of the light. Thus this medium is ideal for a large underground detector for detection of rare events such as proton decay or a search for rare astrophysical particles. The large APDs are expected to play an important role in future particle physics studies if their performance is found to be adequate.

B. CONVENTIONAL HIGH GAIN, DEEP DIFFUSED SILICON AVALANCHE PHOTODIODES

In this section, we cover the basic deep-diffused APD technology that is the foundation for the large planar APDs. An APD is a unique device that combines the advantages of solid state photodetectors with those of PMTs. Like PMTs, APDs have internal current gain due to impact ionization, allowing a high signal-to-noise ratio. Like other solid state devices, APDs have high quantum efficiency and are compact and rugged [Squillante].

An APD is a photodiode operated at a very high reverse bias. The basic physical mechanism upon which avalanche gain depends, impact ionization, occurs when the electric field is sufficiently strong so that an electron colliding with a bound valence electron transfers sufficient energy to ionize it. This creates an additional electron-hole pair. The additional carriers, in turn, can gain sufficient energy from the electric field to cause further impact ionization, creating an avalanche of carriers [Sze]. The current gain resulting from the avalanche process is the primary advantage of an APD relative to a conventional, unity gain photodiode. The high bias requires that special precautions be taken at the edges of the device, where electric fields can be at their highest levels. In earlier devices, this was accomplished by beveling the APD edge (see **Figure 4**) so that the field is reduced by increasing the area over which it is applied [Huth, Farrell 90 & 94]. The beveled edge on an APD must be fabricated by manual processes. This required a skilled technician and was the limiting step in both the yield and cost of producing APDs.

Another unique requirement of APDs is their very deep p-n junction. In order to achieve high gain it is necessary to maintain a moderately high electric field over a very large distance, which requires a wide depletion region. The very high gain APDs made by RMD utilize a depletion region width of more than 150 μm at breakdown. This requires a

very deep p-n junction, which can only be fabricated by using very deep diffusion. Typical APDs with beveled edges manufactured by RMD have areas ranging from 4 mm^2 to 2 cm^2 . They can operate with gains $>10^3$ at room temperature and $>10^4$ cooled to $-30\text{ }^\circ\text{C}$ [Farrell 94]. Important features of these APDs are their high quantum efficiency, having a peak quantum efficiency of 60-80%, and wide spectral response, which are far greater than those for PMTs.

Due to the need to form the hand crafted bevels to produce high gain APDs, it is difficult to fabricate large area devices ($>2\text{ cm}^2$) with such an APD design in a cost effective manner. In the research proposed here, we will address this need, investigating large APDs that can be fabricated for much less cost. The solution is to remove the manual fabrication steps and develop a process that makes use of planar technology. It should be noted that another APD design called a “reach through” device exists which can be fabricated using planar technology [Melle]. This is a planar device, but gains are less than 100, with far worse signal-to-noise ratio than is obtained with the RMD beveled edge design. Also, the “reach-through” design inherently limits the active area of APDs. What is required is a technique to maintain the high gain, i.e. the deep diffusion profile in the bulk Si, and large areas, while terminating the junction using economical planar processes. Our investigation of such an approach has been very promising as discussed in the following section.

C. PLANAR APD FABRICATION

At RMD, we have investigated methods for producing the deep-diffused profiles required to fabricate an ultra-high gain planar APD. Planar techniques require less labor and may produce an array of devices simultaneously, for the processing steps are applied to all the devices on a wafer. We have obtained very promising results in our attempts to form the required doping profile (to terminate the junction at the edges without causing premature breakdown) using a low cost planar process. This innovative approach involves

cutting grooves in the n-type neutron transmutation doped (NTD) silicon wafer used for APD fabrication. The shape of the groove is used to influence the profile of the subsequent p-diffusions. The presence of grooves creates a curved diffusion profile. The resulting p-n junction profile, which is contoured, acts as a planar bevel that can be terminated at a required angle using etching and polishing methods. **Figure 5** outlines the steps involved in this

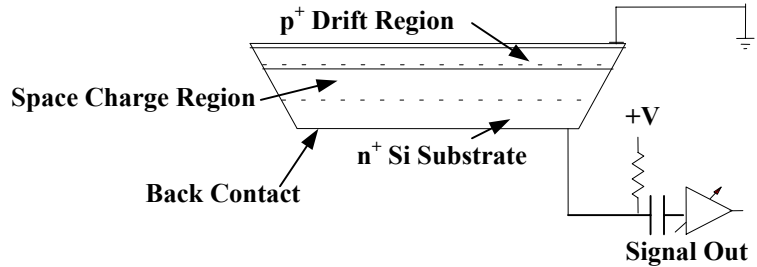


Figure 4. Schematic of beveled edge APD design used previously at RMD.

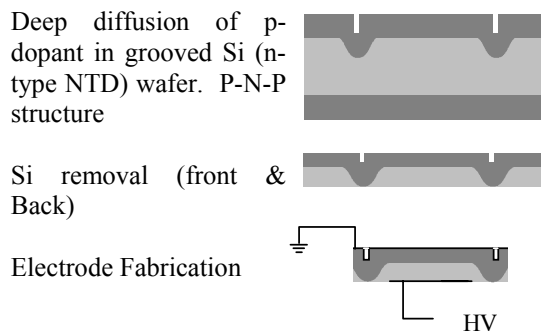


Figure 5. Schematic of planar process used for APD fabrication at RMD.

process, which is very amenable to low cost fabrication of large area APDs and monolithic APD arrays, restricting dead space between elements to $< 350 \mu\text{m}$ [Shah 01].

Previously, we used 2" NTD doped n-type silicon wafers and fabricated large (10 cm^2) APDs as well as APD arrays with 4×4 , 8×8 , 14×14 and 28×28 elements with the planar process. These APD arrays had 1-2 mm pixels. **Figure 6** shows photographs of some planar APDs that have been fabricated at RMD in our research prior to the Phase I program. Such planar devices have been evaluated at RMD in our earlier studies.

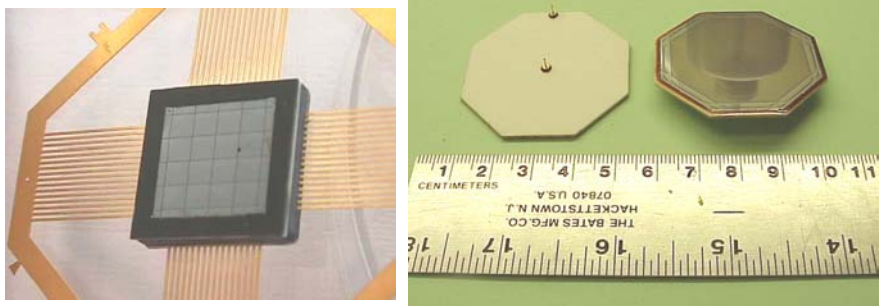


Figure 6. Photographs of planar APDs fabricated at RMD. On left, an APD array (4×4 elements, 2 mm pixels) is shown. On right, a 10 cm^2 APD, packaged on a ceramic substrate is shown.

D. PLANAR DEVICE TESTING

At RMD, we have conducted evaluation of the planar APDs that involved measurement of gain, noise, quantum efficiency and energy resolution studies. Results are reported first for the 4×4 element APD array (2 mm pixels) shown in **Figure 6**, followed by those for a 10 cm^2 planar APD. Using $2 \times 2 \text{ mm}^2$ devices, we have also evaluated radiation hardness properties of the planar APDs.

1. Evaluation of 4×4 Element Planar APD Array:

Testing of the APDs arrays (2 mm pixels) fabricated using planar technique has been conducted. One of the first tasks was to evaluate the gain and noise behavior of the planar APDs and compare the results with those for our standard beveled edge APDs. A low energy X-ray source (^{55}Fe - 5.9 keV X-rays) was used to calibrate the energy scale for gain and noise measurements and a low noise electronic pulse generator was used to quantify noise. The resolution of the 5.9 keV photopeak was measured to be 600 eV (FWHM) for 2 mm pixel size at room temperature. This is comparable to the performance obtained with the manually beveled APDs of similar size. **Figure 7** shows gain versus bias and noise versus bias behavior for 2 mm APD pixel showing that the maximum gain approached 10^4 . The noise of 2 mm planar devices was measured to be 200 eV (FWHM) or 24 electrons (rms) at room temperature. The gain and noise properties of the manually beveled APDs are very similar to the results for planar APDs. Furthermore, the gain of our new planar APDs is higher by a factor of more than 100 as compared to the other “reach through” planar APD design. These results are very encouraging.

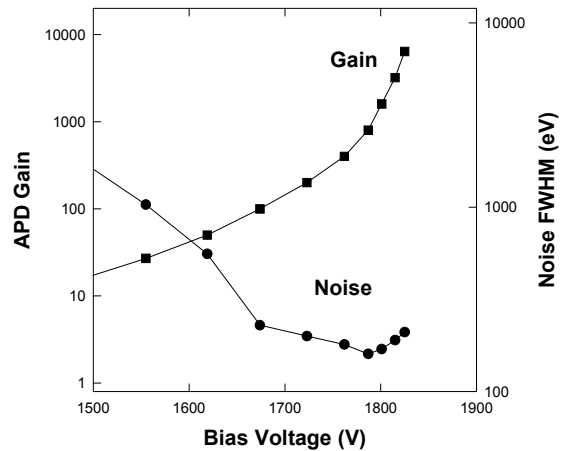


Figure 7. Gain and noise versus bias behavior for 2 mm planar APD pixel.

The quantum efficiency of one planar APD pixel was measured and the results are shown in **Figure 8**. As seen in the figure, the quantum efficiency of these devices is in 60-90% range. The

quantum efficiency of these APDs is significantly higher than that of PMTs. Also, the spectral response range for the APDs is also much broader than that for PMTs. Even higher quantum efficiency, especially in blue region can be achieved upon optimization of the front surface of these APD and adding an anti-reflection coating.

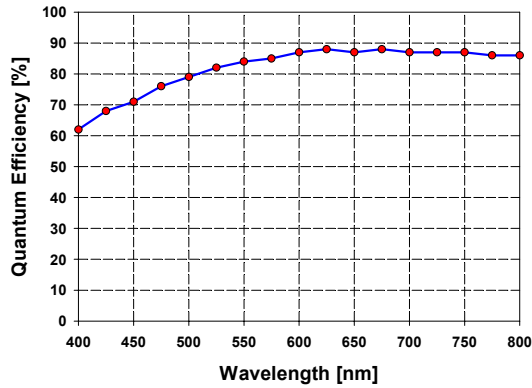


Figure 8. Quantum efficiency versus wavelength for a planar APD.

variation in peak position is $\pm 3.5\%$. The average energy resolution of 5.9 keV peak is 650 eV (FWHM).

The performance of the planar-processed APDs as optical scintillation detectors was investigated. A CsI(Tl) scintillator (2x2x5 mm) which emits optical scintillation light with a peak emission of 540 nm was coupled to a 2 x 2 mm planar APD pixel. The energy resolution of the peak was measured by acquiring a pulse height spectrum of 662 keV gamma rays (^{137}Cs source). The resolution was found to be approximately 6-7% (FWHM) at 20 °C. Our results show that the yield of working devices is very high for the new planar process ($> 95\%$). Cross-talk in adjacent APD pixels has been measured to be $< 0.5\%$. We have cooled 2 mm APD pixels to 77 °K (using LN_2) and have successfully demonstrated single photoelectron detection with such planar APDs.

2. Evaluation of 10 cm² Planar APD

We have also fabricated large APDs using planar process that included a 10 cm² APD with octagonal geometry (see **Figure 6**-right), built on a 2" n-type NTD silicon wafer. Gain and noise properties of the large planar APDs have been measured. Gain was measured using a pulsed LED that irradiated the entire APD surface. The device has unity gain at low bias (200-500 V) and the gain values were computed at higher bias based on the unity gain calibration. Operating gain of such an APD was found to be > 1000 at room temperature where its signal to noise ratio is optimal. Electronic noise of the 10 cm² APD has also been measured. ^{55}Fe source was used for calibration of the energy scale and the resolution of a test pulse was recorded as a function of bias. At the optimal gain value, the noise of the APD is 200 electrons (rms) or 1.7 keV (FWHM) at 20 °C. **Figure 10** shows scintillation spectroscopy, performed by coupling the 10 cm² APD to a CsI(Tl) scintillator

The 4 x 4 APD arrays have also been characterized by measuring their uniformity of response under X-ray irradiation. **Figure 9** shows ^{55}Fe spectra (5.9 keV X-rays) recorded from each of the 16 pixels with the X-ray source placed directly over each pixel during irradiation [Shah 01]. From this data-set, the peak position and integral of X-ray counts for each pixel were computed. The total

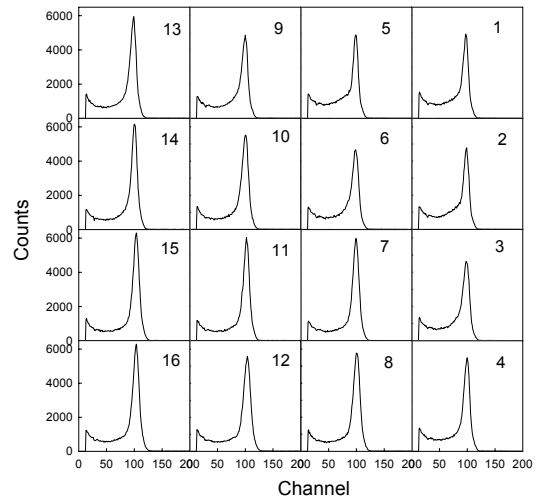


Figure 9. ^{55}Fe spectra recorded with all 16 pixels of an APD array (2 mm pixels).

(3.8 cm diameter, 2.5 cm high). The resolution of 662 keV photopeak (^{137}Cs source) was measured to be 9% (FWHM) at temperature of 16 °C (see **Figure 10**).

3. Radiation Hardness Characteristics of Planar APDs

In a prior investigation, we have evaluated radiation hardness of small planar, high gain APDs with $2 \times 2 \text{ mm}^2$ area. The experiment involved selecting eight discrete planar APDs and measuring their optical quantum efficiency, gain and dark current at operating bias of 1800 V, prior to any radiation exposure. These parameters were selected because quantum efficiency and gain determine the signal generated by the device, while the dark current affects its noise. Next, these devices were irradiated with 72 MeV protons at Paul Scherrer Institute (PSI, Switzerland) with fluence ranging from 1×10^8 to 2×10^{12} protons/cm² by our collaborator Dr. Reucroft at the Northeastern University. After the exposure, the devices were evaluated again, and their gain and dark current (at 1800 V) and their quantum efficiency were re-measured, and the results were compared to the data measured prior to the radiation exposure.

The results of this study are summarized in **Table I**, where the proton exposure, and equivalent 1 MeV neutron exposure (calculated from the proton exposure [Huhtinen]) are listed for each device. Also shown in the table, are the ratios of gain, dark current, and quantum efficiency (at a selected wavelength of 500 nm) for each device, measured after and before the exposure. As seen in the table, gain of the devices does not show any strong correlation to exposure. The dark current of the devices increased at exposure level beyond 10^{12} n/cm². Quantum efficiency, which is the most important parameter from view-point of light detection with APDs appears to be unaffected by radiation exposure up to 10^{12} n/cm² and starts to degrade at higher exposure levels. These results indicate that the APDs show stable performance for exposure level up to $\sim 10^{12}$ n/cm².

These results are very encouraging and indicate that the radiation hardness of our APDs is acceptable for most particle physics studies. Since the basic design and structure of the $2 \times 2 \text{ mm}^2$ planar APDs and the very large APDs that we are building in the proposed effort are similar, we expect the large APDs to exhibit similar radiation hardness characteristics. For certain experiments such as the extreme requirements in CMS, some improvement in radiation hardness of our APDs would be required, which can be achieved by reducing the thickness of APD's front p-type neutral (or drift) region. We have also explored effect of mild thermal annealing on the performance of APDs that suffered some degradation due to high exposure levels (6.5×10^{11} and 2×10^{12} n/cm²). This involved heating the devices to a temperature of 100 °C for a period of 48 hours. The gain, dark current, and quantum efficiency of the devices were re-measured. The ratios for these parameters were calculated based on numbers measured after annealing and the ones measured prior to radiation exposure, and the results are listed in **Table I**. As seen in the table, even with such mild anneal, the parameters approach the pre-radiation values which is very encouraging.

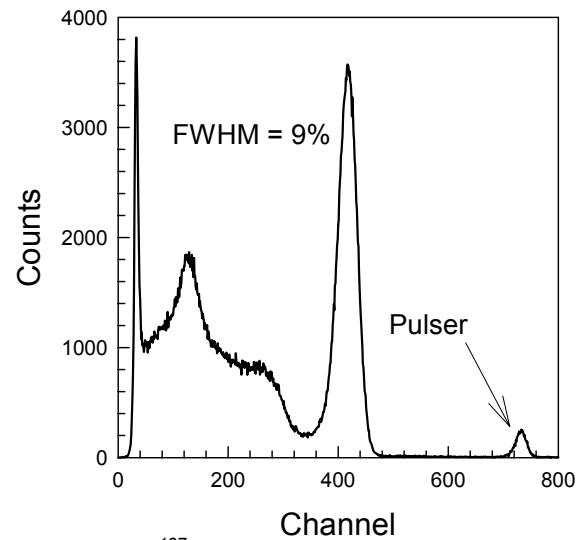


Figure 10. ^{137}Cs spectrum (662 keV γ -rays) recorded with a 10 cm^2 planar APD coupled to CsI(Tl) scintillator at 16 °C.

Table I. Summary of Radiation Hardness and Annealing Experiments

APD #	Proton Exposure [p/cm ²]	Equivalent Neutron Exposure [n/cm ²]	Gain Ratio	Dark Current Ratio	QE Ratio
1	1.09e8	2.29e8	0.81	0.69	0.93
2	1.05e9	2.20e9	1.17	0.84	1.07
3	9.92e9	2.08e10	1.00	1.01	1.21
4	2.95e10	6.20e10	0.86	1.13	1.23
5	9.45e10	1.99e11	0.92	1.08	1.16
6	3.10e11	6.51e11	1.97	2.43	0.95
7	9.85e11	2.07e12	1.42	7.02	0.54
8	2.42e12	5.08e12	1.11	8.11	0.20
annealed 6	3.10e11	6.51e11	2.32	1.19	0.92
annealed 7	9.85e11	2.07e12	1.41	1.94	0.77

These results clearly indicate that planar APD technology is very promising. We have recently upgraded our APD fabrication process to accommodate 4" NTD doped silicon wafers. The ability to process larger wafers allows fabrication of significantly larger devices, which is the focus of the proposed effort. During the proposed Phase I effort the goal was to fabricate APDs with area ≥ 40 cm² using the planar process and extensively characterize the performance of the large APDs. An important aspect of the Phase I research was to cool the large APDs to LN₂ conditions (in order to minimize their noise) and characterize their gain and noise properties. The Phase I project was very successful as discussed in detail in the **Phase I Final Report** section and the feasibility of the proposed effort was adequately demonstrated. Even larger planar APDs (up to 60 cm²) will be built in the Phase II project and possibility of using such APDs for detection of low intensity optical signal will be explored. Planar APDs will be evaluated from view-point of eventual use in various high energy physics applications (discussed earlier) during the Phase II research.

III. ANTICIPATED BENEFITS

The low cost, high gain APDs with very large areas that we plan to produce in the proposed effort will have major impact in a number of high energy physics experiments. This includes eventual implementation in water Cherenkov detectors to study neutrinos from a variety of sources such as the sun, super novae, as well as accelerators. Calorimetry experiments such as KOPIO and MECO are promising near-term applications of the large APDs. Liquid noble gas calorimetry and high energy astrophysics are also potential applications for the large, high gain planar APDs that we plan to explore in the proposed effort.

Such large APDs would also have numerous commercial applications beyond high energy physics research. Medical imaging modalities such as SPECT and PET (with Anger logic design) which involve hundreds of scintillation detectors coupled to optical sensors will directly benefit from advances in the APD technology. The compactness, high gain, high speed and good quantum efficiency of APDs will lead to cheaper and less bulky instrumentation with higher performance. Astronomy and space physics will be another potential application. Non destructive testing, and materials research including synchrotron applications will also be potential markets for the planar APD array technology. Scintillation spectroscopy for nuclear physics research, optical tomography, optical detection of biological and chemical molecules, direct X-ray detection, and charge particle

detection are all potential applications of the proposed technology. Low background, low level radiochemistry experiments are also possible with such large APDs. In view of the promise offered by these APDs, Canberra Industries (Meriden, CT) has shown strong interest in investigation as well as commercialization of these devices.

IV. DEGREE TO WHICH PHASE I DEMONSTRATED TECHNICAL FEASIBILITY

The main objective of the Phase I research was to demonstrate the feasibility of producing large ($\geq 40 \text{ cm}^2$) planar APDs with performance characteristics suitable for high energy physics experimentation. In order to achieve this objective, we had planned to first address design and fabrication aspects for producing such large APDs using the planar process. Packaging and electronic readout aspects were to be investigated. Devices fabricated in this manner were to be extensively investigated which would involve measurement of their gain, noise, and quantum efficiency. Noise of these devices was to be measured, especially at LN_2 temperature in order to analyze the possibility of detecting low intensity optical signal using the large APDs. Timing characteristics of these devices were also to be evaluated.

The Phase I project was very successful and all the Phase I objectives were met or even exceeded (in some cases). During the Phase I project, the planar fabrication process was adapted to allow fabrication of very large APDs. We successfully fabricated planar APDs in two sizes in the Phase I research: 40 cm^2 and 45 cm^2 . These are the largest operational APDs in the world. A new packaging design for these large APDs was developed in order to allow temperature cycling of these devices between room temperature and $77 \text{ }^\circ\text{K}$ (LN_2 temperature) without any mechanical damage to the devices (due to thermal stresses). Both charge sensitive and voltage sensitive preamplifiers were used to evaluate these devices. Initially, gain, noise and quantum efficiency of these devices were evaluated. Quantum efficiency of these devices was measured to be $\sim 60\%$ or higher in the 400 to 900 nm wavelength region. Even at 200 nm, quantum efficiency of $\sim 40\%$ was measured for the planar APDs. At temperature of $-40 \text{ }^\circ\text{C}$, the gain of 45 cm^2 APDs was measured to be 5000 while their noise was 70 electrons (rms). The 45 cm^2 APD was coupled to a CsI(Tl) scintillator and irradiated with 662 keV photons (^{137}Cs source). The energy resolution of the 662 keV photopeak was measured to be 10% (FWHM) at $-40 \text{ }^\circ\text{C}$. The large APDs were also irradiated with 5.5 MeV alpha particles and the signal was observed directly on a digital scope without any shaping. The risetime of the resulting pulse was measured to be $< 2 \text{ ns}$, indicating that the large APDs provide fast response.

The 45 cm^2 APDs were then cooled to liquid nitrogen temperature and their leakage current, and noise were measured. The electronic noise of the device was measured to be ~ 0.8 electron (rms) at $77 \text{ }^\circ\text{K}$ upon optimization of the front-end readout setup. Maximum gain of $\sim 10^4$ was achieved with the large devices at $77 \text{ }^\circ\text{K}$. The ability to detect low intensity optical pulse (with < 8 photoelectrons/pulse) with such large APDs at $77 \text{ }^\circ\text{K}$ was also demonstrated in our research. Based on these results, the feasibility of the proposed research was adequately demonstrated. The Phase I research was a collaboration between RMD and the Brookhaven National Laboratory (BNL) team of Dr. Laurence Littenberg, Dr. Michael Sivertz, Dr. Milind Diwan and Dr. Peter Yamin.

V. THE PHASE I FINAL REPORT

A. DESIGN, SIMULATIONS AND FABRICATION OF LARGE, PLANAR APDS

In the Phase I project, we fabricated very large APDs ($\geq 40 \text{ cm}^2$) using the new planar process at RMD. The basic approach involves cutting a groove in the silicon wafer used for APD fabrication. The shape of the groove is used to influence the profile of the subsequent diffusions. Earlier, **Figure 5** outlined the steps involved in this process that utilizes an automated wafer grooving routine followed by diffusions and polishing methods to form the high gain APD. No manual processing is required in this new fabrication method. The fabrication steps are as follows:

- 1. Fabricate grooves with appropriate depth and thickness into our starting neutron-transmuted doped (NTD) silicon wafers that are normally used for manual processing of large APDs.*
- 2. Carry out standard deep diffusion to define the doping profile.*
- 3. Polish back the front surface and the back side for proper termination of the p-n junction.*
- 4. Define device periphery and fabricate device by applying contacts.*

We have conducted simulations of the dopant profile around the grooves in order to predict the p-n junction profile in the devices. These simulations are discussed here.

1. Simulation of Dopant Profiles and P-N Junction Contours

An important aspect of our new planar fabrication process for APDs involves deep diffusion of p-type dopant into a grooved n-type silicon wafer. The presence of grooves results in a curved diffusion profile in the region near the grooves and a flat profile in the region away from grooves. The resulting p-n junction also has a similar shape. We performed computer simulations of this diffusion process in order to determine the precise distribution of the diffused p-type dopant and the resulting p-n junction contour. One aspect of these simulations was to compare the shape of p-n junction for various groove shapes. The shape of p-n junction is important, and if a sharp bend (or curvature) is present, the device can undergo a premature breakdown, which can limit the gain of the eventual APDs. Since the shape of groove influences the p-n junction shape, a variety of groove shapes were simulated at RMD in a prior investigation.

Although the diffused silicon has a three dimensional profile, symmetry arguments can reduce the problem to two-dimensions. The p-type dopants used in our standard process are gallium and aluminum, which are diffused into n-type NTD silicon wafer (with $30 \text{ } \Omega\text{-cm}$ resistivity) using a carefully controlled process developed by RMD. In our prior research, we have developed a simple mathematical solution for the diffusion process. The process was modeled assuming a constant surface dopant concentration, which is what actually happens in our process. Under this condition, the dopant concentration profile is described by a complimentary error function [Ghandhi]. Since two p-type dopants (Ga and Al) are used in our process, the p-type dopant profile has been modeled as a sum of two diffusion profiles. Once our model was developed, in order to gain confidence in its predictions, we fitted a measured dopant concentration profile for a deep diffused wafer with the model results as shown in **Figure 11**. The experimental data for our deep diffusion profile is based on measurements performed by Solecon, Inc. (San Jose, CA). As seen in **Figure 11**, excellent agreement was observed between the experimental results and our model predictions. Next, we used this model to simulate the dopant profiles for n-type wafers with grooves cut in them.

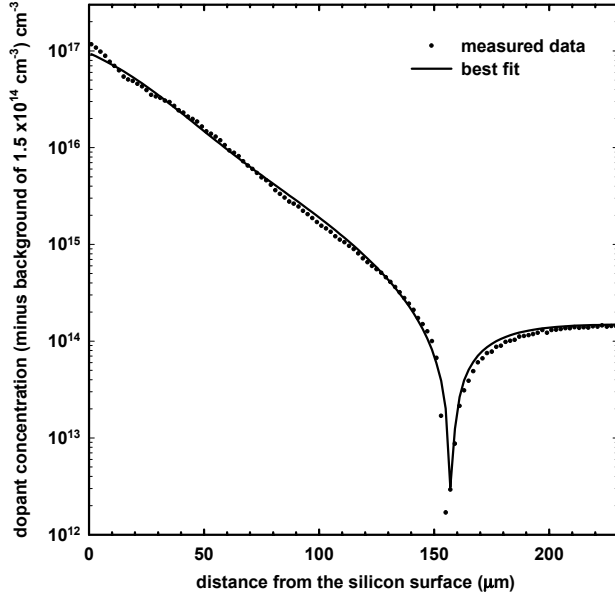


Figure 11. Measured one-dimensional doping profile of an RMD deep diffused silicon wafer and a mathematical fit to that data. The fit used sum of two complementary error functions for p-type diffusion of Ga and Al.

that while the p-n junction curvature is fairly similar for all groove designs, the broad V-shaped and the circular grooves have slightly smoother bending in the p-n junction profile. However, the V or circular groove shapes are harder to fabricate (than the standard rectangular grooves) and they require special blades. As a result, rectangular grooves were chosen for fabrication of very large APDs in the Phase I project. As discussed in later sections, very high gain was achieved with the large APDs having rectangular grooves, which validated this choice.

2. Planar Device Fabrication

While the basic procedure used for APD array fabrication is similar to the process outlined in **Figure 5**, various steps were optimized both prior to and during the Phase I research to enable easier processing, improve the device performance, and allow increased flexibility. **Figure 13** shows a detailed schematic representation of the planar

In this study, the two-dimensional distribution of diffused p-type dopants into the n-type silicon is simulated for wafers having grooves of different shapes. This allowed us to determine whether the curvature of the p-n junction can be significantly altered in these cases (which may have an effect on the breakdown and gain characteristics of the devices). Four groove shapes, all 200 μm deep, were studied: 1) the rectangular grooves, 2) triangular ‘V-shaped’ grooves which have walls at 27° with the ‘z-axis’ (into the silicon), 3) triangular ‘V-shaped’ grooves which have walls at 45° with the z-axis, and 4) round grooves with a radius of 200 μm.

The results of the two-dimensional simulations are shown in **Figure 12**. Also shown in the figure are various groove designs as well as the corresponding p-n junction profiles. From the plots, one can conclude

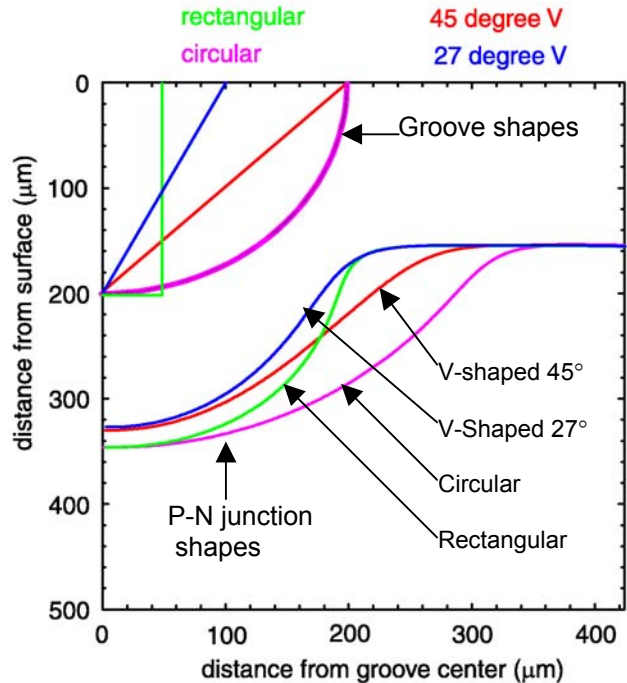


Figure 12. Device designs with various groove shapes (rectangular, V shaped, and circular), and simulated p-n junction shape corresponding to each groove shape (color coded). The simulations assumed a 30 Ω-cm n-type wafer ($1.5 \times 10^{14} \text{ cm}^{-3}$ base concentration).

processed used in the Phase I project for fabrication of very large APDs.

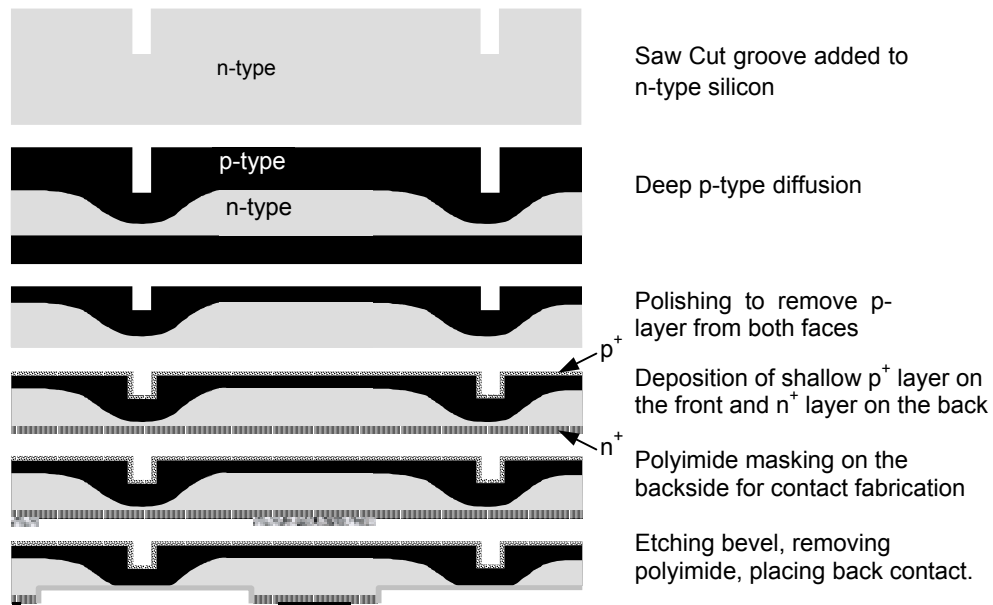


Figure 13. Planar processing of APDs with new polishing and masking methods.

The first step in our APD fabrication effort was selection of silicon wafers. We used neutron transmutation doped (NTD), n-type silicon wafers with 30 Ω -cm resistivity, which were similar to ones used in our manual APD fabrication efforts. Rectangular grooves were cut in the 4" diameter wafers, which in addition to creating planar bevels upon diffusion of p-type dopants, also define the device geometry. Two APD geometries were explored in the Phase I project, one where the grooves defined a square device with 6.35 x 6.35 cm² (or 40 cm²) area, and the second one with an octagonal design having 45 cm² area. The wafers were lightly polished as a service at Semiconductor Processing, Inc. (Boston, MA). Deep diffusion of p-type dopants, gallium and aluminum, was performed using our standard diffusion procedure at RMD. Si material was then removed from the front and back of the wafer. We used our simulations to determine the depths to which the front and backside should be processed in order to allow the p-n junction to meet the silicon surface at a desired angle. This is necessary to prevent surface breakdown in APDs of this design. Initially, the silicon removal was accomplished using etching procedures. However, acid etching is not optimal on the front device face due to the presence of grooves, and we have investigated an alternative method for silicon removal that involves very well controlled polishing of the wafer. Such polishing was performed at Semiconductor Processing, Inc. (Boston, MA), and 100 μ m of p-type material from the front and 200 μ m from the back was removed. This approach was found to be quite reliable and has since been established as a routine step in our process.

The next step was to perform a shallow boron diffusion on the front (grooved) surface which is necessary to improve charge collection near the surface and thereby improve the optical quantum efficiency of the devices. This step is also necessary to 'sharpen' the I-V characteristics of the devices. P⁺ and n⁺ spin-on coated layers were then deposited on the front and backside of the device in order to provide good electrical connections to the APDs. Passivation was then applied and the devices were packaged.

3. Planar APD Packaging

Our typical method for packaging planar processed APDs utilizes a "flip chip" approach (see **Figure 14**). Alumina substrates, with appropriate feed-through connectors, are joined to the APD chip using a combination of mutually compatible silver filled and underfill epoxies. The silver epoxy bumps are used to make electrical connection between the APD contacts and the pins on the alumina substrate. The resulting space between the APD chip and the alumina substrate is then filled

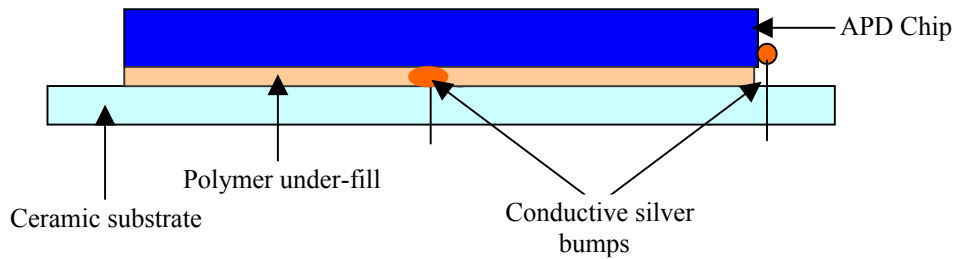


Figure 14. Schematic diagram of polymer "flip-chip" approach for packaging APDs. The top contact is routed to the back via the edge as shown here.

with a non-conducting epoxy to provide mechanical support to the APD chip. Two electrical connections for the front and the back of the APD are provided on the backside of the alumina substrate in form of pins as shown in **Figure 14**. The front connection is routed via the device edge to the backside of the ceramic substrate.

While the basic scheme was similar for packaging the very large APDs that we built in the Phase I project, additional considerations were required. In order to achieve very low noise with these large APDs, they need to be cooled to liquid nitrogen temperature. As a result, the packaging design must be such that the devices can be cycled between room temperature and 77 °K without any mechanical damage to the APD chips due to thermal stresses. As result, the packaging design was modified. For the very large APDs developed in the Phase I program, aluminum nitride substrates are used in place of the alumina ones. Although AlN is somewhat more expensive material than alumina, its thermal expansion coefficient matches that for silicon very well and its thermal conductivity is substantially superior to that of alumina. For underfill, we have used a newly available boron nitride filled material which creates a low stress bond with excellent thermal conductivity, assuring uniform cooling of the APD and its substrate. Since BN filled film requires a high temperature cure, silver filled polyimide was used in place of silver epoxy for making electrical connections. One 45 cm² APD packaged in this way has been cycled between room temperature and 77°K more than dozen times with no degradation in performance. These packaged

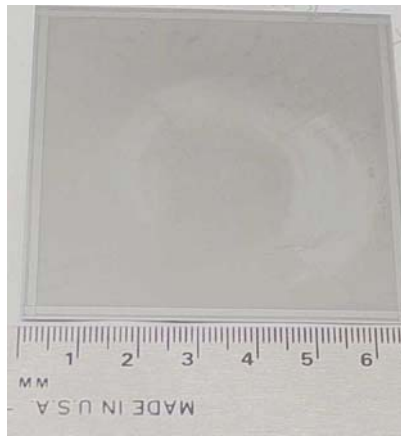
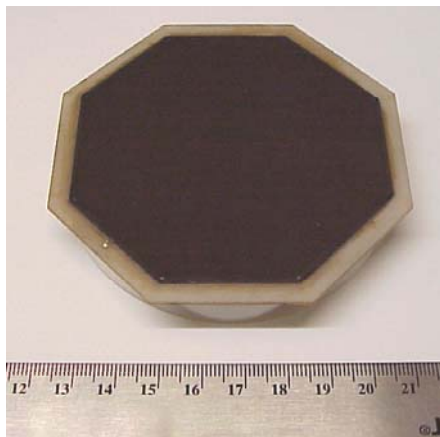


Figure 15. Photographs of an octagonal 45 cm² (left) and a square 40 cm² (right) planar APDs fabricated at RMD.

detectors can sustain cycling across an astounding range of 77 °K and 673 °K and could probably be cooled further. Thus, the packaging scheme that we have developed for the large APDs appears to be very robust and allowed us to evaluate the performance of the large APDs over a wide range of thermal conditions.

Figure 15 shows photographs of 40 cm² and 45 cm² planar

APDs, which are the largest APDs produced in the world so far.

B. BASIC APD EVALUATION

Once the large APD were fabricated, we characterized their performance by measuring important APD properties such as gain, noise, quantum efficiency and timing response. The measurements reported in this section were performed at $-40\text{ }^{\circ}\text{C}$ or at room temperature. Additional measurements of gain and noise were also performed upon cooling the large APDs to liquid nitrogen temperature, which are covered in a later section.

1. Gain and Noise Measurements

Extensive testing of the large APDs was conducted in the Phase I project. One of the first tasks was to evaluate the gain and noise behavior of these APDs. The basic approach for measuring noise and gain involved irradiating an APD with pulsed light (from an LED) and recording the pulse amplitude first at low bias (200-500 V) which represents the unity gain value. Next, the bias is increased and the pulse amplitude is monitored to determine the gain at each bias value. The noise is monitored at the same time by acquiring an ^{55}Fe spectrum to calibrate the energy scale and then recording an energy spectrum of an injected electronic pulse on the calibrated energy scale. By measuring the width of the electronic test pulse peak in the energy spectrum, the noise of device is estimated (in eV or electrons).

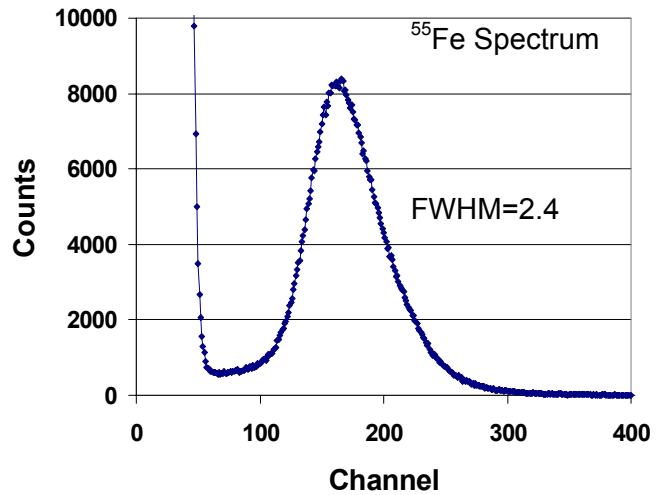


Figure 16. ^{55}Fe spectrum recorded with a 45 cm^2 APD at $-40\text{ }^{\circ}\text{C}$. The resolution of the 5.9 keV X-ray peak is 2.4 keV (FWHM).

These measurements were conducted for the 45 cm^2 octagonal APD at $-40\text{ }^{\circ}\text{C}$. An ^{55}Fe

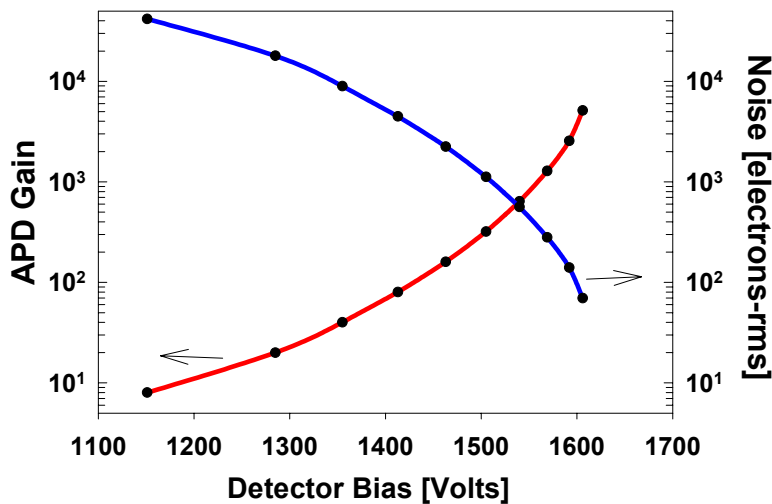


Figure 17. Gain and noise versus bias for a 45 cm^2 planar APD at $-40\text{ }^{\circ}\text{C}$. As seen in the figure, gain of 5000 and noise of 70 e^- (rms) have been recorded.

spectrum (5.9 keV photons) recorded with the 45 cm^2 APD is shown in **Figure 16**. The resolution of 5.9 keV X-rays was measured to be 2.4 keV (FWHM) in this study. Gain and noise of the 45 cm^2 APD as a function of applied bias (at $-40\text{ }^{\circ}\text{C}$) are shown in **Figure 17**. As seen in the figure, the gain of the device approaches ~ 5000 while the corresponding noise is 70 electrons (rms). These studies confirm that the large APDs that we fabricated in the Phase I project are indeed capable of

providing high gain, a characteristic of the deep diffused APD design. Furthermore, upon modest cooling to temperatures that can be achieved with thermoelectric coolers, low noise and low energy X-ray detection can be achieved with the large APDs. Measurements of gain and noise as well as optical detection with the 45 cm² APD at 77 °K are reported in a later section of this report.

2. Quantum Efficiency Measurements

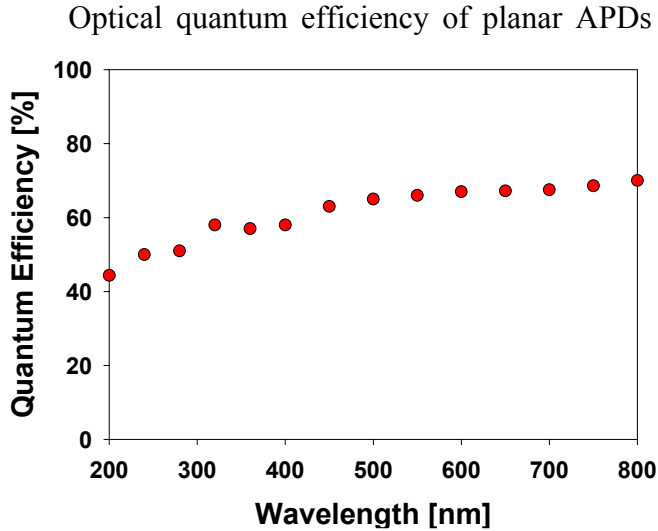


Figure 18. Quantum efficiency versus wavelength for planar APDs.

Optical quantum efficiency of planar APDs has been measured in the 200 nm to 800 nm wavelength region in the Phase I project. The measurement was performed in photovoltaic mode by recording the photocurrent produced by the APD in response to light from a grating monochromator. The current was calibrated to compute absolute quantum efficiency using a standard visible light reference photodiode calibrated for responsivity in A/W. The results are shown in **Figure 18**. The quantum efficiency of the planar APDs is about 40-70% in the 200-800 nm wavelength region, which is significantly higher than the quantum efficiency of PMTs. Even higher quantum efficiency

should be achievable in the Phase II project as the APD front surface is optimized and an anti-reflection coating is deposited for the desired wavelength region. The high quantum efficiency of planar APDs at 200 nm is particularly impressive and the result indicates that APDs can be used for calorimetry based on scintillation from liquid noble gases (for example, liquid Xe). A more detailed evaluation of the quantum efficiency of planar APDs in deep ultra-violet region that covers wavelengths lower than 200 nm will be carried out in the Phase II project.

3. Timing Response of Large APDs

Risetime of the large planar APDs was also investigated. The experiment involved irradiating the APD with 5.5 MeV alpha particles (²⁴¹Am source). The resulting signal from the APD was recorded directly on a digital scope with 50 Ω input impedance without any further amplification or shaping (see **Figure 19**). The risetime of such a pulse was measured to be < 2 ns, indicating that large APDs are capable of providing fast response. It should be noted that direct measurement of the APD response on a digital scope with 50 Ω input impedance represents a voltage sensitive amplification scheme, where the effect of the device

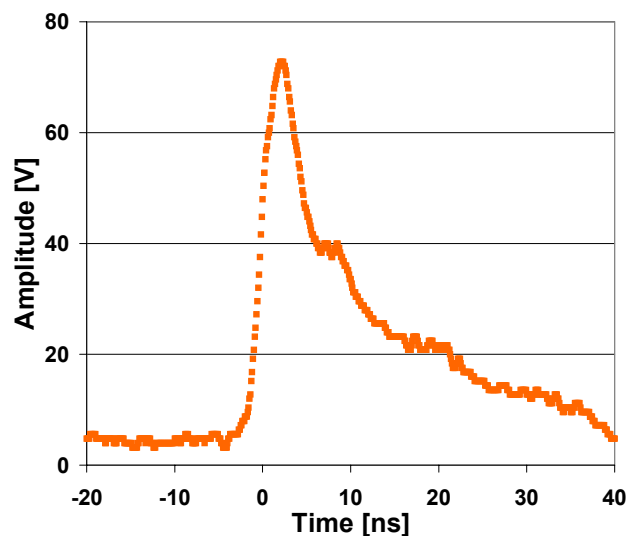


Figure 19. Timing response of a 45 cm² planar APD upon exposure to 5.5 MeV α-particles. The risetime was measured to be <2 ns.

capacitance on the timing response is minimal. This behavior is in sharp contrast to the traditional charge sensitive preamplifiers, where the input capacitance has a strong effect on the timing response. For traditional charge sensitive preamplifiers, the timing response becomes slower as the capacitance of the detector increases. Since the large devices that we are exploring in the proposed effort have high capacitance, voltage sensitive preamplifiers may be better suited, especially for applications where fast response is required. We will explore this issue in greater detail in the Phase II project.

C. SCINTILLATION SPECTROSCOPY WITH LARGE APDS

Based on the gain, noise and quantum efficiency measurements, it is clear that the large planar APDs can be used for scintillation spectroscopy. Evaluation of the large planar APDs for scintillation studies was carried out in the Phase I program. A 45 cm² planar APD was coupled to a CsI(Tl) scintillator (38 mm diameter, 25 mm tall) and irradiated with 662 keV photons (¹³⁷Cs source). Standard nuclear pulse processing electronics were used in this experiment. A ¹³⁷Cs γ -ray spectrum collected in this manner with the APD cooled to -40 °C is shown in **Figure 20**. The resolution of the 662 keV photopeak was estimated to be 10% (FWHM) in this study which is very encouraging. This study indicates

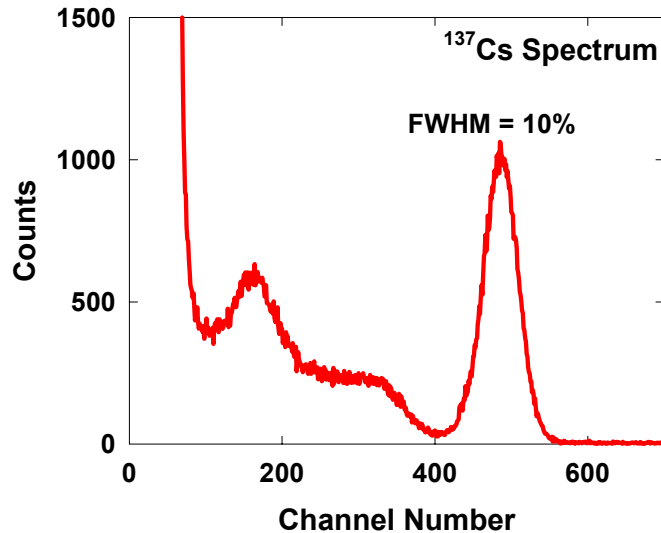


Figure 20. ¹³⁷Cs spectrum collected with a 45 cm² planar APD coupled to a CsI(Tl) scintillator at -40 °C. The resolution of the 662 keV photopeak is estimated to be 10% (FWHM) in this study.

that with modest cooling the large planar APDs that we are investigating in the proposed effort would be suitable for gamma ray spectroscopy based on scintillators. This investigation will be continued in the Phase II project using a variety of scintillators.

D. EVALUATION OF LARGE APDS AT LN₂ TEMPERATURE

Once the basic evaluation of the large APDs was completed, we characterized their performance at 77 °K. The purpose of this study was to reduce the dark noise of the large APDs considerably and evaluate the possibility of using them for detection of low intensity optical signal. In order to perform these studies an experimental setup was first built to allow cooling of the large APDs to 77 °K in a reproducible manner. Gain, dark current and electronic noise of the large APDs were evaluated, and detection of low intensity optical signal was then demonstrated.

1. Experimental Setup

Figure 21 shows a schematic representation of the experimental setup used in this study. The setup consists of an APD test chamber, a light source and the readout electronics.

a. Test Chamber

The test chamber consisted of a die cast aluminum housing (4.75 inches x 7.375 inches x 2 inches high), which contained the APD under test. The APD was supported by nylon screws, which

touched the APD at only a few small points, insuring that the cooling of the APD was done convectively and radiatively rather than conductively. A very small amount of dry nitrogen gas (approximately 0.2 CFH) flowed from a cylinder into the chamber and out of it through small light-tight openings at the opposite sides of the test chamber. This insured that a small positive pressure was maintained with the intention of keeping moisture out. The APDs contacts were attached to wires in the test chamber and the APD output was routed through the chamber wall to the readout electronics via a coaxial cable. This cable was kept short (< 1ft) to minimize electronic noise. One end of an optical fiber was mounted onto the cover of the die cast aluminum test chamber. When the cover was secured to the test chamber, this optical fiber was aimed at the APD (approximately 1 inch away) and was used to supply optical test pulses to the APD. The aluminum test chamber was screwed to a 0.5 inch thick aluminum plate into which was inserted a K-type thermocouple which monitored the temperature of the test chamber. It was assumed throughout the experiments that the thermocouple temperature was equal to the APD temperature because sufficient time was allowed for all measurements for the system to reach equilibrium. Because many thermocouple meters do not work well at low temperatures, we took the approach of connecting a ‘reference’ thermocouple in series with the test thermocouple, and the reference thermocouple was placed in an ice water bath. A sensitive voltmeter was used to measure the voltage across the thermocouples, and this voltage was converted to degrees Celsius using known conversion tables. The test chamber was placed in a stainless steel pan, which was itself placed in a Styrofoam box. Liquid nitrogen was poured into the stainless steel pan to cool the chamber.

b. Light Source

The light source was a pulsed LED with peak wavelength of 590 nm. The electronic pulse that was used to power the LED had a 300 ns duration and a

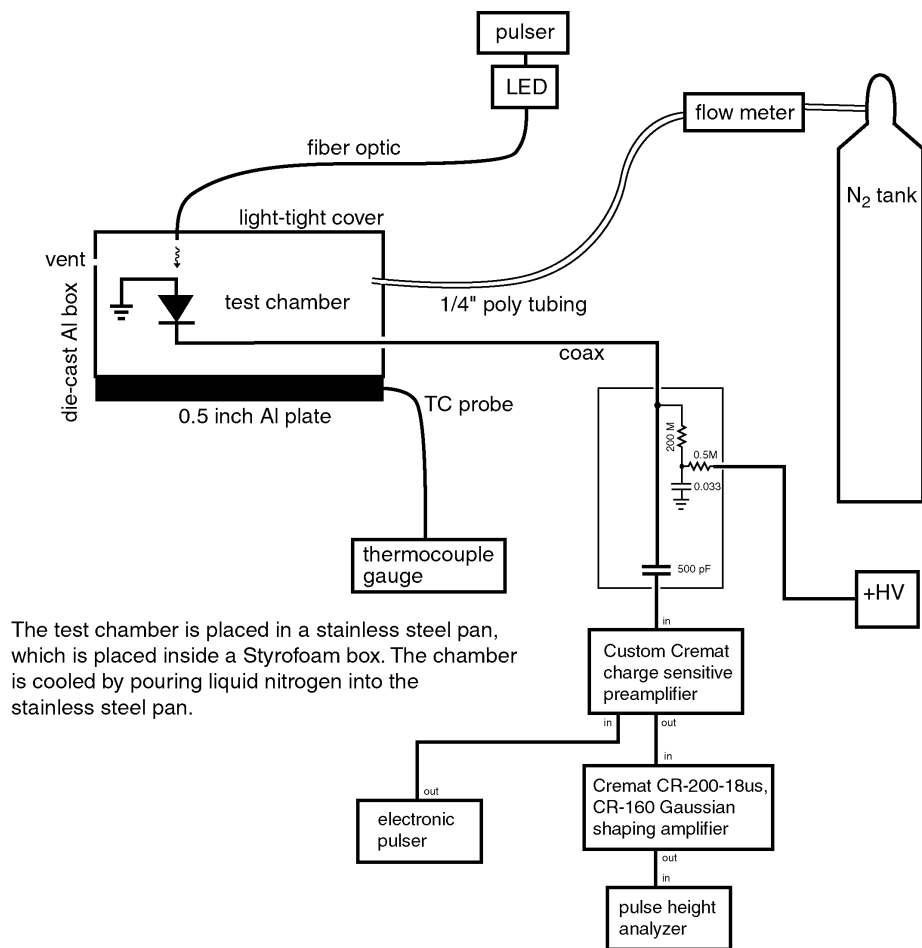


Figure 21. Schematic representation of the experimental setup used in the Phase I project to evaluate the performance of the large APDs at 77 °K.

repetition rate of 600 Hz. The LED irradiated a fiber optic cable, which terminated in the APD test chamber and was aimed at the APD under test (at a distance of about 1” from the APD).

c. Electronics

For the evaluation of the cooled APDs we used a charge sensitive preamplifier (Cremat #110) and a semi-Gaussian (4th order integration) shaping amplifier (Cremat CR-160) along with a pulse height analyzer, high voltage power supply and an electronic test pulser. The detector was AC-coupled because the APD leakage current can become significant at higher temperatures and saturate the preamplifier if it were to be DC coupled. In the preliminary experiments, the coupling capacitors were placed near the detector in the test chamber. It was found that these high voltage ceramic capacitors could not withstand the repeated temperature cycling and as a result the capacitors were placed within the preamplifier housing outside the cryostat in the final setup.

2. Experimental Procedure and Results for Small APDs

To measure the APD dark noise, the APD was first biased to 500 volts, where the APD gain is assumed to be 1. The pulsed LED irradiated the APD and the pulse height was measured using the pulse height analyzer. By recording the position of the LED peak as a function of bias, the gain versus bias relationship for the large APD was determined. The LED was then turned off and the energy scale was calibrated (in eV and then in electrons) by irradiating the APDs with an ⁵⁵Fe source that emits 5.9 keV X-rays. By recording an electronic test pulse spectrum on a calibrated energy scale, the noise of the APD was estimated.

Prior to the measurements with the 45 cm² APDs, experiments were performed with a smaller 2x2 mm² APD to check the apparatus and the experimental procedure. For these small APDs, noise and optical sensitivity experiments were performed at 77 °K. The 2x2 mm² APD was biased to 1430V, where the gain was measured to be 1400. A low intensity LED pulse irradiated the APD on a calibrated energy scale. The LED was turned off and an electronic pulser was injected to the preamplifier input, resulting in the electronic test pulse peak in the spectrum. The measured width of this electronic test pulse peak indicated a dark noise of 0.26 electrons (rms). Successful detection of an optical pulse with intensity corresponding to generation of ~10 photoelectrons/pulse in the 2x2 mm² APD was accomplished. It should be noted that no particular optimization was carried out in this study and the actual noise of the small APD is probably lower. However, this basic study allowed us to verify that the experimental setup was functioning as planned.

3. LN₂ Studies with 45 cm² APDs

a. Dark Current Measurements

In the case of the large (45 cm²) APD, measurements of dark current were performed at a number of different temperatures, spanning the range of 77°K to 250°K. In order to perform these measurements as a function of temperature, the test chamber was first cooled to its coldest (LN₂) temperature. Dark current measurements were made at this temperature, and at warmer temperatures as the test chamber slowly warmed to room temperature (over the course of several hours). The value of the APD dark current is highly dependent on the APD gain, so efforts were made to keep the gain constant as the dark current was measured at varying temperatures. We found that the 45cm² APD could be reliably operated at a gain of 1000 at all temperatures within the tested range (-196°C to -25°C). **Figure 22** shows the variation of the APD operating bias as a function of temperature required to maintain APD gain of 1000 in this study.

The dark current of the 45 cm² APD has been measured as a function of temperature (over 80 °K to 250 °K range) at a constant gain of 1000 (obtained by varying the APD bias as shown in **Figure 22**) and the resulting plot is shown in **Figure 23**. As seen in the plot, the dark current is very low (~30 pA) for the 45 cm² APD at LN₂ temperature, indicating that very low noise should be achievable.

b. Gain Versus APD Bias at 77 °K

The gain versus operating bias relationship for the 45 cm² APD has been measured at temperature of 77 °K. The measurement was performed using the methodology described earlier. The

APD was irradiated with an optical pulse, first at low bias (~500 V). The measured signal amplitude corresponds to a unity gain value. The subsequent signal amplitude measurements at higher bias are normalized with respect to this unity gain value to determine the gain versus bias relationship. The results are shown in **Figure 24** and indicate that very high gain (~10⁴) can be

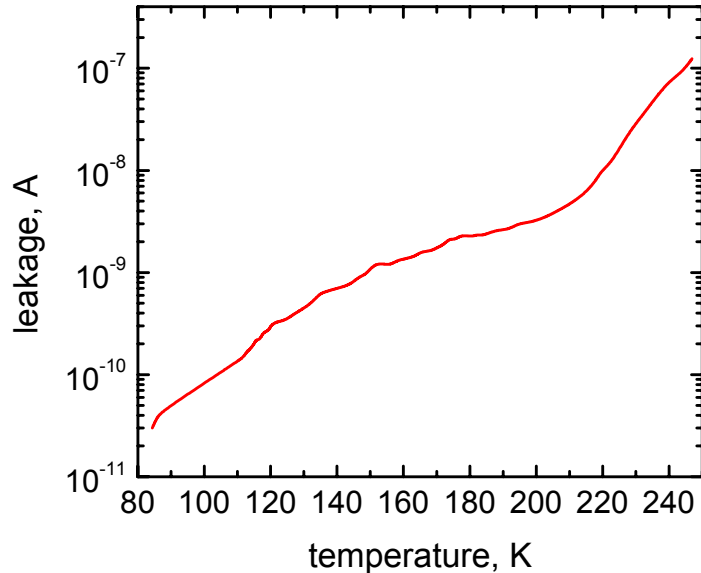


Figure 23. Leakage current versus temperature for a 45 cm² APD at a constant gain of 1000.

the electronic test pulse peak in the spectrum. The measured width of the electronic test pulse peak indicated that the APD noise was ~0.8 electrons (rms).

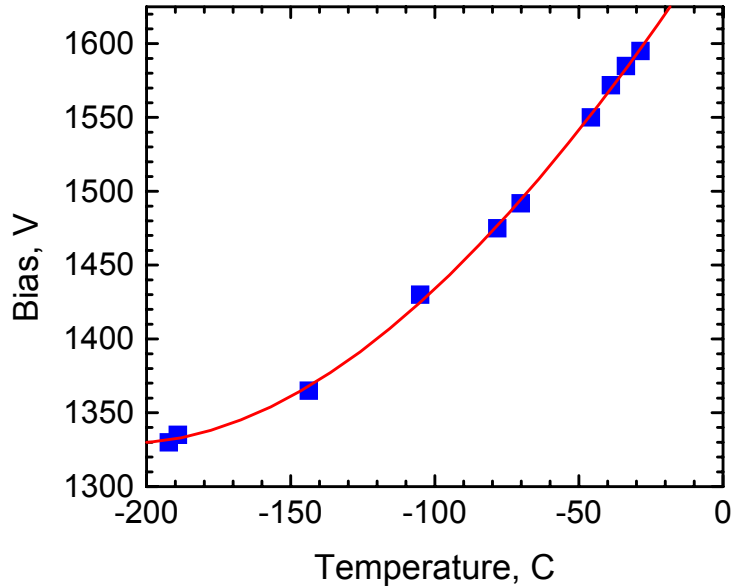


Figure 22. APD bias a function of temperature, required to maintain the gain of 1000 for a 45 cm² planar APD.

achieved with the 45 cm² APD at 77 °K. The optimal gain where the noise is minimized and the device is stable was found to be ~1000 to 2000.

c. Noise and Optical Sensitivity Studies

The final set of measurements in the Phase I project involved measurement of noise of the 45 cm² APD at 77 °K. The APD was operated at gain of ~1000. An ⁵⁵Fe spectrum (5.9 keV X-rays) was used to calibrate the energy scale (in electrons). Next, the APD was irradiated with a low intensity LED pulse and the resulting pulse height spectrum was collected on the calibrated scale. The LED was turned off and an electronic pulser was injected into the preamplifier input, resulting in

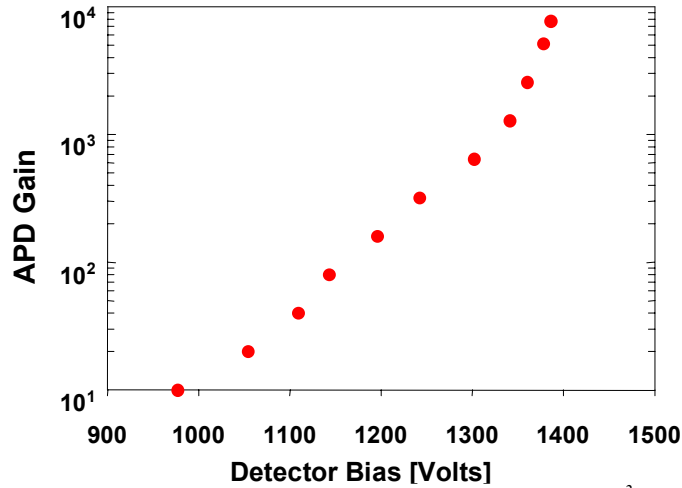


Figure 24. Gain versus bias relationship for a 45 cm² APD at a temperature of 77 °K.

at 77 °K are very encouraging. Further optimization of the APDs and their electronic readout setup in the Phase II project is expected to provide even lower noise. Thus, these large APDs are capable of low intensity optical detection and can play an important role in future high energy physics experiments. Overall, based on high gain, low noise, fast response and high optical quantum efficiency of these 45 cm² APDs, which are the largest functioning APDs in the world, the feasibility of the Phase I research was adequately demonstrated.

Successful detection of an optical LED pulse with intensity of <8 photoelectrons/pulse with the 45 cm² APD is achieved as shown in **Figure 25**. By gating the LED pulse (using an electronic counter), the detection efficiency of the 45 cm² APD at 77 °K for the LED pulse with intensity of ~8 photoelectrons per pulse was estimated to be > 95%. These studies were performed in collaboration with the BNL team.

Overall, the low noise (of ~0.8 electrons-rms) and successful detection of low intensity optical signal (<8 photoelectron/pulse) with the 45 cm² APD

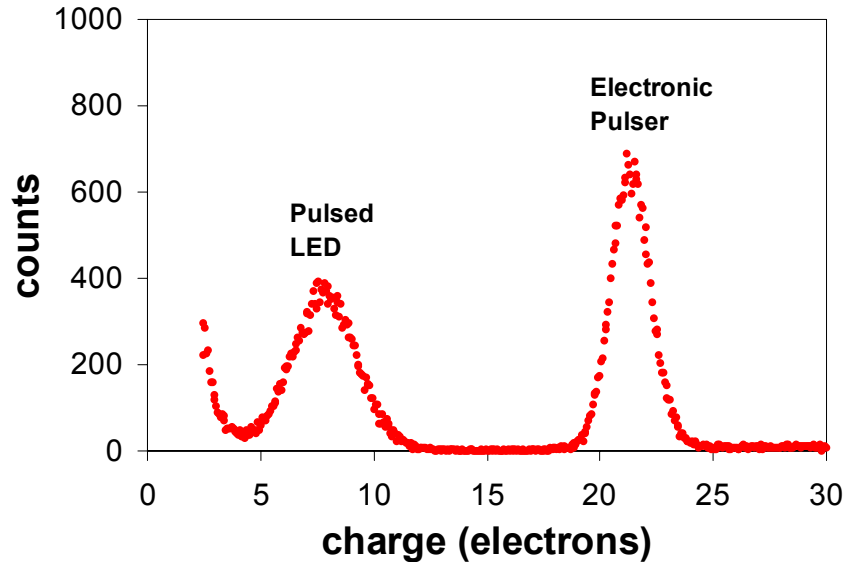


Figure 25. Detection of an optical pulse (<8 photoelectrons per pulse) and an electronic test pulse with a 45 cm² APD at 77 °K. The noise of the APD is ~0.8 electrons (rms).

2.3. THE PHASE II PROJECT:

I. PHASE II TECHNICAL OBJECTIVES

The Phase II research will build on our successful Phase I project and will focus on detailed investigation of the planar technology for fabrication of very large APDs. During the Phase II project, we plan to fabricate APDs as large as 60 cm² in area (with octagonal geometry) for eventual use in high energy physics systems such as water Cherenkov and liquid Xe detectors. Large APDs with appropriate sizes will also be built and evaluated for calorimetry experiments such as KOPIO and MECO during the Phase II project.

In order to achieve these objectives, the design of the planar APDs will be optimized to improve their quantum efficiency, dark current, noise and timing response. This will involve modifications of the front surface layer, thickness of the neutral p-type (or drift) region, and the thickness of the undepleted n-layer on the back. To obtain high quantum efficiency with APDs in a specific wavelength region (for use with scintillation crystals or fibers), use of anti-reflection coating will be explored. Such APDs will be packaged on ceramic substrates such as alumina and AlN using the polymer based flip-chip process. Extensive characterization of large APDs will then be carried out. This will involve measurement of gain, noise, quantum efficiency and timing response of the large APDs. Spatial variation of gain will also be determined in the Phase II project. Direct detection of X-rays and charged particles with the large APDs will be carried out. Scintillation spectroscopy will be conducted using the large APDs coupled to inorganic scintillators such as CsI(Tl). Electronic readout design will be optimized for these large APDs (with high capacitance) to achieve low noise and fast response. Both charge sensitive and voltage sensitive preamplifier designs will be investigated. The large APDs will be cooled to LN₂ temperature and their gain, noise as well as optical sensitivity will be measured. Applicability of these large APDs to high energy physics experiments such as water Cherenkov detection and KOPIO and MECO will be investigated by our collaborators at the Brookhaven National Laboratory (Dr. Laurence Littenberg, Dr. Michael Sivertz, Dr. Milind Diwan and Dr. Peter Yamin). Dr. Reucroft at the Northeastern University will participate in basic APD evaluation including low temperature sensitivity studies in the Phase II project. Dr. Cushman at the University of Minnesota will evaluate the large APDs as UV sensors in liquid Xe detectors in the Phase II project. Thus the technical objectives for the Phase II research are:

1. Optimize the planar process to allow fabrication of very large APDs (up to 60 cm² with octagonal design). Also fabricate APDs with sizes suitable for KOPIO (up to 2x2 cm²) and MECO (up to 1.5x3 cm²) experiments.
2. Explore issues such as front surface processing, thickness of the drift region and the thickness of undepleted n-layer on the back. Evaluate use of silicon with resistivity in 10-30 Ω-cm range.
3. Package the large planar APDs using the polymer flip chip process. Optimize the front end electronics for these large APDs with high capacitance. Explore both charge sensitive and voltage sensitive preamplifier designs.

4. Perform evaluation of the large area APDs including measurement of quantum efficiency, gain, noise and timing response. Map out gain uniformity of large devices in collaboration with Canberra Industries and Dr. Reucroft at the Northeastern University.
5. Perform direct X-ray and charge particle detection with the large APDs. Also, perform scintillation spectroscopy by coupling these large APDs to scintillators.
6. Cool the large APDs to LN₂ temperature and measure gain, noise and sensitivity for low intensity optical signal in collaboration with Dr. Reucroft at the Northeastern University.
7. Evaluate these large APDs from view-point of eventual use in high energy physics experiments such as water Cherenkov detection at BNL.
8. Evaluate large APDs for KOPIO and MECO at BNL
9. Evaluate large APDs as UV sensors in liquid Xe detectors in collaboration with Dr. Cushman at the University of Minnesota.

The Phase II research will be carried out as a collaboration between RMD and BNL team of (Dr. Laurence Littenberg, Dr. Michael Sivertz, Dr. Milind Diwan and Dr. Peter Yamin). Dr. Stephen Reucroft at the Northeastern University and Dr. Priscilla Cushman at the University of Minnesota will also collaborate on the Phase II project. Canberra Industries (Meriden, CT) will also participate in the Phase II project using their own resources. Canberra will participate in optimization of the front APD surface, and in evaluation of APD performance. Canberra will also help in packaging design and electronic readout aspects.

II. PHASE II WORK PLAN

The goal of the Phase II project is to advance the promising, large area (up to 60 cm²), planar APD technology for eventual use in high energy physics experiments. In order to achieve this goal, the Phase II research will cover several diverse areas. The design of the large area planar APDs will be examined and extensive evaluation of the basic properties of large APDs will be conducted. The large APDs will be cooled to LN₂ temperature and their gain, noise and optical sensitivity will be measured. Applicability of these large area APDs to various high energy physics experiments such as water Cherenkov detection and calorimetry will be examined.

A. SIMULATION STUDIES

During the Phase II project, we will conduct extensive simulation studies of the planar APDs which are based on the deep-diffused design. **Figure 26** shows a schematic representation of various regions in a deep-diffused APD. As seen in the figure, the conversion of incident optical photons to current output at the APD anode may be separated into following four processes:

1. Photon absorption in the top p-type layer and generation of photoelectrons.
2. Transport of the minority carrier photoelectrons to the avalanche gain region.
3. Multiplication in the avalanche gain region and subsequent transport of the photoelectrons to the n-type region where they are majority carriers.
4. Majority carrier transport in n-type back layer to the anode.

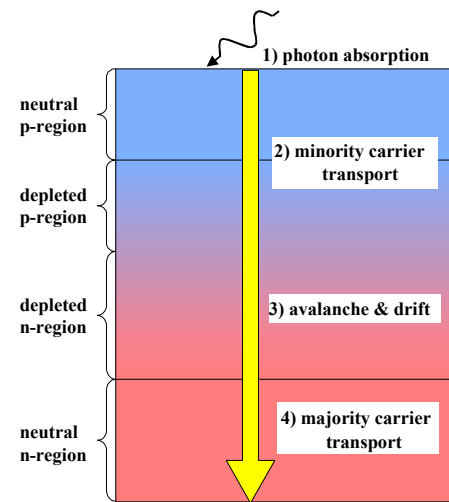


Figure 26. Visualization of current through a deep-diffused APD upon interaction with an optical photon.

The simulation studies in the Phase II project will build upon the tools that we have already established in the Phase I project, but will be more extensive. Specifically, the doping profile, estimated using the method described earlier (in the Phase I Final Report) will be used to compute the electrical properties of the APDs such as electric field profile and depletion region width. Initially, in the Phase II project we will compute the p-type doping profile due to deep diffusion of gallium and aluminum in n-type NTD silicon with varying resistivity. This will be performed using simulation approach that was described earlier. These doping profiles will be the input parameter along with the device geometry and biasing conditions for a semiconductor device program developed at RMD. From the dopant concentration profile, the electric field profile can be estimated by integrating Poisson's equation. The size of depletion region on the p-side and n-side of the junction can be determined on the basis of the charge neutrality requirement [Sze].

For RMD's typical diffusion of p-type dopants (Ga and Al) into a NTD doped n-type silicon wafer with 30 Ω-cm resistivity (for which the dopant concentration profile was shown earlier in **Figure 11**), the computed electric field profile (at gain of 1000) and depletion region width (as a function of bias) are shown in **Figure 27**. As seen in the figure, the region with high electric field is

wider in n-region than in p-region. Furthermore, the high electric field region for this deep diffused APD design is broad as opposed to that for “reach-through” APD design. This allows the deep diffused design to provide high gain with low multiplication noise [Redus, Moszynski]. Similar analysis will be carried out for deep-diffused APDs fabricated from silicon with varying resistivity as well as processing and operating conditions for optimization of the APD design for large area devices. Speed of response of the APDs depends on maintaining high electric field across the APD width and will also be analyzed in this study.

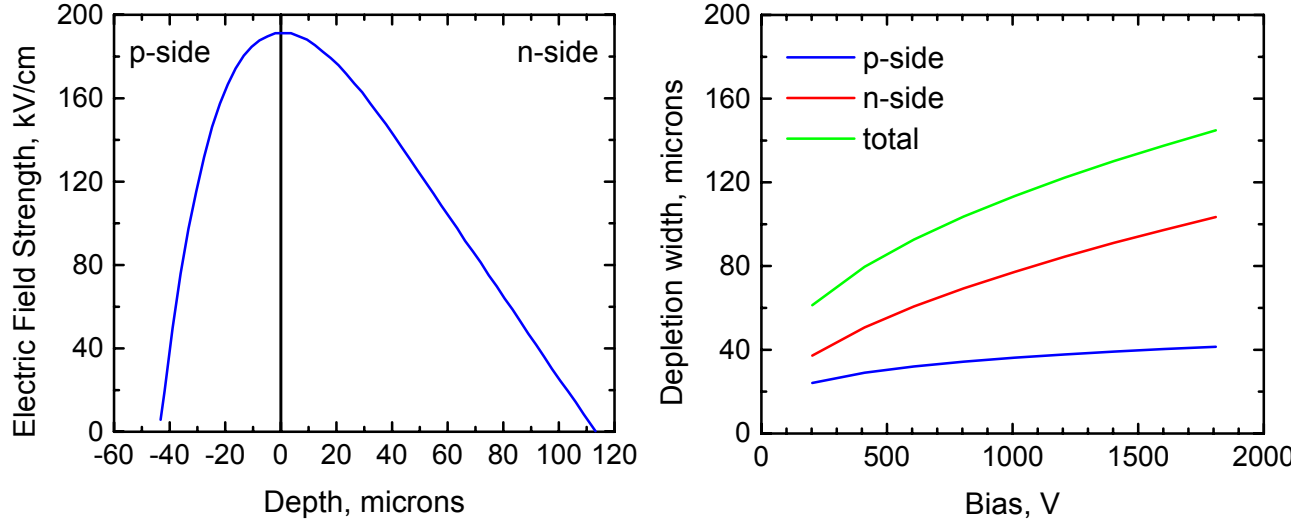


Figure 27. Calculated electric field profile at APD gain of 1000 (left) and depletion width as a function of bias (right) for a deep diffused APD fabricated from a 30 Ω -cm NTD Si wafer. The dopant concentration profile upon RMD’s deep diffusion of p-type Ga and Al in the NTD n-type Si wafer was shown earlier in **Figure 11**.

In addition to this bulk device analysis, we also plan to study the electric field near the front electrode that has thin p^+ layer due to surface boron doping. Since the surface field directly affects the charge collection at surface, which in turn has direct relationship with the quantum efficiency in the blue-UV region, this analysis will help us in optimization of the front p^+ layer processing.

B. LARGE AREA APD FABRICATION

An important emphasis of the Phase II project will be on the optimization of various design and fabrication steps of the planar process (based on the insight gained from the simulations) to produce high gain APDs in very large sizes (up to 60 cm^2 with octagonal design). Large APDs with sizes suitable for KOPIO (up to 2x2 cm^2) and MECO (up to 1.5x3 cm^2) will also be built.

NTD doped n-type silicon wafers in 4” diameter size with resistivity of 30 ohm-cm (which is the standard silicon resistivity for our process) will be purchased from Topsil. Deep diffusion, and polishing (both front and back p-layers) will then be performed in a similar manner as in the Phase I research (see **Figure 13**). Some wafers with lower resistivity (in 10-20 Ω -cm range) will also be used in order to improve timing response of the large APDs. Lower silicon resistivity leads to smaller depletion region width and higher electric field within the bulk, which can lead to improved timing performance. We will also reduce the thickness of the undepleted n-region on the backside of the APD. Initial indications are that this processing improves the APD timing response (see **Figure 28**) as well as reduces the APD noise. The improvement in fall time (shown in **Figure 28**) may be useful in experiments like KOPIO and MECO where very high count-rates are expected.

The front p^+ layer fabrication may be modified based on our simulation studies in order to optimize the quantum efficiency in the blue-UV region. This may involve modification of the standard boron diffusion profile or we may use alternative methods to incorporate boron such as low energy ion implantation followed by pulse laser annealing to create a very thin p^+ layer [Shah 97]. We have performed some early evaluation of this technique on the planar APDs earlier and we will explore it in more detail in the Phase II research. In addition, we will also experiment with the thickness of the p-type neutral (or drift) region, which affects charge collection properties, thereby influencing the optical quantum efficiency. The thickness of the front p-type neutral region (see **Figure 26**) is also expected to influence timing response of the APDs, with thinner drift region expected to provide faster response and lower noise. For example, in a recent study, by reducing the thickness of front p-type neutral region from 15 μm (which is the standard value for planar APDs) to $<5 \mu\text{m}$, we have achieved risetime that is ~ 8 times faster. Quantum efficiency (in blue-UV region) and noise also improved upon such reduction in the thickness of the front p-type neutral region. Hence, we will conduct an investigation of the optimal thickness of the front p-type neutral region. Resistance of the front and back contacts on APD will also be reduced to improve the timing response of large APDs. During the Phase II project, we also plan to fabricate isolation grooves on the backside of the APD as shown in **Figure 29**. These isolation grooves are expected to function as guard rings that reduce the surface leakage current in the devices. Since the surface leakage current can be significant in the large APDs, the new design is expected to reduce the APD noise.

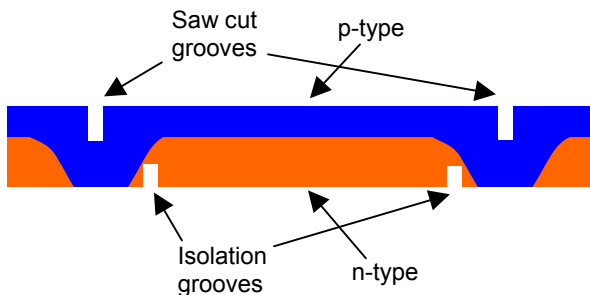


Figure 29. Schematic of an APD with isolation grooves on the backside that function as a guard ring to reduce surface leakage current in the APDs.

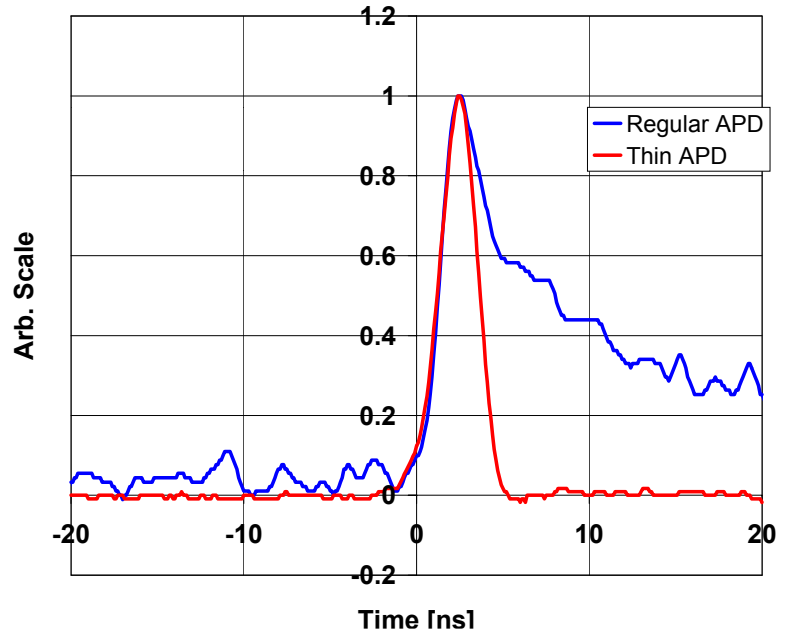


Figure 28. APD time-response upon exposure to 5.5 MeV α -particles, with the signal observed on a digital scope with 50Ω input impedance. Time response is shown for a typical planar APD and for an APD with reduced thickness on the n-side.

In order to improve optical response and quantum efficiency of planar APDs, we will also apply anti-reflection coating (ARC) designed to minimize reflection at desired wavelengths. In applications where scintillators and fibers are coupled to APDs, optical coupling glue is typically used at the interface. Bare silicon has significant reflection, and hence ARC is required to efficiently collect light. An important requirement for ARC is high refractive index. Indeed, using the same refractive index

for the ARC and the optical coupling glue will result in a continuum having the same refractive index. Optical glues typically have refractive index around 1.4-1.5. For this reason, SiO₂ cannot be used together with optical glue because of the proximity of its refractive index with that for a typical glue. We have chosen Ta₂O₅ (with refractive index ~2.2 at 400 nm) as an ARC for APDs. Ta₂O₅ has been used successfully as an anti-reflection coating on Si diodes with excellent results (reflection losses of <3% at desired wavelength) [Evrard]. The optimum ARC thickness d_{opt} can be calculated from the expression:

$$d_{optimum.ARC} = \frac{\lambda_{incident.photon}}{4.n_{ARC}}$$

where n_{ARC} is the refractive index of the ARC coating and λ is the wavelength of incident light. For a given wavelength of interest, the thickness of the ARC (Ta₂O₅) coating can be estimated using the equation presented above. At RMD, we have already deposited with such ARC coatings on APDs, using a spin-coating method. A quantum efficiency plot for an APD processed with a Ta₂O₅ ARC layer (~40 nm thick to optimize the APD response at 370 nm) is shown in **Figure 30**. As seen in the figure, excellent quantum efficiency is observed in the blue region (~80% at 400 nm). We plan to deposit such Ta₂O₅ layers on APDs, optimized for selected wavelengths (for example, ~500 nm where the emission from fibers to be used in KOPIO occurs or 420 nm for peak emission from

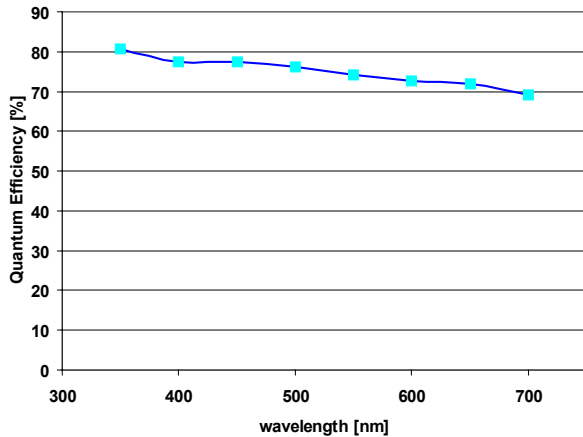


Figure 30. Quantum efficiency of APDs with anti-reflection coating (optimized for 370 nm) being developed at RMD.

PbWO₄ scintillators to be used in MECO) in the Phase II project. We expect the quantum efficiency of APDs to increase substantially as a result of this effort.

The large devices will be packaged in a similar manner as in the Phase I project. In order to allow cooling to LN₂ temperature without mechanical damage due to thermal stresses, APDs will be packaged on AlN ceramic substrates using polymer flip-chip method. A BN based polymeric compound will be used as an under-fill material, while a silver filled polyimide will be used to make electrical connections between the substrate and the APD chip. This packaging scheme (shown in **Figures 14 & 15**) worked very well in the Phase I project and we were able to cycle large APDs between room temperature and 77 °K more than a dozen times without any degradation. Hence, we will continue the same approach to package the large APDs in the Phase II project.

For APDs to be used for water Cherenkov detection in Phase II, an additional consideration will be to develop a packaging scheme that can allow placing APDs in water. A simple housing design will be created to provide water and associated pressure protection for silicon APDs making use of existing commercially available materials. This design basically uses a sealed flange housing to store the APD. One end will be fitted with a quartz window to allow the optical photons to enter while the opposite end will be connected to a metal fitting that has a water-tight feedthrough that allows electrical connections to pass through. Where the quartz and metal feedthrough fittings mate with the flange on either end, o-rings will be used to completely seal the housing from water

leakage. Lastly, waterproof cabling and connectors will be needed to attach to the feedthrough at the back of the housing.

C. LARGE AREA APD EVALUATION

Extensive testing of large area APDs fabricated using the planar process will be conducted in the Phase II project by RMD in collaboration with Canberra and Dr. Reucroft at the Northeastern University. The studies presented in this section will be conducted with the APDs cooled in -25 to -40 °C range that can be achieved with thermoelectric cooling. Detailed evaluation of the APDs will also be carried out at LN₂ temperature, which is presented in a subsequent section.

1. Gain Characteristics

The gain of the large planar APDs will be measured in a manner similar to that used in the Phase I project. The gain measurement will involve recording a pulsed LED peak position first at low bias to measure the pulse height corresponding to unity gain. Next, LED pulse height will be recorded at higher bias values to compute gain versus bias relationship. We will conduct these measurements using APDs with different silicon resistivity in order to compare the gain achieved.

For the very large devices we will also perform a spatial mapping of gain in order to quantify

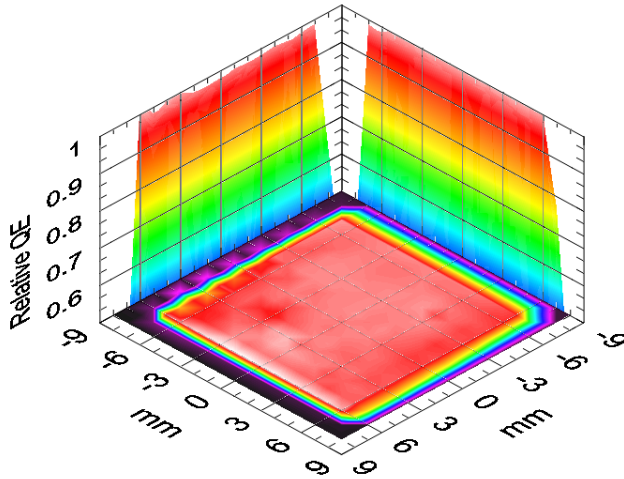


Figure 31. Uniformity of response for a 14x14 mm² APD, generated by scanning a 1 mm diameter optical fiber (illuminated with 550 nm light) across the APD surface. As seen in the figure, the full 14 x 14 mm² area of the device appears in red section of the response map, indicating that the optical response is high and uniform over the full area of the device.

variation of gain over large silicon surface. Since the spatial gain non-uniformity can act as a source of resolution broadening, these measurements will be very helpful in understanding the characteristics of the large devices. We have already performed similar measurements using a 14x14 mm² APD, where its surface was scanned with a 1 mm optical fiber illuminated with 550 nm light. The results are shown in **Figure 31** and indicate that the optical response of the full active area of the device is fairly uniform. The red section (which represents uniform, high response) is $\sim 14 \times 14$ mm², and the lower response (represented by yellow and green periphery around the red section) occurs when the fiber is passed over the APD grooves. The gain of the device was ~ 1000 in this study.

2. Electronic Noise Properties

A detailed study of the electronic noise of the large area, planar APDs is planned for the Phase II project. Dark noise measurements of the Phase II APDs will be made using methods similar to those used in Phase I. Low energy X-rays (5.9 keV photons) will be used to calibrate the energy scale and an electronic test pulse peak recorded on the calibrated scale will provide estimation of noise. The spectral characteristics of the measured noise will be analyzed in order to identify the principal noise sources in the detection system. This will be done at a variety of APD gains. From this information, the optimal APD gain will be determined. At the optimal gain, where the signal to noise ratio is maximum, we will also measure noise as a function of amplifier integration time. Using the noise data at different

integration times, we will estimate the individual noise components such as parallel thermal noise (or other parallel white noise sources such as ‘shot’ noise), series thermal noise, series ‘1/f’, and parallel ‘f’ noise [Radeka] using computer program already setup at RMD [Redus]. An equivalent circuit diagram for various noise sources in an APD coupled to a charge sensitive preamplifier is shown in **Figure 32**. For the large APDs that we are investigating in this project, the shot noise due to APD

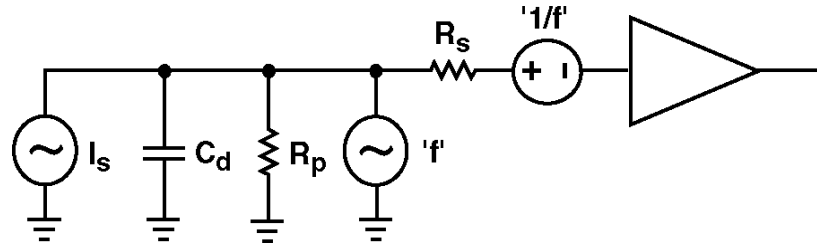


Figure 32. Circuit model for a generalized detector of capacitance C_d coupled to a charge sensitive preamplifier. The preamplifier is modeled as an ideal charge sensitive preamplifier, the APD is modeled as a capacitor, and the various dark noise sources in the system are combined into the four different current and voltage noise sources shown. Characteristics of both the APD and preamplifier are combined into each of the noise sources shown; none of them are due entirely to either the APD or preamplifier alone. For example, the value of R_p reflects a combination of the shot noise due to the properties of the APD and the feedback resistor in the preamplifier. Shown in the figure are the signal current source (I_s), detector capacitance (C_d), equivalent parallel thermal resistance (R_p), equivalent series thermal resistance (R_s), parallel ‘f’ noise current source, and series ‘1/f’ noise voltage source. APD ‘excess noise’ is excluded in this model – only dark (or electronic) noise sources are shown.

leakage current (modeled, in part, by the thermal current noise of an equivalent parallel resistor R_p in **Figure 32**) can be expected to be the dominant noise source at temperatures above $-50\text{ }^\circ\text{C}$. At lower temperatures, where leakage current (and thus shot noise) is relatively low, the noise due to the relatively large detector capacitance is expected to become the dominant noise source. This noise component is modeled by the thermal voltage noise of a resistor placed in series with the preamplifiers input (R_s in **Figure 32**).

3. Excess Noise Measurements

a. Overview of Excess Noise

In addition to the electronic noise discussed in the previous section, signals from APDs and other detectors with gain (such as PMTs) are also affected by distortions resulting from the charge multiplication process [McIntyre, Webb]. The avalanche gain of an APD is a consequence of the effect of *charge multiplication*: an incoming photon ionizes the silicon near the surface, producing a small amount of ionized charge. This charge is immediately accelerated by a strong electric field inside the APD and reaches sufficient velocity, whereby the charge multiplies through the effect of *impact ionization*. Because impact ionization is a stochastic process, identical consecutive signals incident on the APD will undergo slightly different levels of gain. Because each incoming signal pulse on the APD undergoes a slightly different gain, a pulse height spectrum taken using an APD detector will exhibit an additional broadening factor due to this affect.

This effect is traditionally referred to as ‘excess noise’, and quantified by the excess noise factor F , which is defined by: [Webb]

$$F = \frac{\langle M^2 \rangle}{\langle M \rangle^2}$$

where M is the average APD gain. F is known to be a function of gain: for unity gain detectors, F=1. For typical PMTs, F is ~1.4. In APDs, the excess noise factor (F) is dependent on the operating gain, and on other aspects of the APD, such as the doping profile. At moderate gains, F for RMD's APDs is ~2, which is much lower than that for other APDs (as discussed in a later section). The spectrum broadening for an APD-based detection system is given by: [Moszynski]

$$\sigma_{st}^2 = \sigma_n^2 + N_{eh}(F - 1) + \delta_{noise}^2$$

where σ_{st}^2 is the variance in the output signal, σ_n^2 is the variance due to the statistical error in the input signal, N_{eh} is the number of 'primary photoelectrons' created by the incoming photons and δ_{noise} is the electronic dark noise (discussed earlier). In cases of light detection, the first term in the above equation is determined by Poisson statistics ($\sigma_n^2 = N_{eh}$), so the above equation is reduced to:

$$\sigma_{st}^2 = N_{eh} F + \delta_{noise}^2$$

From this equation, we can see that for large signals (N_{eh} large), the spectrum broadening in an APD detection system is proportional to the square root of the incoming signal, as well as the square root of the excess noise factor F. To develop high performance APDs capable of low light detection and minimal spectrum broadening, we must strive not only to produce APD detection systems with low electronic noise, but we also need APDs operating with low excess noise factor F.

b. Excess Noise Dependence on the APD Doping Profile

The excess noise factor F in an avalanche photodiode is known to depend on the APD's doping profile, as well as its operating gain. Because we are interested in developing APDs capable of high resolution spectral performance, we are interested in determining the doping profile which minimizes the excess noise factor F (for a given gain of 1000).

APDs are fabricated by deep diffusing gallium and aluminum into NTD doped (phosphorus) silicon, producing a deep p-n junction. The deepness of the diffusion is important, with deep diffusions offering higher gains and improved signal to noise. Practical constraints, however, prevent us from deepening the diffusion much more than what is typically done now at RMD. One parameter open to our control is the resistivity of the starting silicon wafer. Changing the wafer resistivity would alter the doping profile near the junction and possibly alter the excess noise factor F at a given operating gain. In Phase II, we will fabricate and test large APDs made with different resistivity starting silicon in order to determine if changes in the doping profile significantly affect the excess noise. If the doping profile is found to play significant role in determining F, further studies will be implemented to identify an optimal doping profile minimizing F.

c. Excess Noise Measurements

To measure the excess noise in Phase II, we will use the test setup shown in **Figure 21**. This setup was also used in Phase I to detect light pulses from an LED with large area APDs. In Phase II, we will again use this setup to detect LED light pulses. To measure the excess noise factor F, the APD under test will be stabilized at its operating temperature and the bias voltage will be adjusted so that the APD gain is 1000. Pulse height spectra will then be acquired, which will show a single peak representing a histogram of the detected pulse heights. The shape of the histogram peak should be a simple Gaussian distribution. The spectral broadening can be simply measured by measuring the width of this Gaussian distribution. After the broadening is measured and the magnitude of the input signal noted, this procedure will be repeated for a range of different the input signal

magnitudes. Finally, a plot of the square of the broadening (σ_{st}^2) versus input signal (N_{eh}) will be made. The form of the data should be:

$$\sigma_{st}^2 = N_{eh} F + \delta_{noise}^2$$

The excess noise factor F should be the slope of the line and will be measured in this manner. Because F is known to be a function of APD gain, it is important to make these measurements at a constant gain. This also implies that a constant temperature be maintained, so measurements will be performed at room temperature and at LN₂ temperature. Similar studies will be conducted at different APD gains in order establish excess noise factor versus gain relationship for APDs with varying doping profile. APD designs that minimizes F will be identified from these experiments.

4. Timing Characteristics and Investigation of Voltage-Sensitive Preamplifiers

In Phase I, most measurements of the large APDs were made using conventional charge-sensitive preamplifiers (CSPs). The use of CSPs is standard in nuclear measurement. The advantage of the CSP design is that the gain is independent of the detector capacitance. This is important in situations where very good energy resolution is required and where the detector capacitance may drift over the measurement period. One disadvantage, however, is that the risetime of the output pulse is proportional to the input capacitance. Because the large APDs in this project have relatively high capacitance, the output risetime can be relatively long. While it is true that the risetime can be quickened somewhat by using high transconductance input JFETs in the front end of the CSPs (which would reduce the input impedance Z_{in} of the CSP), the risetime is also limited by the contact resistance in the APDs. For this reason, we would not expect the risetime of the very large APDs to improve dramatically as long as CSPs were used in their readout.

To illustrate why CSPs have this slowed risetime, consider an APD detector (as shown in **Figure 33**) with capacitance C_d and contact resistance R_c , attached to a CSP. The CSP output at a given time is proportional to the charge from the APD which has flowed into the preamplifier input up to that time. The detected ionized charge, which is initially stored on the APD capacitance, must discharge through two impedances: the contact resistance R_c and the preamplifier input impedance Z_{in} . The charge is discharged in an exponential manner, with a time constant $(R_c + Z_{in}) * C_d$. This slow discharge of the APD is responsible for the slow risetime of the output signal.

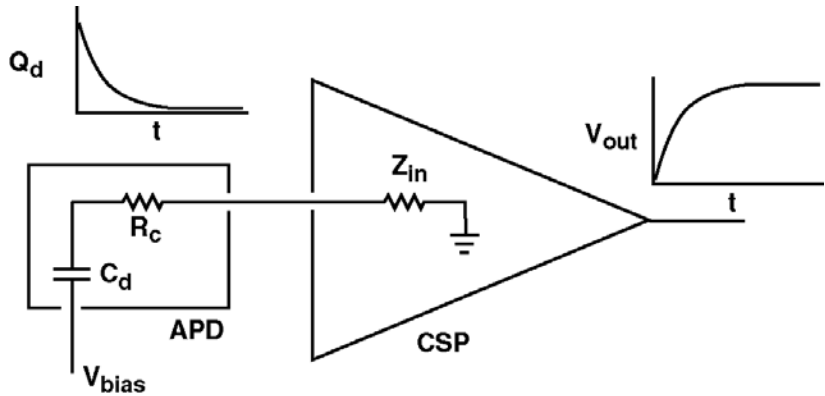


Figure 33: A large APD is modeled by a large capacitance C_d (70 pF/cm² APD) in series with a contact resistance R_c (may be as high as a few hundred ohms). This is connected to a charge sensitive preamplifier (CSP) having input impedance (Z_{in}) of typically a few hundred ohms. The charge (Q_d) on the APD capacitance (C_d), discharges through the impedances R_c and Z_{in} , with a time constant $(R_c + Z_{in}) * C_d$. This time constant is reflected in the output pulse from the preamplifier.

Voltage sensitive preamplifiers (VSPs), on the other hand, do not suffer this effect. VSPs have high input impedance and sense the jump in voltage across the APD caused by the signal rather than integrating the current from the APD. Voltage sensitive amplifiers can be made very fast and do not need to discharge the APD in order to provide an output signal [Spieler].

In Phase II we propose to design, build, and test VSPs for use with large APD detectors. This work, which will be conducted by Cremat, Inc. (Newton, MA) on a fee for service basis, will be aimed at producing preamplifiers having low noise and a risetime considerably faster than that which is possible using a conventional CSP. The fact that the gain of the VSP is a function of the APD capacitance (which may drift if the temperature drifts) is not a critical issue because the APD temperature must be controlled anyway, due to the fact that the APD gain is a function of temperature. Canberra engineers will also guide us in these studies.

a. Signal shape expected from a VSP.

A VSP coupled to an APD is diagrammed in **Figure 34**. A load resistor (R_L) is used to couple the APD to ground, and the VSP measures the voltage formed across R_L . To keep the electronic noise low, R_L should be relatively low: about 1000 ohms should be appropriate. When an incoming event quickly charges up the APD, there is a small jump in voltage across the APD, which appears at the node with R_L . This is detected and amplified by the VSP, which has a high input impedance. The risetime of the signal at the output of the VSP is limited by the bandwidth of the VSP, which can be reasonably fast. The charge on the APD discharges through the resistors R_c and R_L with a time constant $(R_c+R_L)*C_d$. The fast fall time for VSP is faster compared to the CSP, and different techniques may be required to process these faster-falling signals.

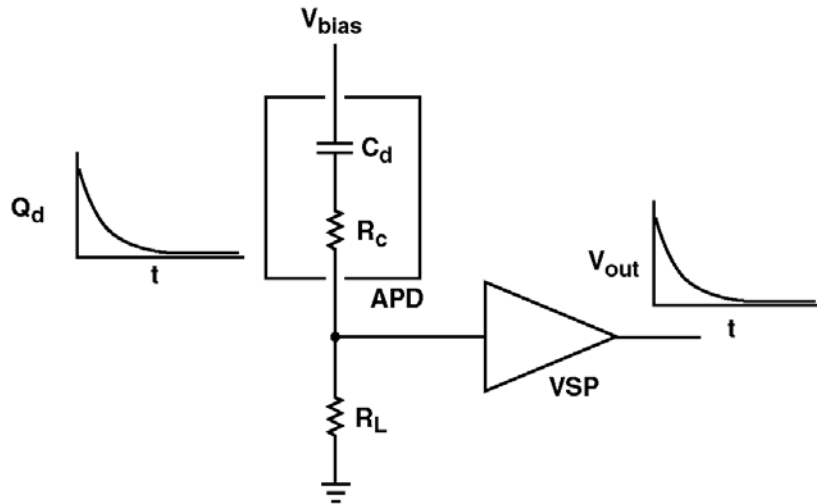


Figure 34. Voltage sensitive preamplifier (VSP) reading out a large APD. The signal charges the APD capacitance C_d to a voltage proportional to the ionized charge in the APD times the APD gain, and inversely proportional to C_d . This voltage change is quickly sensed by the VSP connected to the APD and a jump in the output voltage quickly follows. The APD is discharged through the APD contact resistance R_c and a load resistor R_L , with a time constant $(R_c+R_L)*C_d$. For noise considerations, R_L should be kept relatively low: approximately 1k ohm.

The noise produced in a VSP detection system can be roughly estimated using the published noise values of popular high performance operational amplifiers. Cremat has performed noise analysis for a VSP system consisting of Intersil's EL2125, a state-of-the-art low noise, high speed operational amplifier. Their analysis suggests that using a load resistor, R_L of 1 k Ω , the equivalent charge noise of the VSP system for large APD readout would be only marginally higher than the

charge sensitive preamplifier setup used in the Phase I project. A detailed analysis of risetime and noise for CSP and VSP amplifiers for APD readout will be performed in the Phase II project.

b. Timing Studies with APDs

During Phase II we will study the timing properties of the large APDs. More specifically, we will measure both the risetime and the coincidence timing resolution; this will be done using APDs of various sizes that we fabricate in the Phase II program.

We will measure the risetime and fall time by irradiating the APD with a fast optical pulse (<1 ns pulse width) using a frequency doubled YAG laser available at RMD (Uniphase #NG-10120-101). We will record the resulting signals from the APD on a digital oscilloscope. In place of the laser, we will also use the direct detection of alpha particles (5.5 MeV, ^{241}Am source) as a large fast signal. Again, the risetime and fall time of the signals from the large APDs will be directly observed and measured with the aid of a digital oscilloscope.

The measurement of coincidence timing resolution will utilize the standard instrumentation, with two independent channels detecting the two 511 keV gamma rays from a positron annihilation source (^{22}Na) [Knoll]. The analog pulses from each channel are fed to *constant fraction discriminators*, which provide fast ‘timing’ pulses for each channel. The timing pulses from the two detection channels are fed as the ‘start’ and ‘stop’ pulses in a time-to-amplitude converter (TAC). A histogram of the resulting pulse heights reveals the ‘timing spectrum’, which is typically a Gaussian-shaped peak, the width of which is the ‘timing resolution’. We will use a BaF_2 scintillator coupled to PMT as the ‘start’ channel (known to be a detector with excellent timing resolution) while the APD under test coupled to a second BaF_2 crystal will be used on the ‘stop’ channel in the experimental setup. Measurement of the APD timing resolution using this standard method will provide unambiguous determination of the timing resolution of APDs of various sizes.

Both charge-sensitive and voltage-sensitive preamplifiers will be used with APDs in these experiments in order to compare the timing resolution obtained with these different preamplifier designs. As discussed in the previous section, we expect voltage sensitive preamplifiers (VSPs) to provide much faster risetime performance than the more commonly used charge sensitive preamplifier (CSP) in this application. The faster risetime performance of the VSP design is expected to result in improved timing resolution, however we plan to verify this experimentally in the Phase II study.

5. Quantum Efficiency

The quantum efficiency of APDs will be measured in the Phase II program using a monochromator, a light source, and a calibrated silicon diode in similar manner as in the Phase I project. The optical efficiency will be measured in the 200-900 nm region. One aspect of this investigation will be to study the effectiveness of our new surface doping and other surface treatments on the quantum efficiency of our devices in the blue-UV region. We also plan to perform quantum efficiency measurements with the large APDs in deep ultra-violet region (120-200 nm) using the facilities at Rutgers University (in New Jersey). Rutgers Ultraviolet Detector Laboratory has three monochromators for UV studies, an Acton 502 for wavelength coverage from 120 to 300 nm, a McPherson 247 for 5 to 120 nm, and an Oriel for 200 to 600 nm [<http://www.physics.rutgers.edu/~cjoseph/ast-uvlab.htm>]. Preliminary measurements at Rutgers University indicate that the planar APDs have quantum efficiency of ~40% or higher in the 150-200 nm region, which is attractive for applications such as UV sensing in LXe detectors. Detailed

experiments with the large APDs will be performed on a fee for service basis at Rutgers during the Phase II project. Quantum efficiency measurements will also be performed over the entire wavelength region of interest (UV to visible) as a function of APD temperature (from room temperature to LN₂ temperature).

6. Scintillation Spectroscopy and Charged Particle Detection

Once the gain, noise and quantum efficiency of the large APDs have been characterized, we will measure their scintillation performance. Standard NIM electronics will be used and a low noise charge sensitive as well as voltage sensitive preamplifier will be tried. The APDs, cooled to -25 to -40 °C range, will be coupled to scintillators such as CsI(Tl) and NaI(Tl) and irradiated with isotopic sources such as ¹³⁷Cs, ⁵⁷Co, ⁶⁰Co and ²²Na. The energy resolution of various gamma ray photopeaks will be measured along with the electronic pulser resolution. The dominant resolution broadening mechanism will be estimated from these results. Some measurements will also be made with BaF₂ and plastic scintillators. For the very large devices, we will procure scintillators with matched size from Saint Gobain Crystals and Detectors to perform scintillation studies.

Direct detection of charged particles such as 5.5 MeV alpha particles (²⁴¹Am source) and ⁹⁰Sr beta particles ($E_{\text{max}} = 2.27$ MeV, $E_{\text{avg}} = 0.5$ MeV) with the large APDs will also be carried out in the Phase II project. Standard nuclear pulse processing electronics will be used and the energy spectra resulting from the interaction of these charged particles with the APDs will be recorded at temperature in the range of $+25$ to -40 °C.

D. GAIN, NOISE AND OPTICAL SENSITIVITY AT LN₂ TEMPERATURE

During the Phase II project, we will perform evaluation of the gain, noise and optical sensitivity of the large APDs at LN₂ temperature. These experiments will be similar to those performed in the Phase I project but will be more detailed than what was possible in the limited time frame of the Phase I program. Dr. Reucroft at Northeastern University will participate in this study.

The cooling setup along with the optical source and the pulse processing electronics that we had built in the Phase I project will be used, though a more optimized front end electronics setup will be employed along with appropriate blocking capacitors, amplifier shaping time and load resistors. This will allow us to achieve lower noise with the very large APDs. APDs with area up to 60 cm² will be investigated in the Phase II project. Initially, the gain versus bias relationship of the large APDs will be evaluated at 77 °K. As discussed earlier, an optical pulse spectrum will be recorded for a large APD cooled to 77 °K at low bias (~ 500 V) to determine the pulse height at unity gain. The APD bias will be increased and the resulting pulse height for the same optical exposure will be recorded to determine the gain versus bias relationship at 77 °K. Based on the Phase I results, we expect to achieve APD gain of 10^4 or more with the large devices.

The noise of the large APDs will also be measured at 77 °K in this study, where an ⁵⁵Fe source (5.9 keV X-rays) will be used to calibrate the energy scale (in eV and electrons). Pulse height spectra will then be recorded for an injected electronic pulse on the calibrated scale. The width of the resulting peak (for the injected electronic pulse) will be used to quantify noise in eV and in electrons. These studies will be performed as a function of the APD bias and over a wide range of amplifier shaping times to determine conditions under which the effective APD noise is minimized. Based on the Phase I results as well as the optimization that we plan to perform in the Phase II project, we expect to achieve noise < 1 electron (rms) at 77 °K for even the largest devices (60 cm²) that we plan to build in the Phase II project.

Finally, we will determine optical sensitivity of the large APDs at 77 °K. **Figure 35** shows a schematic representation of the experimental setup that we plan to use for these measurements. An optical fiber coupled to an LED on one side will be attached to an APD on the other end. The LED will be operated in a pulsed mode using a pulser (or a pulse generator). The signal from the pulser will be split with one line going to the LED and the other line going into a single channel analyzer and then into a gate and delay generator. This other line produces a gate every time the LED is flashed. The number of gates during a specified time window will be counted. Gated energy spectra will then be recorded from the APD producing a peak corresponding to the LED signal. The number of photons corresponding to the LED spectrum recorded by the APD will be determined by calibrating the energy scale using ⁵⁵Fe X-rays and by taking into account the APD quantum efficiency. The detection efficiency for the number of photons estimated in this manner will then computed as:

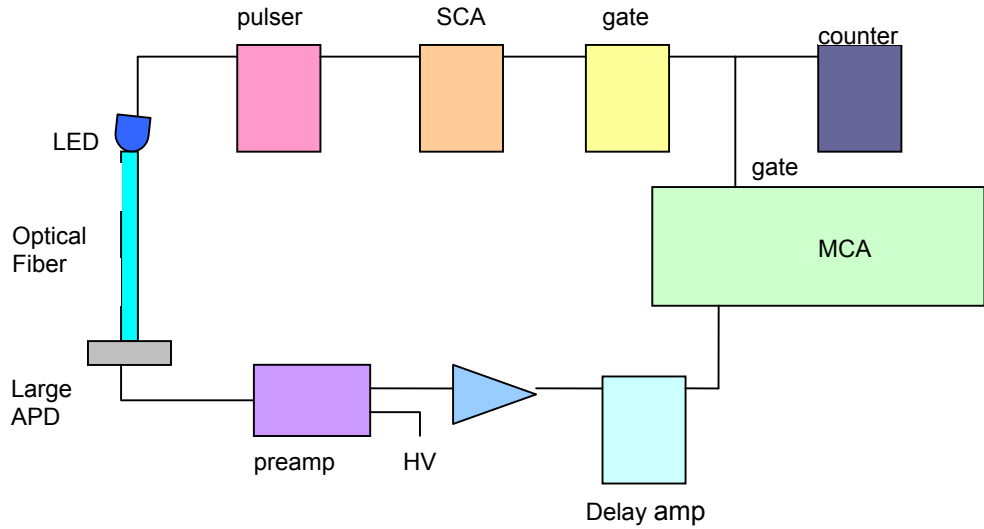


Figure 35. Setup to be used for measuring APD detection efficiency.

The LED will be operated in a pulsed mode using a pulser (or a pulse generator). The signal from the pulser will be split with one line going to the LED and the other line going into a single channel analyzer and then into a gate and delay generator. This other line produces a gate every time the LED is flashed. The number of gates during a specified time window will be counted. Gated energy spectra will then be recorded from the APD producing a peak corresponding to the LED signal. The number of photons corresponding to the LED spectrum recorded by the APD will be determined by calibrating the energy scale using ⁵⁵Fe X-rays and by taking into account the APD quantum efficiency. The detection efficiency for the number of photons estimated in this manner will then computed as:

$$\frac{\text{integral of the number of counts in the gated APD energy spectrum}}{\text{number of gates produced by the pulser in the same time interval}}$$

These experiments will be carried out with the optical intensity on APD varying from ~50 photons per pulse down to the level of a few photons per pulse. Ability of the large APDs to detect single photoelectrons will also be evaluated in this study. In this manner the ability of the large APDs to detect low intensity optical signals at 77 °K with high efficiency will be determined.

E. EVALUATION OF APDS FOR WATER CHERENKOV DETECTION AT BNL:

During the Phase II project, our BNL collaborators will investigate planar APDs for water Cherenkov detection. The Cherenkov light emission (N) in water per unit wavelength and per unit path length of a charged particle is described by the following formula:

$$\frac{d^2N}{dx d\lambda} = \frac{2\pi\alpha z^2}{\lambda^2} \times \left(1 - \frac{1}{\beta^2 n^2(\lambda)}\right)$$

Here λ is the wavelength of light, x is the pathlength, β is the velocity of the particle in units of the speed of light, and n is the index of refraction. In addition, α and z are the fine structure constant and the charge of the particle in unit of e . When we integrate the above equation over the 300 to 600 nm wavelength region, the light yield should be ~328 photons per cm of track. Absorption of the light in water and the efficiency of photo-sensor lower the observed yield as we describe below.

We will evaluate APDs for water Cherenkov detectors on the basis of three criteria.

1) **Performance for low intensity light:** In a large water Cherenkov detector with 10 to 20 % of the surface area covered with photosensors, one expects to observe very few photons per photosensor. It is therefore important to keep improving the APDs to achieve signal to noise ratios that will allow single photon detection with good efficiency. As shown in Phase I of this project, a large APD with area of 45 cm² was operated with 0.8 electron (rms) noise at temperature of 77 K (LN₂). While this result is very encouraging, underwater use of such a device will require special packaging to separate the cold detector from water. We will continue to develop novel APD geometries as well as readout techniques while increasing the sensitive area of new APDs. As discussed earlier mirrors or lenses could also be used to focus the Cherenkov light onto an array of photosensors or a single position sensitive photosensor [Antonioli]. A large imaging APD with pixilated readout (APD pixel sizes of ~ 1 cm²) could be well suited for such an application. An optimum size for APD pixel size could be obtained by considering the requirements for imaging resolution and the noise in each pixel. The efficiency and noise characteristics of large APDs in the water Cherenkov environment will be characterized, and simulation studies will also be conducted.

2) **Efficiency in near ultra-violet:** In **Figure 36** we show the calculated spectrum of photons in pure water versus wavelength in nm. The spectrum was calculated using full GEANT simulation in which 1 GeV/c muons were simulated at the center of a 50 meter diameter and 50 meter high water tank. The Cherenkov light produced by the muon (as well as associated delta rays) was transported through water (to the inner surface of the tank) accounting for absorption using the measured absorption lengths [Pope]. The upper curve in **Figure 36** is the spectrum expected at the inner surface of the tank normalized to unit area. The Cherenkov spectrum, as shown in the equation (on the previous page), increases at lower wavelengths as $1/\lambda^2$. This increase at lower

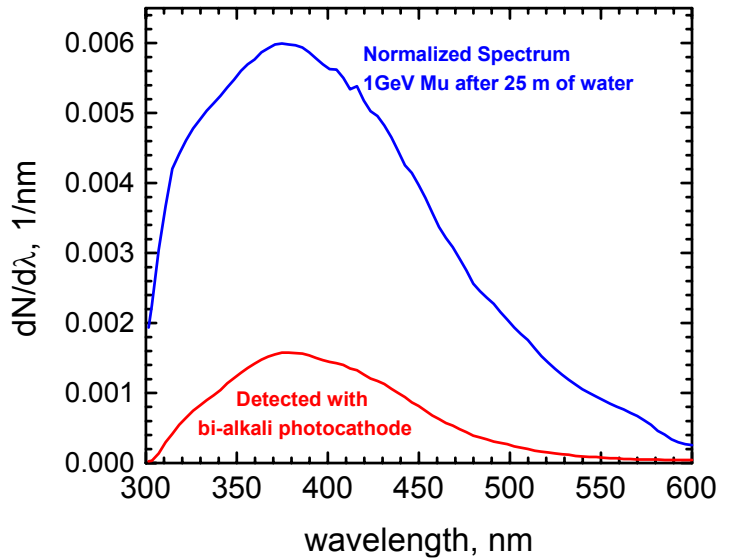


Figure 36. Spectrum of Cherenkov light in pure water calculated for a 1 GeV/c muon at the center of a tank of 50 m diameter. The spectrum includes the effects of absorption as the light travels to the inner surface of the tank. The bottom curve shows the spectrum after including the quantum efficiency of a typical bi-alkali photocathode.

wavelengths gets sharply cut off because of absorption around 300 nm. There is also rapid absorption above 600 nm. Traditional photocathode efficiency peaks around 370 nm. The second curve in **Figure 36** shows the spectrum after accounting for the quantum efficiency of a typical bi-alkali photocathode. It is clear that significant improvement is possible if a new photosensor can be more efficient in the 300 to 400 nm (near ultraviolet) region. The APD appears to fit this requirement very well as shown by our work in Phase I of this project (see

Figure 18). We will characterize the wavelength dependence of the APD efficiency with more precision in Phase II. We will also try to understand by simulation the implications of this efficiency gain at blue-UV wavelengths for the physics capabilities of a future large water Cherenkov detector.

- 3) **Underwater performance:** To gain complete understanding of the photoelectron yield and APD performance we intend to build a small water Cherenkov test tank at BNL. The tank will be approximately 1 meter in diameter and 2 meters high. Light from vertical cosmic ray muons will be focused onto photosensors of interest by using a ~10 cm diameter mirror. The photon yield on the floor of the tank for a vertical muon using the spectrum in **Figure 36** is $\sim 300/(2\pi L)$ per cm^2 , where L is the distance in cm on the floor from the muon. A pair of scintillation counters will be used to select muons of the correct geometry. We calculate that the primary photoelectron yield for an APD should be ~50 per muon for a mirror located 50 cm from the muon track. The exact yield will depend on many parameters: the efficiency of the APDs for Cherenkov light, the purity of water, the surface treatments and packaging of the APD. The data from this small tank will provide very valuable information about the suitability of APDs as an underwater detector. To our knowledge there has been no previous attempt to use APDs in this manner. Therefore we consider this exercise a very important part of detector research for high energy physics.

F. EVALUATION OF APDS FOR KOPIO AT BNL:

During the Phase II project, APDs will be evaluated extensively at BNL for KOPIO. This will include evaluation of APDs for Calorimeter and Outer Veto, Barrel Veto and Downstream Veto, which is discussed here. A schematic diagram of the KOPIO detector was shown earlier in **Figure 2**.

1. Calorimeter and Outer Veto

The KOPIO Calorimeter (CAL) requires 2500 APDs, each with an active area of about 1.5-2 cm^2 (see **Figure 37**). The Outer Veto (OV) requires an additional 600 APDs of the same size. The performance requirements of the CAL and the OV are identical. Each APD views the light transmitted by 144 wavelength-shifting fibers, 1 mm in diameter (see **Figure 38**). This can be accomplished with APDs of 14x14 mm^2 area. The BNL team is currently testing devices of this size as part of the Phase I proposal. APDs are preferred over photomultiplier tubes (PMTs) for this application, because of the need to operate the light collection devices in regions of high magnetic field, where conventional PMTs would not function. The APDs reading out the calorimeter are only a few centimeters from a large magnet, with fringe fields in the range of hundreds of gauss. Standard PMTs suffer loss of gain in such fields. Although there are some field-tolerant PMTs that make use of mesh dynode structure to reduce the effect of the magnetic field, they sacrifice performance and cost significantly more than APDs.

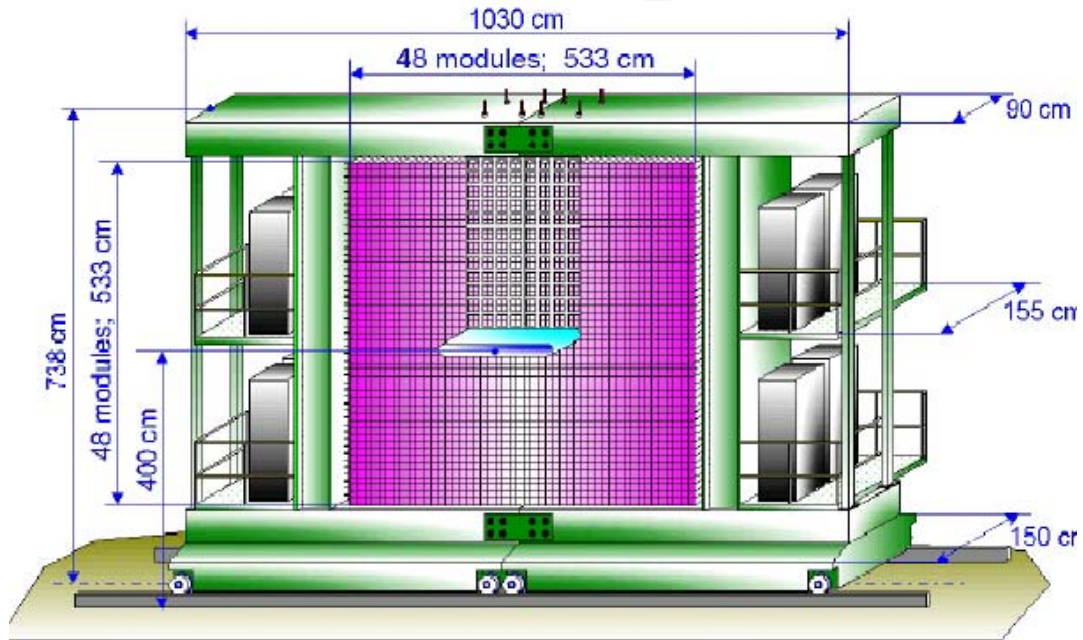


Figure 37: Perspective view of the KOPIO Calorimeter array with 2500 detector modules.

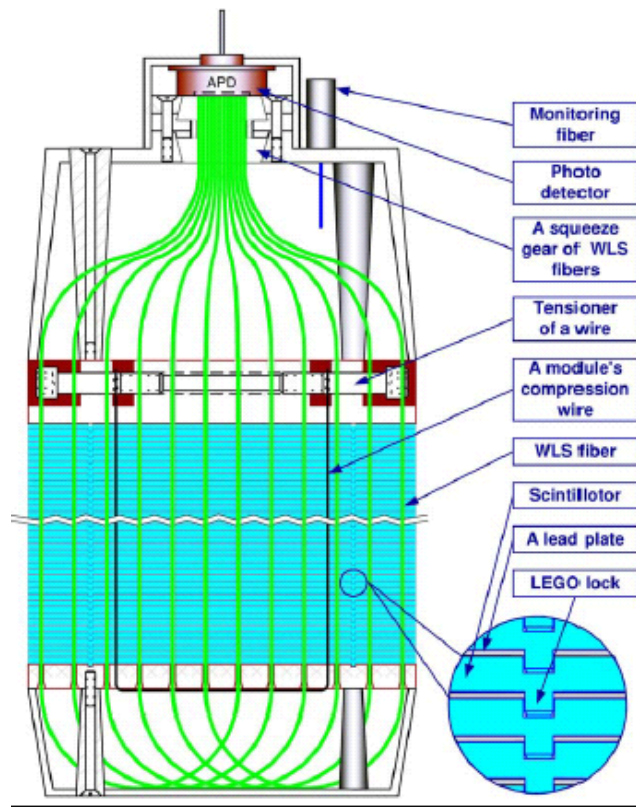


Figure 38: Components of the KOPIO Calorimeter module.

An important requirement of calorimeter readout is that it must be sensitive to low light levels. The KOPIO experiment relies upon the detection of gammas down to energy of about 1 MeV or less. A 1 MeV gamma will produce enough visible photons to deliver approximately 57

visible photons through the wavelength shifting fibers. In order to achieve good efficiency at such low light levels, we must be able to convert those photons into electrical signal in a way that preserves good signal-to-noise ratio, SNR. The quantum efficiency for the existing APDs is measured to be ~ 70 for 500 nm light from the wavelength shifting fibers. This gives 40 photoelectrons for the APD, but only 11 for a standard PMT. This makes the choice of APDs seem very attractive. However, the APD signal has noise contributions that are greater than PMTs. With currently available APDs, we find that we must set a threshold for gamma detection at 1 MeV, while for PMTs the threshold is 0.25 MeV. As mentioned earlier, the Phase II research will focus on reduction in APD noise as well as improving the quantum efficiency of APDs which should enhance the performance of APDs for CAL and OV. The reduction in noise is expected from modifications in APD design (reducing the thickness of neutral (or undepleted) p and n regions and implementation of the isolation grooves on the back of the device, which should reduce the bulk and surface leakage components), and from optimization of the front end preamplifier design. The improvement in quantum efficiency is expected from reduction in the thickness of neutron p-type region on the front face of the APDs and deposition of anti-reflection coating on APD surface. The inherent quantum efficiency of Si can be above 90%. We will determine the how best to optimize the noise and quantum efficiency of the APDs proposed for the CAL and OV in the Phase II study.

The overall noise in APDs can be reduced through cooling. Initial studies have given very promising results for what can be achieved with low cost refrigeration techniques. The BNL team would like to continue the noise studies as a function of temperature, to see what level of cooling is required to achieve high sensitivity for low intensity optical signals. We will be investigating the use of thermoelectric coolers (TECs) that can be bonded to each APD to cool them to -20 to -30 °C. BNL will purchase TECs to conduct tests with prototype APDs. The performance of such modules will be evaluated from the view point of SNR requirements of KOPIO calorimeter and OV systems. This study will complement our Phase I refrigerator study with a final design for mounting cooled APDs on the back of the calorimeter modules. We will measure the effective energy threshold for detecting gammas with APD readout as a function of APD gain and temperature.

APD noise is compounded by an excess noise factor (F) that is larger than PMTs. As discussed earlier, the excess noise factor (F) describes how the response function in a detector with gain (such as APD) differs from a unity gain photodetector where resolution for light detection (in absence of electronic noise) is determined by Poisson statistics only. A typical PMT has an F of 1.4. The BNL team has made measurements of F of 2.2 (at gain of 400-500) for RMD's APDs. As shown in **Figure 39**, F for RMD's APDs is significantly lower than that in other APDs designs, which is encouraging. In general the F of APDs is gain dependent [Hayat], growing as the gain increases, though the slope for RMD's planar APDs is not as steep as that in other APD designs (as shown in **Figure 39**). Because KOPIO is sensitive to noise and the resolution of small signal levels, understanding

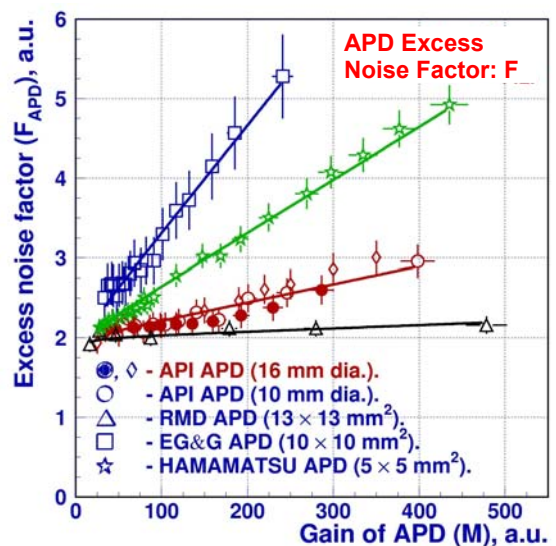


Figure 39: Excess Noise Factor as a function of APD gain, for various APDs.

and control of F is an important priority for the Phase II research with KOPIO.

Fast timing resolution using APDs is required for KOPIO. In order to distinguish between signal gammas and background gammas, one of the most powerful tools is the timing of the hit in the calorimeter. BNL has performed timing resolution measurements using APD readout of plastic scintillators in a test beam study during the Phase I project. Two such detector modules were irradiated with monoenergetic (350 MeV) photon beam. As the beam spot was scanned across the two modules, the photon energy was shared them. The timing resolution was determined by measuring the time difference in the signal between the two modules. When the photon beam energy was shared equally by two modules (~175 MeV detected by each module), timing resolution of ~250 ps was measured. By performing such a study where energy deposition in the two modules is not the same (and the measured timing resolution is dominated by the timing response of the module with less energy), a timing resolution versus incident photon energy relationship of $\sigma_t \approx 86/\sqrt{E}$ was established. Here σ_t is the timing resolution and E is the photon energy in units of ps and GeV, respectively. Similar studies will be continued in the Phase II project upon optimization of APD timing characteristics as well as electronic readout setup. The timing will be determined either by a threshold discriminator and Time to Digital Converter (TDC) or a Wave Form Digitizer (WFD). Based on the optimization of the APD timing response, quantum efficiency and noise that is planned in the Phase II research, we hope to achieve a timing resolution of ~60 ps/ $\sqrt{E(\text{GeV})}$ in the calorimeter. Although the readout scheme for the calorimeter has not yet been finalized, we expect we will require APD signal risetimes of several nanoseconds in order to achieve the time resolution specified. Some of this study will be devoted to the design of a preamplifier. Voltage sensitive preamplifiers usually have faster risetime, but may have slightly higher noise. Charge sensitive preamplifiers give reduced noise, but at the cost of slower rise times. As part of Phase II, we will investigate the best compromise between noise and speed to give the KOPIO calorimeter the optimum performance.

As part of our Phase I research we have operated with APD gains on the order of 10,000, larger than the gains in most applications. In Phase II we will explore the limitations to the stable operation of APDs at gains of 10,000 or greater.

2. Barrel Veto

The Barrel Veto (BV) is an array of lead/scintillator detectors surrounding the decay volume of the KOPIO experiment. **Figure 40** shows a schematic representation of the KOPIO Barrel Veto (*Shashlyk* option). Its purpose is to detect any gammas that accompany the signal, indicating the presence of a background. The BV must be sensitive to gammas of energies below 1 MeV, up to energies of 1 GeV; similar in performance to the CAL. Like the CAL, the BV must be capable of fast timing measurements, and low noise.

There are approximately 1200 light detectors on the BV. In distinction to the CAL, the BV must collect the light from over 400 fibers, so the active area must be larger. APDs of 20x20 mm² area would be adequate. As part of the Phase II program, we plan to evaluate the gain, timing, resolution and noise behavior of these larger 20x20 mm² APDs for the KOPIO BV.

3. Downstream Veto

The Downstream Veto includes a gamma veto (DGV) similar to the BV and a charged particle veto (DCPV). The gamma veto must function inside a strong magnetic field, making PMT use near impossible. Performance for the DGV are just as stringent as the CAL and BV; sensitivity

to gammas down below 1 MeV, with fast risetime and low noise. APD size requirements are not completely specified for the DGV yet, but will be similar to the CAL. The Downstream Charged Particle Veto (DCPV) is a different design from the gamma vetoes. Each DCPV will be a single scintillator tile with wavelength shifting fiber readout. This means that the light collection area will be quite small; a few square mm. For this application, smaller APDs would be appropriate. This makes achieving the low noise operation somewhat easier, and could improve the response time compared to the larger area APDs. As part of Phase II we plan on investigating the design of APD readout of the DCPV.

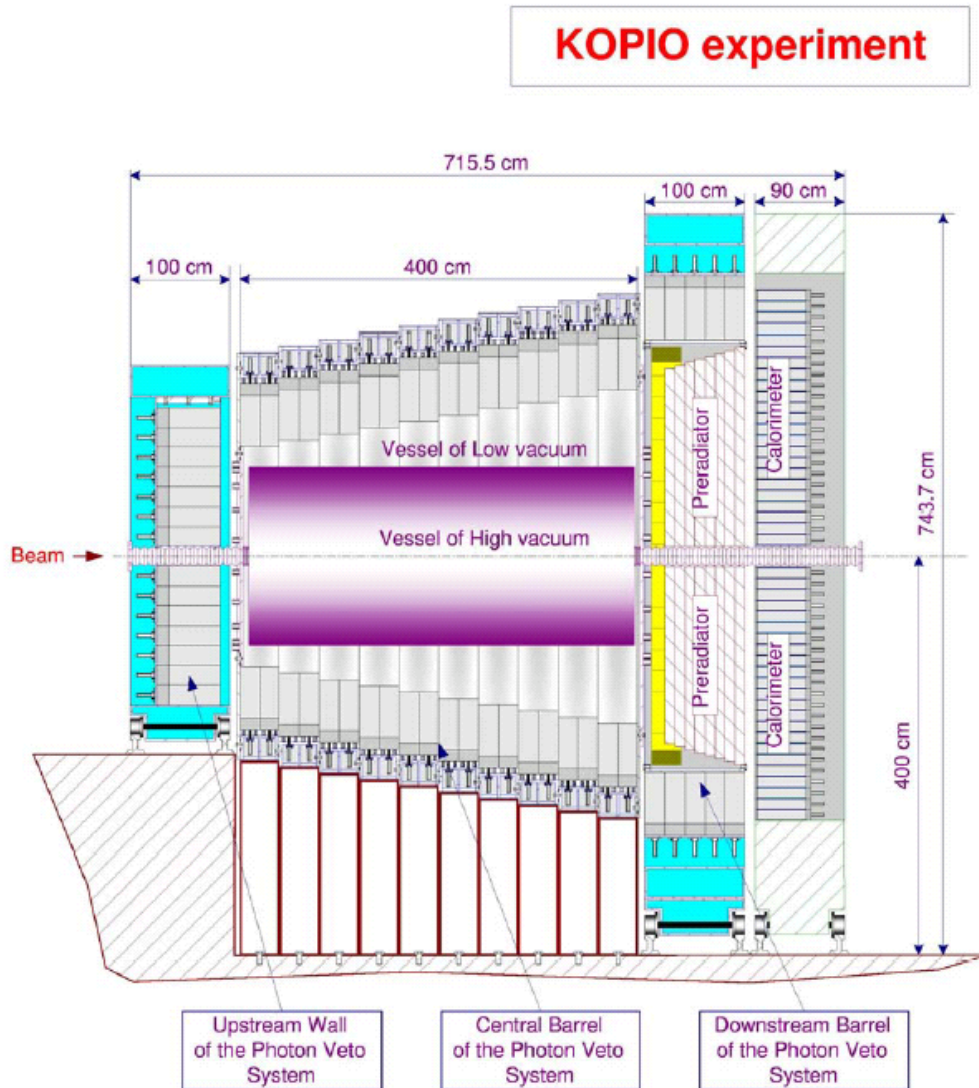


Figure 40: Schematic of the KOPIO Barrel Veto, Shashlyk option.

G. EVALUATION OF APDS FOR MECO AT BNL

Large APDs will also be evaluated for the crystal calorimeter in MECO experiment during the Phase II project in collaboration with the BNL team. A schematic diagram of MECO experiment was shown earlier in **Figure 3**. For MECO, the calorimeter will detect electron from the muon

conversion in the field of a nucleus. These electrons have energy of 105 MeV. The energy detected in the calorimeter will be compared to the momentum measured in the straw-tube spectrometer to reject background so that a signal of 1 event in 10^{17} muon decays can be measured. Very good calorimeter resolution (better than 5%) must be achieved to obtain sufficient background rejection. The calorimeter resolution depends on the amount of light collected by the photosensor, therefore large area APDs are preferred for this application. The calorimeter in MECO is designed to consist of ~ 2000 PbWO_4 crystals, each with $3 \times 3 \times 14$ cm size. **Figure 41** shows a photograph of one such PbWO_4 crystal block along with two examples of APDs that could be used for readout (which includes RMD's 13×13 mm² planar APD). The general requirements for the APDs for MECO are similar to what was described for KOPIO. The time resolution and fall time of the pulse must be in the few ns range to handle high singles rates, the detector must work in a high magnetic field area, and it must collect enough light with low noise so that the high resolution criteria is met.

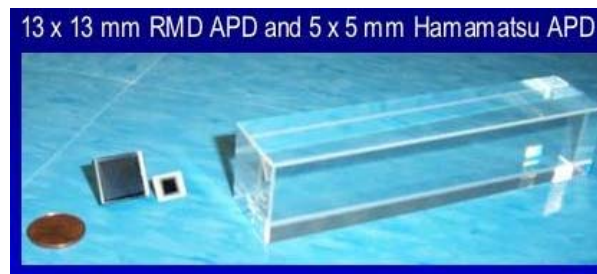


Figure 41. Photograph of $3 \times 3 \times 14$ cm PbWO_4 scintillation block with APDs from RMD and Hamamatsu.

Initial tests of RMD's 13×13 cm² APDs for use in MECO have been performed by New York University (NYU) which is part of the MECO collaboration (along with BNL). The calorimeter and electronics were placed in a freezer and cosmic ray muons were used along with two RMD APDs as shown in **Figure 42**. The combined signal from three plastic scintillators (S1, S2 and S3) was used as a trigger to collect the data from the two APDs coupled to a $3 \times 3 \times 14$ cm PbWO_4 crystal. A lead brick separated S1 and S2 from S3, in order to allow detection of cosmic ray muons. Using this setup, the energy resolution of PbWO_4 crystal can be estimated from the distribution of differences and sums of the two APD signals. Using cosmic ray muon excitation, NYU group has measured energy spectra with two RMD APDs coupled to PbWO_4 crystal. The measured data was processed to create distribution of differences between two APD signals ($A_1 - A_2$), which is shown on the top in the **Figure 43**. Also shown is a plot that depicts the distribution of sum of the signals ($A_1 + A_2$) from the two APDs (see **Figure 43-bottom**). The energy resolution was then estimated to be 4.3% using the following expression:

$$\varepsilon = \frac{\sigma_{A_1 - A_2}}{MPV_{A_1 + A_2}} = \frac{66.14}{1534.0} = 4.3\%$$

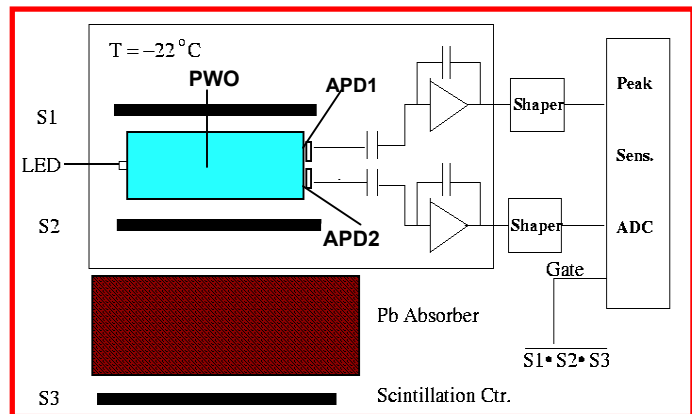


Figure 42. Cosmic ray test stand at NYU for MECO. Two APDs from RMD were attached to a PWO scintillation crystal (shown in blue), and APDs as well as preamplifiers were cooled to increase the scintillation light and reduce the APD dark current. S1, S2, and S3 are plastic scintillators that provide trigger for muon detection.

where ε is the energy resolution, σ_{A1-A2} is the standard deviation for the plot shown on the top in **Figure 43** that depicts the distribution of difference between APD1 and APD2 signals and MVP_{A1+A2} is the mean value for the plot shown on the bottom in **Figure 43** that depicts the distribution of the summed signal for the two APDs [Sculli]. It should be noted that shaping time of 50 ns was used in this study. Upon increasing the shaping time to 200 ns, the energy resolution improved very marginally (to 4.1%). Thus, almost all the light is efficiently collected with shaping time of 50 ns which should allow data collection with high count-rate. In this study, the mean value of energy deposition by cosmic ray muon in $PbWO_4$ was estimated to be 35 MeV. Based on these results, we calculate the energy resolution of the same setup for 100 MeV energy deposition to be $<3\%$.

It should be noted that the NYU group has also performed energy resolution measurements using the setup shown in **Figure 42** where Hamamatsu's $5 \times 5 \text{ mm}^2$ APDs were used. The energy resolution for 35 MeV energy deposition by cosmic ray muons in PWO was measured to be 13.5% at shaping time of 50 ns and 7.6% at shaping time of 200 ns [Sculli]. These results are significantly worse than those achieved with RMD's $13 \times 13 \text{ mm}^2$ APDs. As a result, RMD's APDs appear to be very promising for MECO and we will further optimize their performance in the proposed research.

In the Phase II project, we plan to carry out more extensive tests to determine the temperature dependence of the signal-to-noise ratio of larger APDs built at RMD for MECO experiments. In order to maximize the efficiency of the trigger calorimeter, APDs with sizes larger than the $1.3 \times 1.3 \text{ cm}^2$ ones investigated so far will be explored. We plan to explore planar APDs with $1.5 \times 3 \text{ cm}^2$ in the Phase II project. Two such large APDs will be packaged on the same substrate with $<1 \text{ mm}$ of dead-space between them. These two APDs will be placed on the $3 \times 3 \text{ cm}^2$ end of the $PbWO_4$ crystal (to cover the entire crystal face) in order to increase the light collection efficiency. The basic APD investigation will be similar to the activities described for KOPIO and will involve gain, noise, and timing response measurements as a function of temperature. Both charge sensitive and voltage sensitive preamplifiers will be used. Once such large APDs have been optimized, they will be delivered to BNL (Dr. Peter Yamin) for evaluation. Cosmic ray muon detection experiments

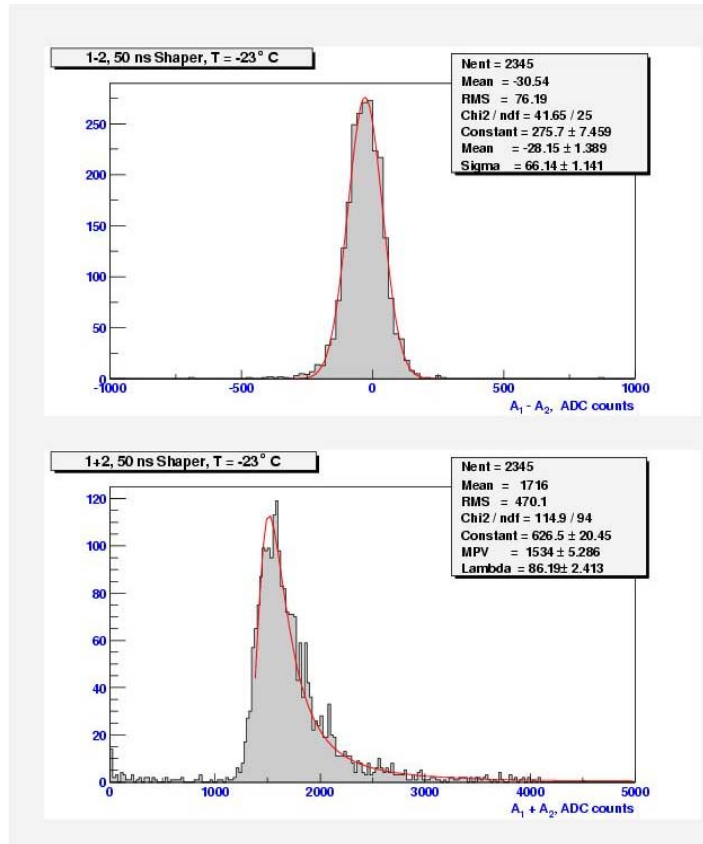


Figure 43. Distribution of differences or $A1-A2$ (top) and sums or $A1+A2$ (bottom) for signals from two APDs coupled to a $3 \times 3 \times 14 \text{ cm}$ $PbWO_4$ crystal upon interaction with cosmic ray muons. RMD APDs were $13 \times 13 \text{ mm}^2$ in area and were coupled to the same $9 \times 9 \text{ cm}^2$ face of a $3 \times 3 \times 14 \text{ cm}^3$ PWO crystal. Energy resolution of 4.3% was achieved at $-23 \text{ }^\circ\text{C}$.

will be performed in similar manner as described above and energy resolution will be measured. Demonstration of high count-rate operation will also be conducted.

H. LARGE APDS FOR UV SENSING IN LIQUID XENON DETECTORS

Another potential application of the large area APD's is in dark matter experiments. The next generation of dark matter experiments will need a large volume of sensitive material in order to push the limits further. A promising candidate is liquid xenon, since it provides a high density, self-shielded detector [Aprile]. Simultaneous measurement of the ionization and scintillation signals provides a natural discrimination between electron recoil (caused by background beta's and gamma's) and nuclear recoil (caused by the dark matter candidate). The scintillation signal is in the UV region at 174 nm. Although there are UV photocathodes, a number of factors make photomultiplier tubes less attractive options for reading out these photons. (1) The direct scintillation signal can be very small for low energy events, favoring a higher quantum efficiency than that available in PMTs. (2) Most PMTs have an unacceptably high background due to radioactivity in the components and in the window. (3) Extra care must be taken that PMTs not break due to the thermal stresses experienced by the cold xenon gas even if suspended above the liquid. Submersion in the -107°C liquid is not envisioned for PMTs, but could be considered for other types of photodetectors.

During the Phase II project, Dr. Priscilla Cushman at the University of Minnesota plans to use the testing facility available in her laboratory to characterize the performance of RMD's large area APDs (up to 60 cm^2 area) as a function of temperature down to LXe temperatures using a liquid nitrogen cooled chamber. The APDs will be attached to an interface board which mates to a Viking sample and hold readout system in order to measure signal to noise ratio at low light levels and as a function of temperature. The uniformity will be measured at room temperature by placing the APD and interface board on a computer-controlled nanomover which intersects a focused light beam. A calibrated diode measures total amount of light. This will be done for a variety of wavelengths down to 175 nm and both gain and quantum efficiency will be estimated from these measurements.

Once the large APDs have been characterized at the University of Minnesota, Dr. Cushman's group will test these large APDs in the prototype liquid Xe detector (see **Figure 44**) being developed at the Columbia University by Dr. Aprile and collaborators as part of the XENON project [Aprile]. Dr. Cushman is a participant on this effort and her team will build a fixture for immersion of the large APD in the prototype detector liquid Xe detector, which will fit into the port which currently houses the readout PMT. Readout electronics for the large APD will

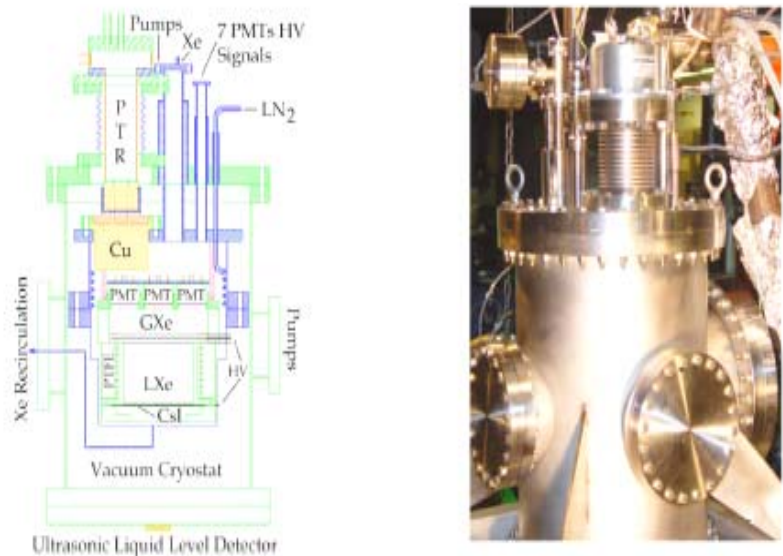


Figure 44. Schematic diagram (left) and photograph (right) of a 10 kg prototype LXe detector built by Dr. Aprile & collaborators.

be setup by Dr. Cushman's team and detection of UV scintillation from liquid Xe with the APD will be accomplished. Important experimental parameters such as detection threshold, efficiency and pulse shape after amplification will be measured and compared with those obtained with PMT readout. Overall, these efforts will lead to better understanding of the applicability of large APDs to various high energy and particle physics instrumentation projects.

I. PHASE II PERFORMANCE SCHEDULE: RMD TO PREPARE THIS SECTION

The Phase II project will focus on investigation of large silicon APDs for high energy physics applications. This effort will require research on following tasks, and numbers in brackets indicate the period in months during which the task will be performed.

- | | |
|---|---------|
| 1. Diffusion and device simulations. | [0-4]. |
| 2. Large area APD fabrication with varying Si resistivity | [1-16]. |
| 3. Testing of APD structures and addressing packaging issues at RMD, Canberra | [1-4]. |
| 4. Addressing the preamplifier issues for large APD readout at RMD, Canberra | [2-6]. |
| 5. Evaluation of large APDs at RMD, Canberra, Northeastern, BNL | [3-18] |
| 6. Evaluation of APDs for KOPIO and MECO at BNL | [3-24] |
| 7. Low temperature studies with large APDs at RMD, Northeastern | [14-18] |
| 8. Evaluation of large APDs for water Cherenkov detection at BNL | [15-23] |
| 9. Evaluation of large APDs in liquid Xe detectors with Dr. Cushman | [18-24] |
| 10. Prepare Phase II final report | [23-24] |

III. LITERATURE CITED

- P. Antonioli et al., The AQUA-RICH atmospheric neutrino experiment, Nucl. Inst. And Meth. A **433** 104-120 (1999).
- E. Aprile *et al.*, The XENON Project: Direct Detection of SUSY Cold Dark Matter in Liquid Xenon, Nov. (2002), www.lngs.infn.it/site/meesem/aprile/GS_DM_2002_mod.pdf
- M. Diwan *et al.*, Very long baseline neutrino oscillation experiments for precise measurements of mixing parameters and CP violating effects, Phys. Rev. **D 68**, 012002 (2003). <http://nwg.phy.bnl.gov>
- T. Doke, K. Masuda, Present status of liquid rare gas scintillation detectors and their new application to gamma ray calorimeters, Nucl. Instrum. Meth. A420 62-80, (1999).
- O. Evrard, M. Keters, L. Van Buul, P. Burger, A novel photodiode array structure for gamma camera applications, Presented at New Developments in Photodetection, Beaune, France, June 17-21, (2002).
- R. Farrell, et al., Large Area Silicon Avalanche Photodiodes for Scintillation Detectors, Nucl. Inst. and Meth., **A288**, p. 137, (1990).
- R. Farrell, K. Vanderpuye, M.R. Squillante, and G. Entine, Radiation Detection Performance of Very High Gain Avalanche Photodiodes, Nucl. Inst. and Meth., **A353**, p. 176 (1994).
- S. Fukuda et al., The Super-Kamiokande detector, Nucl. Inst. And Meth., **A 501** 418-462 (2003).
- S. Ghandhi, **VLSI Fabrication Principles**, John Wiley & Sons, New York, NY (1983).

Hayat, Majeed M., Chen, Zikuan, and Karim, Mohammad, An analytical Approximation for the Excess Noise Factor of Avalanche Photodiode with Dead Space, IEEE Electron Device Letters, V.20, No.7, p 344, 1999.

M. Huhtinen, and P.A. Aarnio, Pion induced displacement damage in silicon devices, Nuc. Inst. & Meth. in Phys. Res, A335, p. 580, (1993).

G.C.Huth, IEEE Trans. Nucl. Sci NS-13 (1966) 36.

K. Kleinknecht, **Detectors for Particle Radiation**, 2nd Edition, Cambridge University Press, (1998).

G. Knoll, **Radiation Detection and Measurement**, 2nd Ed., John Wiley and Sons, (1989).

J. Marler, T. McCauley, S. Reucroft, J. Swain, D. Budil, and S. Kolaczowski, Studies of Avalanche Photodiode Performance in a High Magnetic Field, Nucl. Inst. Meth. A449, p.311, (2000).

McIntyre RJ; Multiplication Noise in Uniform Avalanche Diodes, IEEE Trans. Elect. Dev., **ED-13**, p.164, (1966).

McIntyre RJ; The Distribution of Gains in Uniformly Multiplying Avalanche Photodiodes: Theory, IEEE Trans. Elect. Dev. **ED-19** p.703, (1972).

S. Melle, Laser Focus World, 145, (Oct 1995).

Moszynski M; Szawlowski M; Kapusta M; Balcerzyk; Large Area Avalanche Photodiodes in Scintillation and X-ray Detection; Nucl. Inst. And Meth., **A485**, p.504, (2002).

R. M. Pope, E. S. Fry, "Absorption spectrum (380-700 nm) of pure water. II. Integrating cavity measurements," *Appl. Opt.*,**36**, 8710-8723, (1997).

V. Radeka, Low-Noise Techniques in Detectors, Ann. Rev. Nucl. Part. Sci., **38**, p. 217, (1988).

R. Redus, R. Farrell, Gain and Noise in Avalanche Photodiodes: Theory and Experiment, SPIE Proc. (1995).

John Sculli, New York University, Department of Physics, Private communication.

J. Séguinot, Tischhauser J, Ypsilantis T. Liquid xenon scintillation: photon yield and Fano factor measurements, Nucl Instr and Meth in Phys Res., A354; 280-287. (1995).

K.S. Shah, R. Farrell et al., Large Area APDs and Monolithic APD Arrays, IEEE Trans. Nuc. Sci., V. 48(6), p. 2352 (2001).

K.S. Shah, Gothoskar, P., Farrell, R and Gordon, J. High Efficiency Detection of Tritium Using Silicon Avalanche Photodiodes. IEEE Trans. Nuc. Sci., 44, No. 3, p.774, June (1997).

M. Shiozawa, et al., Search for Proton Decay via $P \rightarrow e^+ \pi^0$ in a Large Water Cerenkov Detector, Phys. Rev. Lett. 81:3319-3323, (1998).

Spieler, H: ICFA Instrumentation School, June 17 – June 28, 2002, Istanbul Technical University, Istanbul, Turkey, published online at <http://www-physics.lbl.gov/~spieler>. See file: III_Electronic_Noise.pdf (2002).

M.R. Squillante et al., Recent Advances in Avalanche Photodiode Technology. Proc. SPIE **2009** X-Ray Detector Physics and Applications II:64-71, (1993).

S.M. Sze, **Physics of Semiconductor Devices**, Wiley, New York, (1981).

Webb PP; McIntyre RJ; Conradi J; Properties of Avalanche Photodiodes, RCA Review, **35**, p.234, (1974).

W.J. Williams, Tracking Detectors in Liquid Helium and Liquid Argon, Talk given at the joint BNL/UCLA-APS workshop on neutrino Super beam, Detectors, and Proton Decay. March 3-5, Brookhaven National Laboratory, Upton NY 11973, <http://www.bnl.gov/physics/superbeam>

V.B. Zalesky, V.A. Pilipovich (Minsk, Inst. Electronics), M.V. Korzhik, O.V. Missevich, A.A.

IV. KEY PERSONNEL AND BIBLIOGRAPHY OF DIRECTLY RELATED WORK

A. MR. KANAI S. SHAH, M.S., DIRECTOR OF RESEARCH, RMD, INC. , P.I.

Mr. Kanai S. Shah is a full time employee of RMD and a citizen (as well as permanent resident) of USA. Mr. Shah obtained his undergraduate training in Chemical Engineering at Gujarat University in India, graduating with a B.E. in 1983, ranking first in his graduating class. He then proceeded to obtain his Master's degree in the same subject at the University of Lowell in Massachusetts in 1987. His master's thesis was a study of mass transfer of carbon dioxide through catheters used in implantable drug delivery systems. He joined the RMD research department in 1985 and was involved in a program aimed at stabilizing HgI₂ low energy X-ray sensors for NASA. Since then he has managed a variety of compound semiconductor detector development and device characterization efforts. The materials he has investigated include PbI₂, HgI₂, TlBr, TlBr_xI_{1-x}, ZnTe, CdTe, CdZnTe, and BP. From 5/92 to 10/93, Mr. Shah worked as a Device Engineer at Canberra Industries, Meriden, CT. At Canberra, he developed a proprietary new contact for germanium detectors, as well as improved yield for an existing process (for HPGe detectors) from 20% to about 70%. He also worked on developing high purity silicon detectors at Canberra. Since rejoining RMD in 11/93, he has been in charge of new semiconductor and scintillator development in form of both single crystals and thick films. His recent area of interest includes development of new detector materials and investigation of high resolution X-ray and gamma ray detectors with imaging capabilities.

Mr. Shah has been a P.I. on several DOE, NIH, DOD, and NSF grants. He has co-authored a chapter entitled "*Other Materials: Status and Prospects*" in "Semiconductors for Room Temp. Nuclear Detector Applications" published by Academic Press in 1995 (E. Schlesinger and R. James, editors). He has also co-authored another chapter on *Photojunction Detectors* in The Measurements, Instrumentation and Sensor Handbook published by CRC press (J.G. Weber, editor) in 1998. Mr. Shah has made several invited presentations at international conferences, has reviewed papers for IEEE and MRS journals, has been a site reviewer for a DOE program, and has authored over 70 technical papers, some of which are listed here.

Book Chapters:

Squillante, M.R. and **Shah, K.S.** Chapter 12: *Other Materials: Status and Prospects*, in Semiconductors for Room Temp. Nuclear Detector Applications, eds. T.E. Schlesinger and R.B. James, New York: Academic Press, 1995.

Squillante, M.R. and **Shah, K.S.**, Chapter VIII, Sect. 8.1.3: *Photojunction Sensors* in **The Measurement, Instrumentation and Sensors Handbook**. Ed. J. G. Webster, CRC Press, Boca Raton, FL. To be published in 1997.

Technical Papers:

K.S. Shah, *et al.*, “Advances in Silicon Avalanche Photodiode Technology”, Presented at IEEE NSS, Portland, Or., Oct, 2003.

K.S. Shah, J. Glodo, M. Klugerman, W. Higgins, P. Wong, W.W. Moses, S.E. Derenzo, M. Weber, and P. Dorenbos, “LuI₃:Ce – A New Scintillator for Gamma Ray Spectroscopy”, presented at IEEE Nuclear Science Symposium, Portland, Or., October, (2003).

K.S. Shah, J. Glodo, W.W. Moses, S.E. Derenzo, M.J. Weber, "LaBr₃:Ce Scintillators for γ -Ray Spectroscopy," *IEEE Trans. Nuc. Sci.*, V50(6), p. 2410, (2003).

K.S. Shah, L. Cirignano, R. Grazioso, M. Klugerman, P.R. Bennett, T.K. Gupta, W.W. Moses, M.J. Weber, and S. Derenzo, "RbGd₂Br₇: Ce Scintillators for Gamma-Ray and Thermal Neutron Detection," *IEEE Transactions on Nucl. Sci.*, Vol. **49**, August 2002.

K.S. Shah, R. Farrell, R. Grazioso, E. Harmon, and E. Karplus, "Position-Sensitive Avalanche Photodiodes for Gamma-Ray Imaging," *IEEE Transactions on Nucl. Sci.*, Vol. **49**, August 2002.

K.S. Shah, J. Glodo, M. Klugerman, L. Cirignano, W.W. Moses, S.E. Derenzo, and M.J. Weber, LaCl₃:Ce Scintillators for Gamma Ray Detection, " Presented at RMA Symposium, Ann Arbor, MI, May, 2002

K.S. Shah, R. Grazioso, R. Farrell, J. Glodo, P. Dokale, and S.R. Cherry, "Position Sensitive APDs for Small Animal PET Imaging," Presented at IEEE Med. Imag. Conf. , Norfolk, VA, Nov., 2002.

Shah, K.S., Street, R.A., Dmitriyev, Y., Bennett, P., Cirignano, L., Klugerman M., Squillante, M.R., Entine, G. “X-ray Imaging with PbI₂-based a –Si:H Flat Panel Detectors”, Nucl. Instr. & Meth. in Physics Res. **A 458** :140-147, 2001.

Shah, K.S., R. Farrell *et al.*, “Large Area APDs and Monolithic APD Arrays,” *IEEE Trans. Nuc. Sci.*, Vol. **48(6) 2**, 2352-6, Dec. 2001.

Farrell, R.F.; **Shah, K.**; Vanderpuye, K.; Entine, G.; et al. *APD Arrays and Large Area APDs via a New Planar Process*, Nucl. Instru. & Meth. In Phys. Res., **A442**, pp. 171-178 (2000).

Shao, Y. S. Cherry, **K.S. Shah**, R. Farrell *et al.*, *Dual APD array Readout of LSO crystals: Optimization of Crystal Surface Treatment*, presented at IEEE Nuc. Sci. Symp., Lyon, France, October, (2000).

Koji Iwata, Soo-Il Kwon, PR Bennett, L Cirignano, **K.S. Shah**, and BH Hasegawa, *Description of a Prototype Combined CT-SPECT System with a Single CdZnTe Detector*, presented at IEEE Nuc. Sci. Symp., Lyon, France, October, (2000).

L. Cirignano, **K. S. Shah**, P. Bennett, L. Li, F. Lu, J. Buturlia, W. Yao, G. Wright, and R.B. James, *Characterization of Multi-element CZT arrays*, Presented at SPIE Annual Meeting, San Diego, CA, July, 2000.

B. RICHARD FARRELL, M.S., SENIOR SCIENTIST, RMD, INC.

Mr. Farrell received his B.S. in Physics in 1964 from Worcester Polytechnic Institute, Worcester, MA and his M.S. in Physics from Brown University, Providence, Rhode Island in 1968. His research experience at Brown included orienting, cutting and polishing semiconductor materials for electroreflectance experiments. During the years 1967 to 1970, he worked at the NASA Electronics Research Center, Cambridge, MA where he carried out R&D in solid state materials, processes and electronic devices. He developed and characterized the first reported SiC backward diode and developed novel encapsulation to allow operation from cryogenic temperatures to above 1300°F.

In 1970 Mr. Farrell went to Device Research, Inc., N. Billerica, MA as Chief Engineer where he developed the first commercial tunnel diode transducer. He also developed several prototype transducer configurations using piezjunction effects in tunnel diodes, backward diodes and transistors. From 1971 to 1973 Mr. Farrell was with Tyco Laboratories in Waltham, MA. While there he was Principal Researcher in the successful development of a CdTe infrared photodetector for use as an aircraft engine fire detector for use by the U.S. Air Force. R&D included device fabrication and encapsulation, development of appropriate electrical contacts for high temperature operation, extensive study of temperature dependence of spectral response of CdTe, noise evaluations, lifetime studies at high temperature, and vibration testing of completed units. In 1973 he established, owned and operated a small ceramics business where he developed new ceramic fabrication techniques.

Mr. Farrell is a full time employee of RMD. In January of 1985 he joined the company as a Senior Scientist working on the silicon avalanche photodiode research. In 1987, he became head of avalanche photodiode research, development and manufacturing and has since been responsible for the technical, as well as, commercial market development of the APD. He is responsible for turning the APD into a standard, product for detection for light, low energy X-rays, and charged particles. In 1994, spearheaded an effort that resulted in an order of magnitude increase in gain over any previous APD's. Mr. Richard Farrell is a member of Sigma Xi and Sigma Alpha Epsilon. Some of his publications are listed here.

K.S. Shah, **R. Farrell** *et al.*, "Advances in Silicon Avalanche Photodiode Technology", Presented at IEEE NSS, Portland, Or., Oct, 2003.

K.S. Shah, **R. Farrell**, R. Grazioso, E. Harmon, and E. Karplus, "Position-Sensitive Avalanche Photodiodes for Gamma-Ray Imaging," *IEEE Transactions on Nucl. Sci.*, Vol. **49**, August 2002.

Shah, K.S., **R. Farrell** *et al.*, "Large Area APDs and Monolithic APD Arrays," *IEEE Trans. Nuc. Sci.*, Vol. **48(6) 2**, 2352-6, Dec. 2001.

Farrell, R.F.; Shah, K.; Vanderpuye, K.; Entine, G.; et al. *APD Arrays and Large Area APDs via a New Planar Process*, Nucl. Instru. & Meth. In Phys. Res., **A442**, pp. 171-178 (2000).

Shao, Y. S. Cherry, K.S. Shah, R. Farrell *et al.*, *Dual APD array Readout of LSO crystals: Optimization of Crystal Surface Treatment*, presented at IEEE Nuc. Sci. Symp., Lyon, France, October, (2000).

Farrell, R., Olschner, F., Shah, K. and Squillante, M.R., *Advances in Semiconductor Photodetectors for Scintillators*, Nuc. Instru. & Meth. in Phys. Res., **A 387**, 194-198 (1997).

Shah, K.S., Gothoskar, P., Farrell, R. and Gordon, J. *High Efficiency Detection of Tritium Using Silicon Avalanche Photodiodes*. Submitted for the IEEE Nuc. Sci. Symp., Anaheim, CA, Nov. (1996).

R. Farrell et al., High gain APD arrays for photon detection, SPIE (1995).

Farrell, R., K. Vanderpuye, L. Cirignano, M.R. Squillante, and G. Entine, *Radiation Detection Performance of Very High Gain Avalanche Photodiodes*, Nucl. Inst. and Meth., **A353**, p. 176 (1994).

F. Martin, G. Entine and **R. Farrell**, *Measurements of the Operating Characteristics of a Large-Area Avalanche Photodiode*, Optical Engineering, **31**, No. 1, 48-52, Jan. (1992).

R. Farrell, K. Vanderpuye, G. Entine and M.R. Squillante, *High Resolution, Low Energy Avalanche Photodiode X-Ray Detectors*, IEEE Trans. Nuc. Sci., **38**, Vol. 2, 144-147, Apr. (1992).

Farrell, R., K. Vanderpuye, G. Entine, and M.R. Squillante, *High Resolution, Low Energy Avalanche Photodiode X-ray Detectors*, IEEE Trans. Nuc. Sci., **NS-38**, p. 144, (1991).

R. Farrell, et al., *Large Area Silicon Avalanche Photodiodes for Scintillation Detectors*, Nucl. Inst. and Meth., **A288**, p. 137, (1990).

C. MR. LEONARD CIRIGNANO, M.S. SENIOR SCIENTIST, RMD, INC.

Mr. Cirignano received his B.S. in physics in 1979 from Boston College and his M.S. in applied physics from the University of Massachusetts, Boston in 1986. While at the University of Massachusetts he worked as a research intern in the semiconductor characterization group at Cabot Corporation in Billerica, MA. While at Cabot his research experience included studying scattering mechanisms in gallium arsenide samples using Hall effect and resistivity measurements.

Mr. Cirignano is a full time employee of RMD. In 1986 he joined RMD as a research scientist. Since joining the company he has contributed to the successful development of both semiconductor radiation detectors and instrumentation for nondestructive testing. Projects which he has helped bring to fruition include a cadmium telluride (CdTe)-based exposure controller for improved mammography and a beta backscatter instrument for determining average atomic number of low Z materials. In addition, he has helped develop an array of photovoltaic CdTe sensors for imaging the intensity profile of radiation therapy beams and a hand-held mini gamma camera based on position sensitive photomultiplier tube technology. His recent research interest includes new detector materials for high resolution gamma ray spectroscopy, gamma ray imaging systems, charged particle and neutron imaging detectors. Mr. Cirignano is a member of the American Physical Society. Some of his publications are listed here.

K.S. Shah, J. Glodo, M. Klugerman, **L. Cirignano**, W.W. Moses, S.E. Derenzo, and M.J. Weber, *LaCl₃:Ce Scintillators for Gamma Ray Detection*, " Presented at RMA Symposium, Ann Arbor, MI, May, 2002

K.S. Shah, **L. Cirignano**, R. Grazioso, M. Klugerman, P.R. Bennett, T.K. Gupta, W.W. Moses, M.J. Weber, and S. Derenzo, "RbGd₂Br₇: Ce Scintillators for Gamma-Ray and Thermal Neutron Detection," *IEEE Transactions on Nucl. Sci.*, Vol. **49**, August 2002.

K.S. Shah, **L. Cirignano**, W.W. Moses, S.E. Derenzo, M.J. Weber, *et. al.* "LaBr₃:Ce Scintillators for γ -Ray Spectroscopy," Presented at IEEE Nucl. Sci. Symp., Norfolk, VA, Nov., 2002.

K.S. Shah, **L. Cirignano**, R. Grazioso, M. Klugerman, P.R. Bennett, T.K. Gupta, W.W. Moses, M.J. Weber, and S. Derenzo, "RbGd₂Br₇: Ce Scintillators for Gamma-Ray and Thermal Neutron Detection," *IEEE Transactions on Nucl. Sci.*, Vol. **49**, August 2002.

K.S. Shah, R. Farrell, R. Grazioso, R. Myers, and **L. Cirignano**, "Large Area APDs and Monolithic APD Arrays," in *Proc. 2001 IEEE Nucl.Sci. Symp. Conf.*, San Diego, (2001).

Squillante, M.R., **Cirignano L.**, Grazioso, R., *Room Temperature Semiconductor Device and Array Configurations*. Nucl. Instr. & Meth. in Physics Res. **A458**:288-296, 2001.

L.Li, F. Lu, K. Shah, M. Squillante, **L. Cirignano**, W. Yao, R.W. Olson, P. Luke, Y. Nemirovsky, A. Burger, G. Wright, and R.B. James, "A New Method of Growing Detector-Grade Cadmium Zinc Telluride Crystals," in *Proc. 2001 IEEE Nuc. Sci. Symp/Med Img. Conf. P*, San Diego.

Shah, K.S., Street, R.A., Dmitriyev, Y., Bennett, P., **Cirignano, L.**, Klugerman M., Squillante, M.R., Entine, G. *X-ray Imaging with PbI₂-based a-Si:H Flat Panel Detectors* Nucl. Instr. & Meth. in Physics Res. **A 458** :140-147, 2001.

Cirignano, L., Shah, K. S., Bennett, P., Li, L., Lu, F., Buturlia, J., Yao, W., Wright, G., James, R., *Characterization of Multi-element CZT Arrays*, Proceedings of SPIE Vol. 4141 pp 23 – 28 2000.

Bennett, P.R., Shah, K.S., **Cirignano, L.J.**, *et al.*, *Multi-element CdZnTe Detectors for Gamma Ray Detection and Imaging*, Submitted to IEEE Nucl. Sci. Symp., Albuquerque, NM, Nov. 1997. Published in IEEE Trans. Nucl. Sci. (1998).

Cirignano, L., Klugerman, M., Dmitriyev, Y, Shah, K.S. *High Efficiency Spectroscopic CZT Array*. Presented at MRS Fall Meeting, Boston, MA, Dec. 1997.

V. RMD FACILITIES/EQUIPMENT AND RELATED RESEARCH

A. RMD OVERVIEW AND FACILITIES/EQUIPMENT

Radiation Monitoring Devices, Inc., was started in 1974 to pursue the development of CdTe nuclear detectors. Today, we are the primary company in the United States devoted to the development of this technology and to the production of CdTe radiation detectors and nuclear instruments for commercial and medical use. RMD is also a pioneer in the silicon APD technology which is being pursued at the company for over 20 years. RMD's laboratories occupy over 30,000 square feet and include equipment for many types of research and development work. RMD has extensive facilities for the fabrication, testing, and packaging of nuclear and optical detectors. Included are such items as crystal shaping equipment, cleaning and evacuation facilities, general bench and hood space for materials handling, glove boxes, and various facilities for crystal cutting, lapping, and polishing. Device fabrication facilities include high vacuum evaporators with thickness monitoring capabilities, diffusion furnaces, micromanipulators and wire bonders. RMD maintains a CAD layout work station, enabling mask layout to be designed and implemented on our premises. This will assist us in the production of rapid and detailed designs. In the way of materials and device characterization facilities, we have optical and infrared microscopes, four point resistivity probes and optical spectrometers as well as several complete sets of nuclear instrumentation. Also available are various specialized test fixtures, a wafer probe station, variable temperature test chambers and a wide variety of isotopic radiation sources as well as two X-ray generators.

B. RELATED RESEARCH AT RMD

Radiation Monitoring Devices, Inc. is involved in several avenues of research that are related directly to the work proposed here. We have worked with silicon avalanche photodiodes for use as optical scintillation detectors, direct X-ray detectors, and beta particle detectors for use with tritium. We have developed compound semiconductors as radiation detectors for over twenty years and we have also developed different types of semiconductor optical detectors, and alpha, beta, gamma, and neutron detectors, as described below.

1. Large Area, High Gain Avalanche Photodiodes

RMD has pioneered the development of large area, high gain silicon avalanche photodiodes. Our work has led to a technological breakthrough in this area, achieving avalanche diode gains of over 10,000 at room temperature and 40,000 at low temperature, a full order of magnitude better than ever previously reported. We have also developed a planar process that will allow low cost production of these promising devices. RMD has produced monolithic, multi-element APD arrays in large format (up to 28 x 28 elements). Large planar APDs (45 cm²) have been built at RMD.

2. Silicon Drift Photodiodes for Scintillation Spectroscopy

This research has the goal of producing silicon drift photodiodes for optical light detection. These are unity gain devices but show very low noise because their capacitance is very small. Specifically, these photodiodes are being optimized for use as scintillation light detectors for high resolution gamma-ray spectroscopy. Research is focusing on optimizing the quantum efficiency of these devices for CsI(Tl) scintillated light (560 nm) by using tuned anti-reflection coatings and optimized doping profiles.

3. Semiconductor Research and Development

RMD was founded in 1974 to pursue the development of CdTe nuclear detectors. Today we are the world's largest commercial supplier of CdTe detectors and associated electronic instrumentation. We have carried out research into the fundamental physics of crystal growth of CdTe using the traveling solvent zone method and studies of the metal/semiconductor barrier. We have developed large volume detectors for spectroscopy, and thin film devices for photovoltaic solar cells. We have worked with various other sensors including PbI₂, HgI₂, and TlBr crystals which have all been prepared and characterized in our laboratories.

VI. COLLABORATORS AND CONSULTANTS

A. DR. LAURENCE LITTENBERG'S TEAM AT BROOKHAVEN NATIONAL LABORATORY

In the Phase I project, we will collaborate with the Brookhaven National Laboratory (BNL) team of Dr. Laurence Littenberg, Dr. Michael Sivertz, and Dr. Milind Diwan. Brief bio-sketches of the BNL team members are provided here and a letter of interest from Dr. Diwan is attached.

1. Dr. Laurence Littenberg, Brookhaven National Laboratory

Dr. Littenberg was a thesis student of the noted high energy physics pioneer Oreste Piccioni, who was himself a student of Enrico Fermi. After working on kaon decay as a graduate student at UCSD, Dr. Littenberg was a postdoc at the Daresbury Laboratory in England for four years, participating in photoproduction experiments with a tagged photon beam from the NINA accelerator. Since then he has been a staff member of the Brookhaven National Laboratory Physics Department where he is presently a Senior Physicist and Group Leader. He is an expert in the subject of kaon decay and is the co-discoverer of a number of kaon decay modes. He has published

several reviews on rare kaon decays, including the recurring one in the Particle Data Book. He has also collaborated on theoretical papers in this and other areas. He has worked extensively with Cherenkov and scintillating detectors. He is a Fellow of the American Physical Society and the winner of the Brookhaven Science and Technology Award.

2. Dr. Michael Sivertz, Brookhaven National Laboratory

Dr. Sivertz has been an innovator in the field of experimental particle physics for more than two decades. As a member of the PHENIX experiment at RHIC, he was responsible for building a novel design of tracking chamber (1998-2001). He served as the Trigger Coordinator for the CLEO experiment at Cornell (1992-98), developing fast electronics for data recording. While at CLEO, he studied the feasibility of using APDs for readout of aerogel Cherenkov counters. He was the CLEO Run Manager for the installation of a Silicon Vertex Tracker, and intensity upgrades of the electron-positron synchrotron. He developed a new type of scintillating fiber calorimetry as a member of the SPACAL Group at CERN where he pioneered APD use in particle physics detectors (1989-92). As a member of the CDF experiment at Fermilab, he worked on the development of a calibration database (1983-86). He constructed Cherenkov counters for electron identification and hodoscopes for muon identification as part of his involvement with the rare kaon decay experiment E-791 at Brookhaven (1986-89). Because of his broad expertise in all types of particle detector technology, he was chosen as a reviewer of detector technology papers for NSF.

3. Dr. Milind Diwan, Brookhaven National Laboratory

Dr. Diwan obtained his Ph.D. in particle physics from Brown University in 1988. His thesis topic was the detection of rare interactions of neutrinos on electrons. He was a postdoc at Stanford University where he worked on rare decays of kaons. He worked at the SSC laboratory to improve the performance of the proposed accelerator and detector complex with regards to the expected intense radiation fields before the project was terminated. Since 1994 he has been a member of the scientific staff at Brookhaven National Laboratory. His recent interests have been kaon decays, neutrino oscillations, and large underground detectors. He is a member of the MINOS collaboration at Fermilab. He recently led a study group at BNL to explore new opportunities for very large neutrino detectors with size of 500kT located deep underground. This study can be found at <http://nwg.phy.bnl.gov> as technical note BNL-69395. Dr. Diwan is a member of the American Physical Society. He has been a leader of many initiatives in particle physics. He has been a member of many national as well as internal review panels.

4. Dr. Peter Yamin, Brookhaven National Laboratory

Dr. Peter Yamin received an S.B in physics in 1960 from the Massachusetts Institute of Technology, an M.S. in physics and a Ph.D. in particle physics from the University of Pennsylvania in 1961 and 1966, respectively. He has served as a postdoc at Brookhaven National Laboratory, a member of the physics faculty of Rutgers University, and a staff physicist in the Accelerator Department at Brookhaven. Currently, he is Special Assistant to the Associate Director, High Energy and Nuclear Physics, at Brookhaven. He was a participant in the experiment at Fermilab in which the polarization of inclusively produced neutral hyperons was discovered and further experiments at Brookhaven in which this phenomenon was explored; as a member of the Fermilab D-Zero experiment he worked on the construction and installation of the uranium-liquid argon calorimeter and the analysis that led to the discovery of the top quark. Dr. Yamin has served on visiting review committees for the Department of Energy and as a proposal reviewer for both the

DOE and the National Science Foundation. He is a collaborator on the MECO experiment. A selection of his publications is provided here.

5. Selected Papers of BNL Team Members

J. McDonald, C. Velissaris, B. Viren, **M. Diwan**, A. Erwin, D. Naples, H. Ping, *Ionization Chambers for Monitoring in High-Intensity Charged Particle Beams*, To Be published in Nucl. Instr. Meth. A. e-print: physics/0205042.

V. M. Abazov, **P. Yamin**, et al., *Search for 3- and 4-Body Decays of the Scalar Top Quark in Proton-Antiproton Collisions at $s^{1/2} = 1.8$ TeV*, Phys. Lett. B581:147-155, 2004.

A. Gordeev, **P. Yamin**, et al., *Technical Design Report of the Forward Pre-Shower Detector for the D0 Upgrade*, Fermilab-Pub 98-416, 2003.

Yu.G. Kudenko, **L. Littenberg**, et al., *EXTRUDED PLASTIC COUNTERS WITH WLS FIBER READOUT*, Nucl. Instrum. Meth. A469:340-346, (2001).

J. Barrette, **M. Sivertz**, et al., *The Pixel Readout System for the Phenix PAD Chambers*, Nucl. Phys. A661:665-668, 1999.

M. Diwan, S. Kahn, R.B. Palmer, *A Solenoidal Capture System for Neutrino Production*, presented at IEEE Particle Accelerator Conference (PAC99), New York, Mar. 29- Apr. 2 1999. Published in Particle Accelerator, Vol. 5, 3023-3025 (1999).

T.K. Komatsubara, **L. Littenberg**, et al., *PERFORMANCE OF FINE MESH PHOTOMULTIPLIER TUBES DESIGNED FOR AN UNDOPEDED CSI ENDCAP PHOTON DETECTOR*, Nucl. Instrum. Meth. A404:315-326, (1998)

M. Sivertz, et al., *A Compact Gas Cherenkov Detector with Novel Optics*, Nucl. Inst. Meth. A385:37-46, 1997.

I.H. Chiang, **L. Littenberg**, et al, *CSI ENDCAP PHOTON DETECTOR FOR A $K^+ \rightarrow \pi^+ \nu$ ANTI-NU EXPERIMENT AT BNL*, IEEE Trans. Nucl. Sci., 42:394-400, (1995)

S. Abachi, **P. Yamin**, et al., *Observation of the Top Quark*, Phys. Rev. Lett. 74:2632-2637, 1995.

J. Badier, **M. Sivertz** et al., *Test Results of an Electromagnetic Calorimeter with 0.5-mm Scintillating Fibers Readout*, Nucl. Inst. Meth. A337:314-325, 1993.

S. Abachi, **P. Yamin**, et al., *Beam Tests of the D0 Uranium-Liquid Argon End Calorimeters*, Nucl.Instrum.Meth. A324:53-76, 1993.

M. Abolins, **P. Yamin**, et al., *Hadron and Electron Response of Uranium-Liquid Argon Calorimeter Modules for the D0 Detector*, Nucl. Instrum. Meth. A:280:36-44, 1989.

L. A. Ahrens, **M. Diwan** et al., *A Massive Fine Grained Detector for the Elastic Reactions Induced by Neutrinos in the GeV Energy Region*, Nucl. Instrm. Meth. A254:515, 1987.

Y. Watase, **M. Diwan**, et al., *A Test of Transition Radiation Detectors for a Colliding Beam Experiment*, Nucl. Instr. Meth. A248: 379-388, 1986.

B. DR. STEVEN REUCROFT AND DR. JOHN SWAIN, NORTHEASTERN UNIVERSITY

Dr. Stephen Reucroft, Distinguished Professor of Physics, Northeastern University, Boston, MA, and his colleague, Dr. John Swain will be our collaborators on this project. Over the past several years Professors. Reucroft and Swain have been involved in high energy physics research on various levels. For example, Prof. Reucroft is one of the inventors and prime motivators of the LEBC high-resolution bubble chamber at CERN and was leader of both CERN and Fermilab experiments, which investigated charm properties. At Northeastern University he has devoted his efforts to experiments at the highest energy colliders. He has successfully developed the scintillating fiber technique and tested it with the tracking system in L3. Prof. Reucroft has concentrated his efforts on the DO upgrade, where he led the upgrade simulation group that was instrumental in winning Fermilab approval of the upgrade project. Prof. Reucroft is presently an active participant in the CMS experiment where he leads eight different university groups. As pointed out in his biography, Prof. Reucroft has over 300 publications related to high energy physics detectors.

Prof. Swain has been involved in software development for the CMS experiment to be built at CERN, forming a joint project agreement with Hewlett Packard (HP), Switzerland, to investigate the use of large numbers of PCs as an alternative to workstations and mainframes for high energy physics computations. He continues to be involved in CMS and L3 software and in the general question of how to deal with future programming environments in high energy physics. Prof. Swain is conducting studies of radiation hardness of photodiodes and is also working on novel scintillating materials. He is an author of more than 150 publications. In the proposed effort, Dr. Reucroft and Dr. Swain will collaborate with us and their letter of support is attached at the end of the proposal.

1. Stephen Reucroft, Ph.D., Professor of Physics, Northeastern University, Boston

Prof. Reucroft received his B. Sc. from Liverpool University in 1965 and his Ph.D. from the same institution in 1969. From 1967 to 1969 he was a Demonstrator at Liverpool University. In 1969 to 1971 he was a Research Fellow, CERN, Geneva. During the years 1971 to 1979, Stephen Reucroft was at the Vanderbilt University, Nashville, first as a Research Associate and then as an Assistant Professor. While at the Max-Planck-Institute, Munich during 1977 Prof. Reucroft was a Staff Scientist. From 1979 to 1986, he held various positions at CERN, Geneva. From 1986 to the present time, he has been with Northeastern University, first as an Associate Professor of Physics and now as a Professor of Physics.

In the years 1988 to 1993, Prof. Reucroft was Chair, Physics Department, Northeastern University and from 1992 to the present, he has been a Matthews Distinguished University Professor. Stephen Reucroft has been spokesman of experiments at CERN and Fermilab and at the SSC. The CERN high resolution bubble chamber LEBC was designed to investigate charm particle properties. Reucroft was one of the inventors and prime motivators of the LEBC technique and he was leader of both CERN and Fermilab experiments which investigated charm properties.

Since leaving CERN and joining Northeastern University in 1986 he has devoted his efforts to experiments at the highest energy colliders. He spent significant time developing the scintillating fiber technique and successfully tested it with the tracking system in L3. In 1990 he was co-spokesman of the TEXAS collaboration which developed an innovative scintillating fiber and calorimeter based detector design for the SSC. After the termination of the SSC project, he concentrated his efforts on the DO upgrade, where he led the upgrade simulation group that was

instrumental in winning Fermilab approval of the upgrade project. Prof. Reucroft is presently an active participant in the CMS experiment where, as NSF liaison, he represents the eight NSF supported university groups. Selected Publications (of more than 300) related to Detectors.

Y. Musinko, **S. Reucroft**, D. Ruuska, and J. Swain, Studies of Neutron Irradiation of Avalanche Photodiodes Using Californium-252, submitted to Nucl. Instr. and Meth (1999)

Y. Musienko, **S. Reucroft**, D. Ruuska, A. Heering, R. Rusack, and J. Swain, Radiation Hardness of Avalanche Photodiodes Using Californium-252, Proceedings of the Fourth Workshop on Electronics for LHC Experiments (LEB98), University of Rome, Sept. 21-25, 1998.

J. Moromisato, Y. Musienko, **S. Reucroft**, D. Ruuska, J. Swain, and E. von Goeler, Novel Electronic Sensors at CMS, Proceedings of the Fourth Workshop on Electronics for LHC Experiments (LEB98), University of Rome, Sept. 21-25, 1998.

S. Reucroft, R. Rusack, D. Ruuska, and J. Swain, Neutron Irradiation Studies of Avalanche Photodiodes Using Californium-252, Proceedings of the First Conference on New Developments in Photodetection, Beaune, France, June 24-28, 1996, Nucl. Instr. and Meth. A387 (1997) 214.

S. Reucroft, R. Rusack, D. Ruuska, and J. Swain, Neutron irradiation damage of APD's using ^{252}Cf , Nucl. Instr. and Meth. A394 (1997) 199.

Y. Musienko, **S. Reucroft**, R. Rusack, D. Ruuska, and J. Swain, Irradiation Damage of APD's for CMS Using Neutrons from ^{252}Cf , Proceedings of SCIFI'97, University of Notre Dame, Notre Dame, Sept. 1997, eds. A. D. Bross *et al.*, AIP Conference Proceedings Volume #450.

S. Reucroft, R. Rusack, R. Ruuska, and J. Swain, *Neutron Irradiation Studies of Avalanche Photodiodes Using Californium-252*, Nucl. Instr. Meth., **A387** (1997) 214, and Proceedings of the First Conference on New Developments in Photodetection, Beaune, France, June 24-28, 1996.

S. Reucroft, R. Rusack, R. Ruuska, and J. Swain, *Neutron Irradiation Damage of APDs Using ^{252}Cf* , to appear in Nucl. Instr. Meth, 1997.

2. John Swain, Ph.D., Assistant Professor of Physics, Northeastern University, Boston

Prof. John Swain received his B. Sc. from the University of Toronto, he was conferred degrees in both physics and computer science in 1985. He received his M. Sc. from the University of Toronto in 1986 and his Ph.D. from the same institution in 1990. Prior to 1990, John Swain held miscellaneous teaching, tutoring and consulting jobs. From 1990 to 1994 he was with CERN in Geneva, first as an Instructor and then as a Research Associate. In November 1994, Prof. Swain was a Visiting Professor of Physics at the , Universidad Nacional de La Plata, Argentina. From 1995 to the present time, John Swain has been an Assistant Professor of Physics, Northeastern University in Boston, MA. He has also been involved in software development for the CMS experiment to be built at CERN, forming a joint project agreement with Hewlett Packard (HP), Switzerland to investigate the use of large numbers of PC's as an alternative to workstations and mainframes for high energy physics computations. He continues to be involved in CMS and L3 software and in the general question of how to deal with future programming environments in high energy physics, and addressed this issue in the HEPVIS 96 conference in Geneva in September of 1996.

Also in the framework of CMS, he has been involved in studies of radiation hardness of avalanche photodiodes, with preliminary results presented at an international conference in Beaune, France in 1996 with further results in preparation. he has been also working on novel scintillating materials. An interest in string-like models of hadrons led to some mathematical work on the approximation of groups of area-preserving diffeomorphisms by classical groups which was presented in a colloquium in La Plata and is in preparation for publication. Since November 1995, he has been the representative of Northeastern University on the collaboration board of the Pierre Auger project, which is designed to search for the origin of the highest energy cosmic rays. He is an author of more than 150 publications.

Y. Musienko, S. Reucroft, D. Ruuska, A. Heering, R. Rusack, and **J. Swain**, Radiation Hardness of Avalanche Photodiodes Using Californium-252, Proceedings of the Fourth Workshop on Electronics for LHC Experiments (LEB98), University of Rome, Sept. 21-25, 1998.

J. Moromisato, Y. Musienko, S. Reucroft, D. Ruuska, **J. Swain**, and E. von Goeler, Novel Electronic Sensors at CMS, Proceedings of the Fourth Workshop on Electronics for LHC Experiments (LEB98), University of Rome, Sept. 21-25, 1998.

S. Reucroft, R. Rusack, D. Ruuska, and **J. Swain**, Neutron Irradiation Studies of Avalanche Photodiodes Using Californium-252, Proceedings of the First Conference on New Developments in Photodetection, Beaune, France, June 24-28, 1996, Nucl. Instr. and Meth. A387 (1997) 214.

S. Reucroft, R. Rusack, D. Ruuska, and **J. Swain**, Neutron irradiation damage of APD's using ^{252}Cf , Nucl. Instr. and Meth. A394 (1997) 199.

Y. Musienko, S. Reucroft, R. Rusack, D. Ruuska, and **J. Swain**, Irradiation Damage of APD's for CMS Using Neutrons from ^{252}Cf , Proceedings of SCIFI'97, University of Notre Dame, Notre Dame, Sept. 1997, eds. A. D. Bross *et al.*, AIP Conference Proceedings Volume \#450.

C. DR. PRISCILLA CUSHMAN, PROFESSOR OF PHYSICS, UNIVERSITY OF MINNESOTA

Dr. Priscilla Cushman at the University of Minnesota will be our collaborator in the Phase II project. Dr. Cushman has considerable experience in area of detectors for high energy physics applications including development of a scintillating fiber preradiator prototype built for SSC to investigation of photodetectors for tile-fiber hadronic calorimeter for CMS. She has active research interest in photodetectors such as Hybrid PhotoDiodes (HPDs) and APDs for high energy physics experiments, including CMS. Extensive electronic readout facilities for evaluation of APDs are available in her laboratory. UNM also has facilities for radiation hardness evaluation of APDs using ^{252}Cf source, which will be carried out under Dr. Cushman's supervision in the Phase II project. A letter of interest and intent from Dr. Cushman is attached in the proposal, and Dr. Cushman's Bio-sketch is included in the next section.

Bio-sketch of Dr. Priscilla Cushman

Education

Harvard University	Physics and Philosophy	AB	1976
Rutgers University	Physics	PhD	1985
Rockefeller University	Exp. Particle Physics	postdoc	1985-88

Professional Experience

2000-present: Professor of Physics, University of Minnesota

1993-2000: Associate Professor of Physics, University of Minnesota
1988-92(93) Assistant (Associate) Professor of Physics, Yale University

Selected Recent Publications

1. P. Cushman, F. Farley, K. Jungman, P. Nemethy, B.L. Roberts, W. Morse, Y. Semertzidis, A Direct Measurement of the Muon Neutrino Mass by $\bar{\nu}$ Decay in Flight in the g-2 Ring, AGS-2000 Experiments for the 21st Century, BNL Formal Report 52512, Littenberg & Sandweiss eds (1996).
2. E. Adelberger, et al., Kinematical Probes of Neutrino Mass, Proceedings of the 1994 Summer Study on High Energy Physics (Snowmass, Colorado) World Scientific (1995).
3. H.N. Brown et al. (g-2 Collaboration), Improved Measurement of the Positive Muon Anomalous Magnetic Moment, Physical Review D62:091101,2000, Sept 2000.
4. P. Cushman, A. Heering, and A. Ronzhin, Custom HPD Readout System for the CMS Hadronic Calorimeter, Nuclear Instruments and Methods A442, 289 (2000).
5. S. A. Sedykh et al. (Detector SubGroup of the g-2 Collaboration), Electromagnetic Calorimeters for the BNL Muon (g-2) Experiment, Nuclear Instruments and Methods A455, 346 (2000).

Other Publications

1. P. Cushman, Electromagnetic and Hadronic Calorimeters, Chapter 4 of "Instrumentation for High Energy Physics", ed Fabio Sauli. Vol 9 of the series "Directions in High Energy Physics", World Scientific (1992) pp. 281-386.
2. P. Cushman, Status of the Brookhaven g-2 Experiment, International Europhysics Conf. on High Energy Physics, Tampere, Finland, July 1999, Published by IoP (2000) p.694 (ISBN 0-7503-0661-0)
3. R. Carey et al. (g-2 Collaboration), A New Measurement of the Anomalous Magnetic Moment of the μ^+ , Physical Review Letters 82, 1632 (1999).
4. P. Cushman, A. Heering, and J. Nelson, The Effects of Neutron Irradiation on Multi-Pixel Hybrid Photodiode Tubes, Nuclear Instruments and Methods A411, 304 (1998).
5. P. Cushman, A. Heering, and A. Ronzhin, Studies of Hybrid Photomultiplier Tubes in Magnetic Fields up to 5 Tesla, Nuclear Instruments and Methods A418, 300 (1998).

Synergistic Activities

1. Director of Undergraduate Studies (Physics) for the University of Minnesota. Developed new physics curriculum for Liberal Arts: wrote textbook: Energy and the Environment: Physics Principles and Applications, P.Cushman, ISBN 0-7872-5391-X, Kendall/Hunt Publishers (1998).
2. Brookhaven User's Executive Committee (1997-1999)
3. Member-at-large, APS Topical Group on Fundamental Constants, 1996-98.
4. Science Editor (pro bona) Carolrhoda Books (division of Lerner) - Biographies for Middle Schools, Einstein, Farnsworth, etc.
5. "Science Works!" a Minneapolis public schools systematic reform effort in K-8 science. A program supported in part by the National Science Foundation and Medtronic. Worked in the Partnership Teaching program and the Science Kit Training Sessions for Elementary Teachers.

D. CANBERRA INDUSTRIES, MERIDEN, CT

Canberra Industries (in Meriden, CT) is a world leader in the area of particle detectors, instrumentation and electronics and they have shown keen interest in our new APD technology. Canberra has committed \$150,000 of their own resources in the Phase II project for the advancement of the large planar APD technology. Canberra will collaborate with us in the Phase II project and will evaluate our devices in their laboratories using their extensive electronic and

instrumentation facilities. Their efforts in the Phase II project will serve as a platform for the Phase III commercialization effort that we plan to pursue together and for which Canberra will invest their own resources (\$1,000,000). The Phase III commercialization effort will benefit from the extensive planar silicon fabrication facilities, nuclear instrumentation, as well as world wide marketing and distribution setup available at Canberra. In fact, Canberra is one of leading suppliers of silicon and germanium nuclear detectors. Their p-i-n silicon sensors are fabricated using a planar process setup very similar to the one that would be required to mass produce APDs.

Many potential applications of the proposed planar APDs such as particle physics, synchrotron studies, health physics, nuclear waste characterization, space research, non destructive evaluation, and logging studies are already being covered by Canberra. This will be particularly helpful in bringing the APD technology to commercial stage in a rapid manner. A letter of interest from Mr. Orren Tench, Vice President of Canberra Industries is included in the proposal. Mr. Tench is in charge of detector division at Canberra and he and his engineering staff have extensive expertise and experience in the area of semiconductor and optical detectors. As a result, we expect a mutually beneficial collaboration in Phase II and Phase III projects.

VII. COMMERCIALIZATION RECORD: RADIATION MONITORING DEVICES, INC.

A SUCCESS RECORD FOR SBIR RESEARCH

Radiation Monitoring Devices has been an active participant in the SBIR program since its inception. Over the years, the company has conducted many successful SBIR projects ranging from applied research contracts focused on creating new technologies requiring many years of development to reach the market, to engineering projects leading straight to a marketable item before the completion of Phase II.

The success of some of our SBIR derived products cannot be measured directly in sales of these products. For example, we have built non-destructive test equipment that has improved the productivity of large manufacturers, and while the total sales of equipment is significant, it is tiny relative to the amount of money saved by these manufacturers in reduced losses and increased productivity. For example, many millions of dollars have been saved in the manufacture of reinforced plastics alone because of the Compuglass Analyzer developed at RMD with NSF SBIR funding. It is even harder to quantify the benefit of systems that are designed to prevent loss. We designed and built an inspection system based on similar technology to Compuglass, but improved during a subsequent Army funded SBIR program. This system was modified to meet a specific need of America's largest manufacturer of television tubes. The total sales were over \$3,000,000 and, although the units increase productivity by reducing the time required for quality control testing, the true benefit of the system is that it virtually eliminates the possibility of a financially devastating recall of defective TV sets which could represent many millions of dollars in losses.

Some of our most important successes go beyond financial, in the medical area we have built instruments that have had a significant impact on the quality of life of patients after surgery. There are several examples of systems that have resulted in improvements in surgical technique which have been documented to reduce the probability of post operative problems and increase patient recovery rates, some are discussed below. Our new success, the lead-in-paint analyzer is not only a hot new product, but will help ensure the safety of children in homes that might have lead paint. Similarly, our new product, a surgical probe, is not only a commercial success, but helps in fight against diseases, especially the breast cancer.

B. RMD'S TECHNOLOGICAL CONTRIBUTIONS AND COLLABORATIONS

Employment at RMD since their first NSF SBIR award has increased from 11 to over 70 today. SBIR collaborations, principally relating to SBIR funded research, total 65. They include the following universities: New Jersey Institute of Technology, Massachusetts Institute of Technology, Boston, UMass (Lowell), Stanford, Michigan, Northeastern, New Hampshire, Minnesota, California (SF, LA, Berkeley, and Davis), Johns Hopkins, and Harvard; the following industrial corporations: Schlumberger, Xerox, Fisher Medical, Varian, General Electric, Analogic, Saint Gobain, and Canberra; as well as, national laboratory collaborations with Lawrence Livermore/Berkeley, Sandia, Argonne, Oak Ridge and Los Alamos. SBIR contracts and grants have allowed RMD to provide over a million dollars in funding to universities and other small companies. Over two-hundred technical articles and four book chapters have resulted from SBIR research funded by NSF and other agencies

C NEW PORTABLE XRF SYSTEM FOR LEAD PAINT ANALYSIS

This recent NIH sponsored project has already resulted in our commercial release of the best lead in paint analyzer on the market. The technology used grew from continued development of the core technology that resulted from the army SBIR research that also led to the TV inspection system discussed above. The lead paint analyzer which is designed to sell for \$14,000 weighs 3 pounds and can produce a non-destructive measurement of the lead content of painted surfaces in under 10 seconds. Thus compares very favorably with the competitive units which weigh as much as 20 pounds and take two minutes per reading. The system was introduced at several trade shows and has been awarded a listing on the GSA schedule as an approved instrument for government use. Our company now manufactures and sells this product with sales of several million dollars per year. Sales are rising and we now have over 50% of the market of XRF lead paint analyzers. We estimate that there are presently well over 2000 inspectors employed using this system and that over 35,000 homes have been inspected, helping to protect the children that live in those homes. Total sales of over \$27,000,000 have been achieved with this system.

D. INTRAOPERATIVE SURGICAL PROBES

Initially investigated through NIH sponsored project, RMD has tied up with US Surgical to market a CdTe based imaging probe that is used to detect radiolabeled tumors during surgery. The probe acts a guide during surgery to differentiate normal tissue from tumors. It can be used to locate lymphnode(s) that influence cancer also. Total commercial sale over \$13,000,000 has been achieved with this technology.

E. IMAGING SURVEY METER

Initial work on this product was funded by a Navy Phase I SBIR contract. Although Phase II was not awarded, additional funding was obtained from DOE. The DOE sponsored Phase II SBIR project (Grant No. DE-FG02-93ER81530) has already resulted in the release of a new product, an Imaging Nuclear Survey Meter. This instrument is designed to safely and remotely locate radioactive material by providing a gamma ray image of the distribution of radiation superimposed on a video picture. This allows radiation surveys to be conducted with dramatically reduced radiation exposure, lowered cost, and improved documentation. We have begun commercialization of this instrument in parallel with the continued technical development. We participated in the DOE Commercialization Assistance Program (Dawnbreaker) in order to speed up commercialization. To date, units for a total of over \$600,000 have been sold. We are actively

marketing the instrument to a variety of government and commercial customers. Sales are only beginning, because the product was introduced to the market only recently.

F. RAPID NONDESTRUCTIVE DETERMINATION OF THE RESIN/GLASS CONTENT OF REINFORCED PLASTIC COMPOSITES

This project, one of our first SBIR grants, funded by the NSF, resulted in a successful line of products sold under the trade name "Compuglass" to the automotive industry. RMD both manufactures and sells the Compuglass with over \$3,000,000 in total sales internationally.

G. INTRAOPERATIVE REGIONAL MYOCARDIAL BLOOD FLOW MONITOR

This unusual instrument, funded by the NIH and completed in September 1990 resulted in renewed worldwide interest in regional cerebral blood flow measurements. Using this equipment, our collaborators at Bowman Gray School of Medicine were able to answer crucial questions relating to the causes of permanent neurological damage which affected over two-thirds of all patients undergoing open-heart surgery. As a result of that research, major changes were made in the protocols used in such operations and tens of thousands of patients have experienced improved outcomes at hospitals around the world. The product is manufactured and distributed by our Phase III collaborator, while our company is the supplier to them of the nuclear sensors used in the instrument. We have also directly manufactured and sold several hundred thousand dollars of custom blood flow monitoring systems which is permitted under our agreement with our partner.

H. HIGH RESOLUTION DIGITAL RADIOGRAPHY SYSTEM FOR MEDICAL DIAGNOSIS

While still working on the Phase II of this NIH sponsored project we reached a Phase III commercialization and manufacturing agreement with a major medical equipment manufacturer. This manufacturer has provided funding to build a complete sensor fabrication plant at RMD and has signed a manufacturing agreement to purchase hundreds of the sensors over the next five years. The initial capitalization contract was for \$280,000 and if this Phase III effort succeeds, the manufacturing contract will reach several millions of dollars.

I. LARGE AREA PbI_2 SEMICONDUCTOR FILMS FOR DIGITAL RADIOGRAPHY

Initial, very exploratory research on an exciting new material, PbI_2 , was funded by an NSF SBIR grant. This research resulted in the first working X-ray detector made from PbI_2 . Several tens of thousands of dollars of detector prototypes were sold as a result of the Phase II effort. More importantly, this NSF funding led directly to a new use of PbI_2 , large area thick films for digital radiography. As a result of an SBIR Phase II program funded by NIH we have been able to enter into Phase III agreement with three companies for a total of over \$1,500,000.

VIII. PHASE II AND PHASE III FUNDING COMMITMENTS

The large planar processed APD technology that we have developed in the Phase I project has produced excellent initial results, and appears to have significant commercial potential. Due to the large existing and expected market for these planar APDs, we have secured Phase II and Phase III funding agreement from Canberra Industries, Meriden, CT. RMD will work with Canberra in the Phase II and Phase III projects to bring the planar APD technology to mass-production with low cost targets. Canberra has committed significant resources towards this effort.

During the Phase II project, RMD will supply the devices to Canberra for evaluation at their facilities. Canberra will conduct its evaluation of these APDs. RMD and Canberra will jointly define specifications for the APDs for high energy and particle physics, medical imaging and other

markets. Canberra will also contribute towards the Phase II effort in areas of device design, processing, packaging and evaluation. Canberra has committed their own resources (\$150,000) for this evaluation effort in the Phase II program. Thus, the total cost sharing in the Phase II project will be \$150,000 or 20% of the funds requested from DOE.

During the Phase III project, Canberra will provide >\$1,000,000 required for manufacturing the APDs for various commercial applications. A full silicon processing line available at Canberra will be modified to fabricate APDs using design and knowledge base that has been gained (at RMD) during the proposed Phase II project. The APD fabrication line will be capable of mass production of these devices in an economical fashion. Both RMD and Canberra staff have excellent skills in area of packaging of detectors, which will be very useful. Canberra will provide marketing and financial infrastructure in the Phase III effort. We expect these new APDs to be applicable to high energy and particle physics, health physics, synchrotron studies, space applications, medical imaging (SPECT, PET, CT), non destructive evaluation, nuclear waste characterization, nuclear treaty verification, and logging. Other applications, which would use these APDs without scintillators would include X-ray and charge particle detection studies and optical applications such as LIDAR, LADAR, Adaptive Optics, optical communications, inter-satellite links, surveillance, and tracking. Because of such wide scope for these devices in diverse fields, Canberra has committed to fund the Phase III commercialization effort. This commitment is based on both the technical success of this project as well as the continued relevance of this technology at the end of the Phase II project. RMD and Canberra have the financial and technical resources as well as the desire to fulfill such a commitment. A letter from Canberra covering the details of the Phase II and Phase III commitments is included in the proposal.

2.4. BUDGET JUSTIFICATION

The Phase II project will be managed by Mr. Kanai Shah, P.I., at RMD. He will be involved in design of experiments and analysis of results. He will also be responsible for co-ordination with our collaborators. Mr. Richard Farrell at RMD will be responsible for the APD design and fabrication efforts. Mr. Leonard Cirignano will be in charge of APD evaluation experiments. They will be assisted by staff scientists/technicians to perform basic wafer processing as well as routine electronic assembly. The materials and supplies budget for the project (~\$26K) includes silicon wafers, processing chemicals, routine fabrication services and supplies, some electronic components, and packaging supplies, as well as outside commercial services for testing and evaluation. We have budgeted \$194,556 for the BNL team of Dr. Laurence Littenberg, Dr. Michael Sivertz, Dr. Milind Diwan and Dr. Peter Yamin where the large APDs will be evaluated for high energy physics applications.

We have budgeted \$25K for a subcontract to Dr. Priscilla Cushman at the University of Minnesota (UMN), where the large APDs will be evaluated as UV sensors in a LXe detector. Our collaborators, Dr. Reucroft and Dr. Swain at Northeastern University will evaluate basic performance of the large APDs and participate in low temperature studies. \$10K has been budgeted for their team.